From the Research Center Borstel
Leibniz Lung Center
Priority Research Area Infections
Director: Prof. Dr. Stefan Niemann

Research Group Host Determinants in Lung Infections
Dr. Bianca Schneider

Sex differences in vaccine induced immunity and protection against *Mycobacterium tuberculosis*

Dissertation
for Fulfillment of
Requirements
for the Doctoral Degree
of the University of Lübeck

from the Department of Natural Sciences

Submitted by
Gishnu Harikumar Parvathy
from Kollam, India

Lübeck 2024

First referee: PD Dr. rer. nat. Norbert Reiling, Forschungszentrum Borstel

Second referee: Prof. Dr. rer. nat. Rudolf A. Manz, Universität zu Lübeck

Date of oral examination: January 15th, 2025

Approved for printing. Lübeck, January 24th, 2025

Table of Contents

Abbreviations

AID	Activation induced deaminase
AIM-2	Absent-in-melanoma–2
AM	Alveolar macrophages
AR	Androgen receptor
BCG	Bacillus Calmette-Guérin
BSL	Biosafety level
cAMP	Cyclic adenosine-monophosphate
CD	Cluster of differentiation
CD40LG	*CD40 ligand*
CFU	Colony forming unit
ConA	Concanavalin A
cRPMI	complete Roswell Park Memorial Institute medium
CTLA4	Cytotoxic T-lymphocyte-associated Protein 4
CYBB	*Cytochrome b-245, beta chain*
DC	Dendritic cells
DC-SIGN	Dendritic cell-specific intercellular adhesion molecule-3-grabbing non-integrin
Ddx3x	*DEAD Box Helicase 3 X-Linked*
DNA	Deoxyribonucleic acid
EDTA	Ethylenediamine tetraacetic acid
ELISA	Enzyme linked immunosorbent assay
Eomes	Eomesodermin
ESAT-6	Early secreted antigenic target 6
ESCRT	Endosomal sorting complex required for transport
FACS	Fluorescence assisted cell sorting
FOXO3	forkhead box O3
GrALT	Granuloma associated lymphoid tissue
H&E	Hematoxylin and Eosin
IAVI	International AIDS vaccine initiative
Ig	Immunoglobulin
IKKG	*Inhibitor of nuclear factor kappa-B kinase subunit gamma*
IL	Interleukin
$KHCO_3$	Potassium bicarbonate
L (as in CD40L)	Ligand
LN	Lymph node
MHC	Major histocompatibility complex
Mtb	*Mycobacterium tuberculosis*
NADPH	Nicotinamide adenine dinucleotide phosphate oxidase
NaN_3	Sodium azide
NaOH	Sodium hydroxide
NH_4Cl	Ammonium chloride

NLRP3	Nucleotide-binding domain leucine-rich–containing family pyrin domain–containing-3
OADC	Oleic Albumin Dextrose Catalase Growth Supplement
PBS	Phosphate buffered saline
PC	Principal component
PCA	Principal component analysis
PFA	Paraformaldehyde
PGE_2	Prostaglandin E_2
RBC	Red blood cell
rBCG	Recombinant Bacillus Calmette-Guérin
restim	Restimulation *ex-vivo*
RNA	Ribonucleic acid
ROS	Reactive oxygen species
RPMI	Roswell Park Memorial Institute medium
s.c.	Subcutaneous
SARS-CoV-2	Severe Acute Respiratory Syndrome Corona Virus – 2
scRNA sequencing	Single-cell ribonucleic acid sequencing
TB	Tuberculosis
TBS	Tris-buffered saline
TCF-1	T cell factor 1
TCF-7	*Transcription factor 7*
TLR	Toll-like receptor
TLS	Tertiary lymphoid structure
UMAP	Unified Manifold Approximation and Projection
UTX	*Ubiquitously transcribed tetratricopeptide repeat, X chromosome*

Summary

Tuberculosis (TB), a disease killing over a million people per annum, shows a strong male preponderance in disease development. Although increased male affliction for TB has long been known from an epidemiological perspective, the mechanistic understanding of those differences is relatively recent. The only approved vaccine for TB, Bacillus Calmette Guérin (BCG), shows high variability in its protective efficacy – necessitating the development of effective vaccine candidates. However, whether the male-biased susceptibility to TB also applies to the efficacy of the BCG vaccine, has been scarcely explored. In the current study, a male specific failure of BCG is demonstrated in the C57BL/6 mouse model. However, two recombinant derivatives of BCG (rBCGs) - VPM1002 and BCGΔBCG1419c - were found to ameliorate this male specific vulnerability of BCG by significantly improving survival rates in males upon *Mycobacterium tuberculosis* (*Mtb)* challenge. The disparities in survival between rBCGs and BCG vaccinated males were not attributable to their ability to reduce lung colony forming units (CFUs). Further analysis revealed that BCGΔBCG1419c, used as a representative of VPM1002 and BCGΔBCG1419c, significantly enhances CD8 T cell responses 90 days post-vaccination compared to BCG, specifically in males. This enhancement shows a strong positive correlation with improved survival following *Mtb* challenge. In addition, significant positive correlations were identified between the CD4 T cell response on day 28 post-vaccination and the CD8 T cell response on day 90 post-vaccination, as well as between the CD4 T and B cell responses on day 28 post-vaccination. The CD4 T cell response at day 28 post-vaccination also showed a significant direct correlation with survival following *Mtb* challenge. Lastly, 28 days post-vaccination, CD8 T cell populations in the spleen showed distinct global differences between sexes, with specific clusters varying between males and females, independent of vaccine type. In summary, the current study identified a male specific failure of BCG in the C57BL/6 mouse model of TB and the ability of rBCGs to significantly improve the protective efficacy specifically in males. The underlying differences in post-vaccine immune responses that correlate with vaccine efficacy, as well as, those differences between sexes were identified. Elucidating how sex-specific differences in CD8 T cell responses influence vaccine efficacy, as well as the potential role of CD4 T cells and B cells in the sex-specific development of different CD8 T cell populations open new avenues for future studies.

Zusammenfasung

Tuberkulose (TB), an der jährlich über eine Million Menschen sterben, betrifft in besonders hohem Maße Männer. Obwohl das häufigere Auftreten von TB bei Männern aus epidemiologischer Sicht seit langem bekannt ist, ist das mechanistische Verständnis dieser Unterschiede relativ neu. Der einzige zugelassene TB-Impfstoff, Bacillus Calmette Guérin (BCG), weist eine unzureichende Wirksamkeit auf, was die Entwicklung effektiverer Impfstoffe erforderlich macht. Über Geschlechterunterschiede in der Wirksamkeit von BCG ist jedoch nur wenig bekannt. In der vorliegenden Arbeit wurde erstmals die fehlende Wirksamkeit von BCG speziell bei männlichen Tieren im C57BL/6-Mausmodell gezeigt. Zwei rekombinante BCG-Derivate (rBCG) - VPM1002 and BCGΔBCG1419c - konnten hingegen das Überleben nach einer *Mycobacterium tuberculosis* (*Mtb*)-Infektion speziell bei männlichen Mäusen gegenüber der BCG-Impfung signifikant verlängern und zeigten somit eine deutlich verbesserte Wirksamkeit. Die Unterschiede in der Überlebensrate zwischen rBCG- und BCG-geimpften Männchen waren dabei nicht auf ihre Fähigkeit zurückzuführen, die Anzahl der koloniebildenden Einheiten (KBE) in der Lunge zu reduzieren. Darüber hinaus wurde gezeigt, dass BCGΔBCG1419c, das als Vertreter der beiden rBCGs verwendet wurde, 90 Tage nach der Impfung die CD8-T-Zell-Antworten im Vergleich zu BCG speziell bei männlichen Mäusen signifikant erhöht - eine Eigenschaft, die eine signifikante positive Korrelation mit dem Überleben nach *Mtb*-Belastung aufwies. Desweiteren wurden signifikante positive Korrelationen zwischen der CD4-T-Zellreaktion am Tag 28 nach der Impfung und der CD8-T-Zellreaktion am Tag 90 nach der Impfung sowie zwischen der CD4-T- und der B-Zellreaktion am Tag 28 nach der Impfung festgestellt. Die CD4-T-Zell-Antwort am Tag 28 nach der Impfung zeigte ebenfalls eine signifikante Korrelation mit dem Überleben nach einer *Mtb*-Infektion. Schließlich zeigten sich zwischen den Geschlechtern globale Unterschiede in den CD8-T-Zell Populationen in der Milz 28 Tage nach Impfung, wobei sich unabhängig vom Impfstoff spezifische Cluster zwischen Weibchen und Männchen unterschieden. Zusammenfassend zeigt diese Studie eine geschlechtsspezifisch fehlende Wirksamkeit von BCG bei männlichen C57BL/6-Mäusen, und dass neuere rBCG-Derivate die Wirksamkeit bei Männchen signifikant verbessern. Die zugrundeliegenden Unterschiede in der Immunantwort nach der Impfung, die mit der Wirksamkeit des Impfstoffs korrelieren, sowie die Unterschiede in der Immunantwort nach der Impfung zwischen den Geschlechtern wurden ermittelt. Die Aufklärung, wie geschlechtsspezifische Unterschiede in den CD8-T-Zell-Antworten die Impfstoffwirksamkeit

beeinflussen, sowie die mögliche Rolle von CD4-T-Zellen und B-Zellen für die geschlechtsspezifische Entwicklung von verschiedenen CD8-T-Zell-Populationen, eröffnet neue Wege für weiterführende Studien.

1. Introduction

1.1. Tuberculosis: a background to the disease, its history, and why sex of the individual matters

Tuberculosis (TB) is a disease that has been estimated to have been with us for about 3 million years[1], having been responsible for hundreds of millions of deaths in the course of human history – which, although abated, continues to this day in its role as the number one infectious disease killer on the planet, except for a brief interruption during the pandemic years by the Severe Acute Respiratory Syndrome Corona Virus – 2 (SARS-CoV-2)[2–4]. Indeed, SARS-CoV-2 pandemic has set back years of progress in TB control, with TB deaths rising for the first time in more than a decade[5,6]. Currently, TB often affects populations in countries of Asian and African continents, showing an inverse relationship with their socio-demographic index[7], which is a composite index of development status taking into account the education, income and fertility rate of a population[8]. Over the past 200 years, TB has been estimated to be responsible for over a billion deaths[9].

TB deaths overwhelmingly affect the male population[10], with TB being a disease that shows a male predilection in disease development – having a male-female ratio of 1.9 in Germany[11], but going up to a male-female ratio as high as 4.5 in Vietnam[12]. Previously such differences in TB disease development have been attributed to factors such as alcoholism, smoking, drug abuse, among other debilitating habits. Habits that were common in males, particularly, in high burden regions of the world which also showed a strong gender inequality in their social construct. Nevertheless, this alone would not be able to account for such differences as nations with more gender equal social constructs such as Germany also shows a male-female ratio of 1.9 in TB incidence[11,13]. Meanwhile, in the past years the underlying biology of sex differences in immune responses has begun to unravel. An increasing detail of such sex specific determinants of immunity – such as the contribution of immune-related genes encoded in sex chromosomes, sex specific differences in epigenetic marks, the effects of sex hormones on immune cells – have started to uncover the mechanistic basis of infectious diseases generally resulting in increased mortality and severity in males relative to females[14–19]. Such sex specific differences in immune responses have also been extended to vaccinations, especially for those diseases where specific high affinity antibody titers demonstrate a strong positive correlation with protection, unlike TB[20,21]. Nevertheless, the role of individual sex in Bacillus Calmette-

Guérin (BCG) vaccination – the only vaccine currently approved for TB in clinical use – has largely remained unexplored despite being in use for over 100 years. Therefore, delineating the contribution of sex in the protective efficacy of BCG as well as newer recombinant variations of BCG currently in various stages of development as well as that of other vaccine candidates would be essential if the most medically vulnerable adult population group, the male sex, is to be protected by a (prospective) vaccine.

In the following chapters, I will explore in brief, the background of TB disease development including some of the peculiarities of its causative agent, the vaccines in development focusing on the vaccine candidates that were tested in this project, the current knowledge of sex differences particularly in TB and vaccination – providing a background on the research questions that were investigated in the current project.

1.2. Influence of biological sex on immunity, disease and vaccination

Incidence of diseases such as TB, atherosclerotic heart disease, autoimmune diseases including systemic lupus erythematosus and primary biliary cirrhosis, as well as, development of life-threatening complications from infections including sepsis and COVID-19 morbidities, all show differences between females and males[22–25]. However, whether it was overwhelmingly due to gender associated factors (referring to socially constructed roles, behaviors and activities associated with femininity and masculinity in communities[26]) contributing to differing risks and outcomes in disease remained unsolved for most of human history. In recent years, the work of several research groups have begun to uncover the mechanistic details that contribute to sex differences in immunity[19,25,27,28]. Among them, the role of sex hormones, sex chromosomes, gene dosage, the differing epigenetic landscape associated with age and sex – all working to confer a sex specific identity to the immune system has been increasingly detailed[25,27–33], such as the escape of *toll-like receptor 7 (TLR7)* gene from X chromosomal inactivation contributing to systemic lupus erythematosus in females while conferring them with enhanced resistance to severe COVID-19 disease course[34], the engagement of androgen receptor by androgens suppressing *Transcription factor 7 (TCF-7)* gene expression leading to decreased self-renewal capacity and increased T-cell exhaustion[35]. Indeed, female individuals have a higher number of circulating B cells, plasma cells, naïve cluster of differentiation (CD)8 T cells – while males have higher numbers of circulatory monocytes and myeloid cells[36–40].

To illustrate sex specific influences on the molecular phenotypes of immune cells with an example in TB, mutations in X-linked *cytochrome b-245, beta chain (CYBB)* gene affecting the nicotinamide adenine dinucleotide phosphate oxidase (NADPH) activity - and thus the oxidative burst in macrophages encountering mycobacteria – provide a permissive environment that is associated with predisposition to tuberculous mycobacterial disease with a male bias[41]. Together with other examples, such as mutations in inhibitor of *nuclear factor kappa-B kinase subunit gamma (IKKG)* regulating the activation of NF-kappaB affecting inflammation, immune cell function and survival or mutations in *ubiquitously transcribed tetratricopeptide repeat, X chromosome (UTX)* encoding a histone demethylase and *DEAD Box Helicase 3 X-Linked (Ddx3x)* sensing viral ribonucleic acid (RNA) in immune cells affecting the immune response to intracellular pathogens in a sex specific manner[25,42–47] – the example of *CYBB* highlights the potential of complex interplay at multiple levels. This include gene dosage (associated with (incomplete) X-chromosomal inactivation in females), metabolism, cytokine production and inflammatory profile (also profoundly dictated by cellular metabolism) as well as cellular identity, being particularly identified with macrophages in the context of *CYBB* - together contributing to sex specific immune responses in diseases such as TB. Sex specific differences in TB has also been associated with differences in B cell follicles, with male mice showing smaller as well as poorly organized tertiary lymphoid structures identified to contain B cell follicles in immunohistochemical staining[48]. Thus, although individual factors influencing the outcome might differ contextually, females in general have a more protective immune response, including against chronic infections such as TB[27,28].

Similar differences on account biological sex have been described for vaccinations – especially for viral illnesses such as SARS-CoV-2 and influenza – where higher antibody titers, as described in females, correlate with protective efficacy of the vaccine[28,49,50]. However, whether these observed sex specific differences would translate to enhanced male vulnerability in case of BCG vaccination for TB – where antibody titers themselves are a poor correlate of protection[51] – remains scarcely explored.

1.3. TB disease and its causative agent *Mycobacterium tuberculosis*

Known from ancient times and referred to in documents dating back 3300 and 2300 years ago from India and China, it is estimated that the *Mycobacterium* genus first appeared about 150 million years ago[52]. *Mycobacterium tuberculosis* (*Mtb*) itself has survived for about 70,000

years, currently affecting 25% of the world's population or 2 billion people[53–55]. The vast majority of these people are latently infected, with the potential for future reactivations. There are about 10.6 million new cases reported every year, with about 1.3 million recorded deaths per annum[10]. 5.8 million of the recorded TB cases in 2022 were in men and 3.5 million were in women[56], while 1.3 million were in children.

The causative agent of TB, *Mtb*, identified by Robert Koch in 1882[54], is an acid-fast, slow growing, lipid-rich aerobic bacillus with humans as their only known reservoir[57]. It is armed with an array of protein and non-protein virulence factors, able to interact with the host in a variety of ways including phagosomal maturation arrest and escape, subversion of autophagy, modulation of cell-death pathways, affecting the activity of pattern recognition receptors such as TLR 2 and regulating cytokine production, among others[58–66]. Yet another effect of virulence factors is to modify the behavior of *Mtb,* such as Trehalose Dimycolate, which promotes formation of long filaments (chords) with biofilm-like properties. Chording confers *Mtb* with the ability to penetrate between cells and infect new tissue niches, impair the host immune response by compressing the host cell nucleus, and provides protection from antibiotic clearance[67]. Pulmonary TB, the most common manifestation of TB, is also the most relevant disease manifestation that allows for its spread in the natural environment – causing medical and economic hardships in resource constrained parts of the world where TB is endemic[68,69]. Nevertheless, *Mtb* can infect almost all tissues and organs from human brain to deep within the spine (Pott's disease), resulting in a crippling and lethal disease course which is often difficult to treat, requiring prolonged treatment with an appreciable and sometimes high failure rate (up to 67% for TB meningitis)[70–72]. Therefore, the ability of preventive measures, such as vaccination, to especially prevent pulmonary form of TB is essential to arrest its spread in the population, as well as, to reduce the socio-economic burden and health impact of the disease at a population level[73,74]. Arresting TB spread would in-turn reduce the incidence of extra-pulmonary manifestations of *Mtb*, reduce the burden on a strained healthcare system and lay a permissive ground for socio-economic development in resource-constrained endemic regions of the world – all in addition to its direct impact on reducing pulmonary TB.

In order for any preventive intervention to be effective, it is imperative that the chosen intervention protects the vulnerable population in endemic regions. Because sex of the individual is strongly associated with disease susceptibility, with males exhibiting at least about

2-fold more susceptibility than females, any new vaccine candidate or vaccine strategy should offer considerable efficacy to the most vulnerable among its target population in order to successfully control TB in endemic settings.

1.4. Tuberculous granuloma and its immune landscape

One of the most striking features of *Mtb* infection in humans is the formation of (necrotizing) granulomas. Identified as a classical histological feature in TB over a 100 years ago, its role in *Mtb* infection remained unsolved for decades[75]. Granulomas are 3-dimensional structures with a central macrophage core that can be cellular, necrotizing (caseating or cheese-like), mineralized or suppurative (with profound neutrophilic infiltration)[75,76]. *Mtb*, acquired as a droplet infection, infects the alveolar macrophages (AMs). These infected AMs migrate to the interstitium, allowing *Mtb* access to lung parenchyma. Here, the progressive infection leads to recruitment of immune cell populations such as macrophages. These motile macrophages undergo epitheloid differentiation, characterized by tight interdigitations and aggregation, associated with the characteristic morphology of a granuloma[75,77]. Macrophages are also present in the inner layers of the granuloma, forming a scaffold for other recruited cell populations. They are joined by cell types such as dendritic cells (DCs), neutrophils, mast cells, lipid laden and foamy macrophages, multi-nucleated giant cells, T cells, B cells, innate lymphoid cells, natural-killer cells, fibroblasts and epithelial cells – with T and B cell populations forming a rim around epitheloid cells in later stages of granuloma formation, once adaptive immune response has developed following the priming of B and T cells[75,77–79]. It is also characterized by new blood vessel formation and a collagen cuff[75,80]. Originally described purely as a host protective structure, in part due to its purported ability to "wall-off" the bacteria, studies in the zebrafish model and the hyper conserved virulence factors in *Mtb* aiding granuloma formation point to the potential role of granulomas in *Mtb* dissemination[76]. Although several open questions remain, the diverse roles a granuloma plays in *Mtb* infection, both from the host and pathogen perspective is being increasingly appreciated – in part, reflecting the diversity of granulomas that can be found in the same infected lung[81,82].

These granulomas are sites for immune exhaustion – a condition characterized by dysfunctional immune cells occurring in response to chronic antigen stimulation, that are unable to clear the infected or cancerous cells[83–87]. Generally, these dysfunctional immune cells are enriched for immune checkpoint markers – which are regulators of immune response,

serving to prevent an exaggerated response against innocuous antigens and regulate the immune response to remain within physiological limits during encounter with pathogens[88]. In diseases such as cancer and chronic infections, the dysfunctional immune cells enriched in immune checkpoints provide a context of pathological tolerance allowing the infection or cancer to flourish in the background of an immune response inadequate for their clearance[88–93]. The co-expression of immune checkpoint markers in various immune cell types and deficiency of antigen presentation in granuloma associated DCs correlate with dysfunctional T cells in the granuloma microenvironment[89]. Deficient antigen presentation, enrichment of regulatory T cells and myeloid derived suppressor cells, enrichment of immune checkpoint markers, competition for metabolic substrates - such L-arginine being required for both inducible nitric oxide synthase driving microbicidal nitric oxide production or arginase-1 driving ornithine synthesis, associated with resolution of inflammation, angiogenesis and treatment failure in tumors in cells such as macrophages[94,95] – together drive exhaustion in the immune landscape of TB granuloma[78,96–98]. Granulomas exhibiting features of exhaustion are present across several Mycobacterium species, including *Mycobacterium marinum* in zebra fish infection model and *Mycobacterium bovis*. Granuloma formation with BCG in presence of co-morbidities enhancing immune dysfunction, such as cancer, have also been reported[99]. The ability of BCG to cause disease features generally associated with immune dysfunction makes its inefficiency as vaccine in adult populations unsurprising, due to its potential ability to generate dysfunctional immune cells upon vaccination, especially if part of the population is predisposed to have a less robust adaptive immune response such as the male sex.

Further, it has been noted that the establishment of organized lymphoid aggregates containing DCs, B and T cells – tertiary lymphoid structures (TLS) or granuloma associated lymphoid tissue (GrALT) in *Mtb*-infected lungs – correlate positively with disease control of chronic conditions such as TB and cancer[100–103]. Poor organization of lymphoid aggregates has also been associated with TB susceptibility in male mice[48,104–106] – and has also been associated with the efficacy of at least one TB vaccine candidate administered via aerosol route of immunization[102]. Whether such organized lymphoid aggregates are associated with vaccine efficacy for the vulnerable male sex in TB remains unknown.

1.5. BCG and newer vaccine candidates – VPM1002 and BCGΔBCG1419c

BCG, derived by the attenuation of *Mycobacterium bovis* through successive passages in-vitro, has been the only approved vaccine against TB[107]. The vaccine, approved over a 100 years ago, is largely insufficient to protect against pulmonary TB in regions of the world where TB is endemic[108]. A wide variety of peculiarities in immune response, shared among many mycobacterial species with some being unique to virulent strains, are thought to contribute to this deficiency in preventing TB [84,109,110]. As such, several newer vaccine candidates are in various stages of development. New vaccine(s) administered alone or in combination, tending to the peculiarities of a population – such as co-morbidities, age, individual sex, previous exposure to *Mtb* strains or BCG – will become necessary to fully address the deficiencies of BCG. Among those vaccine candidates in development, VPM1002 and BCGΔBCG1419c are two live recombinant derivatives of BCG, that have independently demonstrated significant advantage over BCG in animal models[111–115]. VPM1002 is currently in clinical trials[116,117].

VPM1002 has an exchange of the gene encoding Urease C with that for listeriolysin O. Urease C is an enzyme that diminishes the acidic pH of the phago-lysosomal compartment upon phagocytosis of live BCG following vaccination. Because acidic pH is essential in phago-lysosomal compartments for efficient processing of antigens by cathepsins and other enzymes, absence of Urease C gene allows for enhanced antigen processing via the major histocompatibility complex (MHC) II pathway. Lysteriolysin O, replacing Urease C, is a pore forming toxin from *Listeria monocytogenes*, that functions in the acidic pH of the phago-lysosomal compartment. Thus, VPM1002 mediates formation of pores in the phago-lysosomal membrane, allowing for the leakage of antigens into the cytosol. This potentially enhances cross-presentation via MHC I pathway, with the aim to prime CD8 T cells more efficiently as compared to BCG – a feature that has been experimentally demonstrated[111,116,118–121]. Indeed, *Mtb* too has been shown to establish itself in lysosome poor macrophages with deficient cathepsin activity in a recent study[122].

The second vaccine candidate, BCGΔBCG1419c, has a gene deletion for *1419c*, encoding for a phosphodiesterase that metabolizes cyclic adenosine-monophosphate (cAMP) in BCG. In the absence of *1419c* gene, the enhanced cAMP allows for increased pellicle formation in BCG akin to biofilm. Pellicle in BCG has shared similarities to *Mtb*, and BCGΔBCG1419c has been

demonstrated to enhance CD8 T cell memory and reduce lung pathology in a murine model of TB, as compared to BCG[114,115,123].

However, the sex specific effects of VPM1002 and BCGΔBCG1419c, as well as how each of those candidates fare in comparison to one another remains to be investigated.

1.6. Immune response to *Mtb* with a perspective on individual sex and vaccine candidates VPM1002 and BCGΔBCG1419c

Mtb, having habituated and adapted itself to the human immune system for thousands of years, its only natural reservoir, has co-evolved with its host during this time and exerts a diverse range of effects on various components of the host immune response. The earliest encounter of *Mtb* occurs with the alveolar lining fluid – a mixture of various protein and lipids secreted by alveolar epithelial cells[124,125]. Various components of the alveolar lining fluid such as surfactant and hydrolases interact with mycobacterial glycolipids and deficiency in surfactant production due to smoking or inflammageing has been shown to aid TB disease development[125–128]. On passing this barrier, *Mtb* encounters AMs and alveolar epithelial cells. *Mtb* can infect alveolar epithelial cells, spreading its glycolipids on the host cell membrane, affecting the interaction of the infected epithelial cell with other host cells[129–131]. Subpopulations of AMs provide a largely permissive niche for *Mtb*, especially in the first 2 weeks of infection. During this time, *Mtb* traverses the interstitium via infected AMs in an interleukin (IL)-1 beta and early secreted antigenic target 6 (ESAT-6) dependent manner - and diversify their niche to neutrophils, DCs and other macrophages[132–135]. Indeed, selective deletion of AMs in mice has been shown to reduce *Mtb* burden in lungs[136]. Generally, (alveolar) macrophages that are restrictive to *Mtb* growth display pronounced glycolysis while those that are permissive to *Mtb* are largely skewed towards oxidative phosphorylation[137]. Therefore, the metabolic dependencies of immune cells could diversely affect the outcome of *Mtb* infection in an infection-stage (and consequently cell type) dependent manner – with a skewing towards glycolysis benefiting the restriction of *Mtb* in innate immune cells such as macrophages[137]. At this point, it is worthwhile to note that sex hormones such as testosterone and estradiol have profound metabolic effects in a dose dependent manner[138–140]. Indeed, males have been shown to have a higher background level of circulating inflammatory markers, especially as they age compared to females[141]. In females, the risk of several diseases with underlying chronic inflammatory background, such as atherosclerotic heart disease where the role of

innate immune cells such as macrophages and mechanistic pathways such as inflammasome activation are recognized as contributory factors, increases after menopause – which is associated with a fall in the circulating level of female sex hormones[142–144]. In agreement, supplementation with estrogen after menopause has been shown to reduce the risk of atherosclerotic heart disease in post-menopausal women compared to control group without hormone replacement[145].

After the transfer of *Mtb* to various immune cells including macrophages, DCs and neutrophils following the crossing over of AMs to lung interstitium, *Mtb* employs a wide variety of effectors and techniques to stall the ongoing immune response from being effective in its complete eradication[133,146]. When successful, this results in the arrest of phagosome maturation and phago-lysosomal fusion, inhibition of the function of antimicrobial effectors such as reactive oxygen species (ROS), disruption of the integrity of phagolysosmal membrane as well as the ability of macrophages to repair the defect caused in the endolysosomal system, modulating the activity of absent-in-melanoma-2 (AIM-2) and Nucleotide-binding domain leucine-rich–containing family pyrin domain–containing-3 (NLRP3) inflammasomes in the cytosol[133,147–152]. It also results in down regulating and/or cleaving the immunodominant antigens of *Mtb*, as well as in inhibiting the efficient loading of antigens for robust antigen presentation (for example by disrupting the endosomal sorting complex required for transport (ESCRT) machinery) and exporting *Mtb* antigens by kinase-2 dependent vesicular transport to divert them from MHC II mediated antigen presentation[133,147,153–155]. These strategies are employed to various degrees in disease stage dependent and immune cell subpopulation dependent ways[133] - particularly in macrophages, DCs and neutrophils - in a manner that is just beginning to be understood. The infected DCs, therefore, exhibit deficiency in migration and T cell priming and depend in-part on bystander DCs in draining lymph nodes (LNs) to capture the exported *Mtb* antigens and prime T cells – further delaying the initiation of a robust T cell response[147,156,157]. BCG, derived from *Mycobacterium bovis* which causes comparable disease in cattle, shares many functional outcomes of *Mtb* in generating inadequate immune response, including deficiencies in antigen processing in DCs as well as insufficient T cell responses[158,159]. The efficacy of BCG as a vaccine shows a large variability, ranging from 0-80% across populations[160,161]. Newer live vaccine candidates derived from BCG, such as VPM1002, have made specific genetic modifications to overcome deficiencies in particular steps of antigen

processing and presentation of BCG[120] – allowing for better antigen processing and enhanced MHC I and II antigen presentation in VPM1002 vaccine strain.

Upon priming of CD4 and CD8 T cells with varying degrees of success during infection, the engagement of these antigen experienced CD4 and CD8 T cells with *Mtb* infected cell populations such as permissive macrophages are further hindered by the downregulation or modification of immunodominant antigens with which the T cells were primed – rendering those antigen experienced T cells largely unable to engage the infected cells for want of cognate peptide recognition[162,163]. The most immunodominant antigens of *Mtb* have also been shown to drive T cells, in yet ununderstood ways, to a terminal fate[163] – rendering them quickly ineffective for long term control. In contrast, priming of T cells with cryptic or non-immunodominant antigens which are still capable of eliciting an immune response have been shown to result in polyclonal populations of T cells that correlate with better protection against *Mtb*[162,164,165]. This knowledge has also informed the development of various vaccine candidates, including live vaccine candidates on the background of BCG such as BCGΔBCG1419c. BCGΔBCG1419c shows an enhanced production of pellicle or biofilm - a virulence factor with shared similarities between *Mtb* and BCG[115,166,167] – in the hope of providing a sustained pool of memory T cells capable of responding rapidly to actual encounter with *Mtb*[114].

Moreover, persistent expressions of antigens have been demonstrated to lead T cells to an exhausted phenotype, as is prevalent in the immune landscape of TB granulomas[163,168,169]. Indeed, inefficacy of BCG vaccination has been associated with attrition of T cell functions, including loss of cytotoxicity, proliferative potential and upregulation of inhibitory markers[170]. Other BCG responsive diseases such as bladder cancer, having many commonalities with the immune landscape of TB[171,172], is also associated with elevated T cell exhaustion in those patient populations unresponsive to BCG treatment - in contrast to about of 40-50% of those non-muscle invasive bladder cancer patients being responsive to BCG[83,173]. The exact nature of factors predicting response to BCG and how it allows the development of a phenotype of elevated T cell exhaustion in the unresponsive patient population remain open areas of investigation in the field[173]. This points to an independent ability of BCG to at least allow the development of elevated T cell exhaustion in other permissive environments such as in vaccine draining LNs, independent of *Mtb* infection. It further impresses on us the urgency to test

newer vaccine candidates that have a broader and greater protective profile against potential deficiencies in BCG induced immune responses, affecting at least a part of the target population. Whether that target population of BCG vaccinated individuals, in the context of providing protection against TB, will be at least in-part be dictated by the sex of the individual is a question that has been scantly explored considering the deficiencies of the male immune system to mount efficient immune responses to chronic infections such as TB and cancer[27,28,174]. The male immune landscape also exhibits an increase in exhausted CD8 T cells and T exhausted progenitors in chronic conditions such as TB and cancer[30,93,133,175]. B cells in germinal centers of females exhibit higher expression of the enzyme activation induced deaminase (AID) and increased rates of somatic hypermutation, demonstrating enhanced development of high affinity antibodies[33,176–178]. These and other effects described in the following chapter point to a potential deficiency of male sex in long term vaccine induced immunity against TB – a deficiency that maybe partially ameliorated by newer recombinant derivatives of BCG made specifically to enhance the immunogenicity of BCG vaccine.

1.7. Influence of individual sex and BCG/*Mtb* in T cell priming and CD8 T cell memory

The work from Dibbern, J and colleagues has shown, for the first time, that males exhibit accelerated disease progression upon infection with *Mtb* compared to their female counterparts in a resistant murine model of TB[27,105]. Although the underlying immunology of these differences could extend from the first innate immune cells that *Mtb* encounters in the lung to the time-lapsed establishment of adaptive immune response, this section will focus primarily on the priming process and generation of T cell responses – considering the established role of T cells in TB protection[157,164,179–181] and the scope of the current project to investigate potential sex specific functional differences in protection upon vaccination against TB. The two newer vaccine candidates that were tested in this study have been implicated to enhance CD8 T cell responses[111,114,120]. However, their sex specific effects and efficacy remains unelucidated to the best of my knowledge.

In vaccination, directed at generation of memory T (and B) cell responses, professional antigen presenting cells such as DCs presenting the vaccine antigens direct the fate of T cells to an activated effector phenotype or a tolerogenic phenotype by directing them to undergo anergy or apoptosis - or the expansion of regulatory T cells[179,182–187]. In addition, they inform naive CD4 T cells to differentiate into various helper T cell subsets having diverse functions[188]. DCs

execute this function by employing a diverse array of co-stimulatory molecules (CD80/CD86) engaging stimulatory (CD28) or inhibitory (CTLA4; cytotoxic T-lymphocyte-associated Protein 4) receptors in T cells, as well as, through cytokines. Described respectively as signals 2 and 3, with signal 1 being the peptide loaded MHC presenting cognate antigen to the naïve T cell, they supply contextual information to the engaging naïve T cell[188–192]. Such contextual information determines the difference between autoreactive T cells recognizing innocuous endogenous and exogenous antigens such as apoptotic bodies, food and commensal microbiota being eliminated in the periphery or being directed to a regulatory T cell fate versus directing the development of a clonally expanding effector - and subsequently memory - population of T cells directed against microbial invaders or cancer cells[193–197]. Activated T cells on the other hand, interact with CD40 on DCs via CD40L providing a positive feedback loop, "licensing" DCs to provide cytokines such as IL-12 aiding T cell differentiation and enhancing expression of CD80/CD86 by DCs[198].

In TB disease protection, the ability of DCs to activate appropriate T cells is paramount to stall disease progression. As such, the ability of any vaccine against TB to engage appropriate DC populations to direct T cell fates, generating long-lasting memory responses are necessary. In TB, the prominent role of CD8 T cell mediated immunity[109,114,180,181,199–203] and the necessary role of CD4 T cells are established, among others, by work demonstrating that DCs pulsed with both CD8 T cell and CD4 T cell peptides provide protection against TB while those pulsed with either alone do not significantly improve protection against TB[204–206]. This is in line with the established functions of CD8 T cells to engage and neutralize infected cells and the ability of CD4 T cells to aid CD8 T cell functions, especially in the context of chronic inflammation such as *Mtb* infection resulting in CD8 T cell exhaustion[205] - a phenomenon that is generally more prominent in males relative to females[28,175,207].

BCG and *Mtb* subvert antigen processing by DCs with their ability to arrest phagocyte maturation, phago-lysosomal fusion and inhibition of cathepsins[58,208,209]. Engagement of scavenger receptors such as dendritic cell-specific intercellular adhesion molecule-3-grabbing non-integrin (DC-SIGN) also directs the phagocytotic vacuole away from lysosomes[210,211]. Thus, BCG, while being a vaccine, suppresses efficient antigen presentation – possibly precluding its own function as a vaccine. The nature of newer derivatives of BCG such as VPM1002 and BCGΔBCG1419c, providing respectively for more efficient antigen cross presentation[111] and

increased production of immunogenic biofilm on a BCG background[110,115], aim to provide an enhanced pool of memory CD8 T cell population[114,180,212,213].

These effects have generally been associated with the sex of the individual, with females demonstrating a more robust antigen presentation[214–216] and subsequent adaptive immune responses. Genes involved in the process such as *CD40 ligand (CD40LG)* are located on X chromosome[217]. Estradiol has been known to positively influence DC differentiation[214] and production of type 1 interferons[138,218,219]. Indeed, females were shown to have lower frequency of forkhead box O3 (FOXO3)+ tolerogenic DCs in the immune landscape of chronic diseases[220,221] – in line with findings of an increased exhausted landscape in males in chronic conditions such as cancer[220], in many ways mimicking the exhausted landscape of chronic infections such as TB[84,98,172]. Monocyte derived DCs, a DC subset that have been shown to have a significant role in the generation of memory CD8 T cell population – via upregulation of T-cell Factor 1 (TCF-1) and Eomesodermin (Eomes) in T cells through low level IL-2 signaling[222] – is increased in females. Estradiol directs the generation of monocyte derived DCs during inflammation[216,223–225] – potentially encouraging robust generation of CD8 T cell memory responses that could exaggerate sex differences when an inadequately protective vaccine such as BCG is used. Separately, Androgen receptor (AR) receptor-ligand engagement downregulates TCF-1 in CD8 T cells – and has been mechanistically linked to reduced CD8 T cell stemness and memory in males[30,35]. Further, a new study has demonstrated the role of Prostaglandin E2 (PGE_2) to inhibit the expansion of antigen experienced CD8 T cells in tumors by disrupting IL-2 signaling and mitochondrial function[226,227] - a finding of potential prominence in the context of sex differences in immunity with the as yet inadequately characterized dose dependent regulation of PGE_2 by sex steroids[228] and the known role of IL-2 to improve T cell dysfunction in TB[168].

In agreement, sex specific differences across diverse immune cells including inflammatory monocytes, neutrophils, T cells and in structures such as lymphoid follicles are also increasingly being described in TB[48,105,174,229]. However, whether the post-vaccination immune landscape of BCG mirrors such a male specific deficiency in (CD8) T cell recall response – an enhancement of which was pursued by the two newer BCG derivatives that was tested remains unknown to the best of my knowledge. Also, whether such newer recombinant derivatives of BCG are at least partially able to overcome a potential male specific deficiency in BCG remain open to

investigation. Investigation of potential male specific CD8 T cell deficiency in the context of BCG vaccination – as well as its correlation with vaccine efficacy – would especially contribute to the pre-clinical and early assessment of newer vaccine candidates against TB, particularly those derived from BCG, for its efficacy in the vulnerable male sex.

In short, there is increasing appreciation of sex in chronic diseases such as TB and cancer, in many ways sharing similar immune landscapes[28,172,230–232], as well as for vaccines where high affinity antibody titers correlate with protection - with females showing an increased ability to affinity mature antibodies[33,177,178,233]. However, the role of individual sex in vaccines aimed at generating a sustained T cell response requiring to overcome a landscape of exhaustion as in TB remains poorly elucidated. To my knowledge, only one study has so far explored the biology of BCG vaccine efficacy in TB protection separately in female and male sex in a disease model[229]. Because that study was in a susceptible model of TB, there exists a paucity of information on how a resistant model of TB would respond in a sex specific way to BCG, in line with most humans being able to resist the development of active disease or control it for a long time[234] – and whether it would mirror the male vulnerability observed in TB disease[27]. Further, it is unexplored whether the newer derivatives of BCG – currently in clinical trials and in pre-clinical studies are able to ameliorate the potential male vulnerability in BCG vaccine efficacy. My PhD work aims to clarify these questions.

2. Objectives

1. Identify whether BCG differs in its protective efficacy between females and males – particularly whether BCG offers reduced efficacy for males in a resistant mouse model of Tuberculosis (C57BL/6 mice).
2. If there exists a male specific deficiency in BCG mediated protection, examine whether newer recombinant derivatives of BCG – VPM1002 and BCGΔBCG1419c – can ameliorate the male specific inefficacy of BCG vaccination.
3. Begin to identify the specific features of post-vaccination immune responses in the best performing male vaccine – pointing to peculiarities in post-vaccination male immune response that the chosen recombinant vaccine candidate addresses – paving way for future work on the mechanistic details of potential male specific vulnerability in TB vaccination.

3. Materials

Table 1 – Consumables and manufacturer list

Consumables	**Manufacturer**
7H11	BD Biosciences
7H9	BD Biosciences
Activated charcoal	Sigma-Aldrich
Albumin Fraction V (Bovine Serum Albumin)	Serva
Alkaline phosphate conjugated anti-mouse IgA	Southern Biotech
Alkaline phosphate conjugated anti-mouse IgG	Southern Biotech
Alkaline phosphate conjugated anti-mouse IgG2a	Southern Biotech
Alkaline phosphate conjugated anti-mouse IgM	Southern Biotech
Bovine serum	Biowest
CD16/32	Clone 93, Biolegend
CellTrace™ Violet	Thermo Fisher Scientific
Ceramic beads (for mechanical organ disintegration)	Bertin Technologies
Chloralhydrate	Sigma-Aldrich
Citric acid-Monohydrate	Roth
Concanavalin A (ConA)	Pharmacia (kindly provided by Dr. Zane Orinska, Research center Borstel)
distilled H_20 (dH_2O)	Water purification system for dH_20, Research Center Borstel (in-house)
DNAase I	Roche
Dulbecco's phosphate buffered saline (PBS)	PAN Biotech
Ethylenediamine tetraacetic acid (EDTA)	Roth
Enzyme Linked Immunosorbent Assay (ELISA) plates	Nunc-Immuno™, Sigma-Aldrich
Eosin	Merck
Ethanol	Merck
Fetal calf serum	Biochrom AG

Glycerol	Roth
Haematoxylin	Merck
Hamster serum	Abcam
HEPES	PAN Biotech
Kaliumaluminiumsulfate-Dodecahydrate/Alaun	Roth
$KHCO_3$	Roth
L-Glutamine	PAN Biotech
Liberase™ TL	Sigma-Aldrich
Minilys ® tubes	VWR (Cell viability Incorporated)
Mouse serum	PAN Biotech
Mtb whole-cell lysate	BEI Resources
NaN_3	Roth
Natriumiodide	Merck
NH_4Cl	Roth
OADC (Oleic acid, Albumin, Dextrose, Catalase)	BD Biosciences
Paraformaldehyde (PFA)	Roth
pNitrophenylphosphate	Merck
Proteinase inhibitor cocktail	Roche
Rat serum	PAN Biotech
Roswell Park Memorial Institute (RPMI) medium without: L-Glutamine, with: 2,0 g/l $NaHCO_3$	PAN Biotech
Sealing Tape, optical clear (for 96-well plates)	Sarstedt AG & Co. KG
Sodium pyruvate	PAN Biotech
Syringes and canula	B. Braun SE
ß-Mercaptoethanol (50mM)	PAN Biotech
Tris(hydroxymethyl)aminomethane	Roth
Tween 20	Sigma-Aldrich
Tween 80	Sigma-Aldrich

Vi-cell counter kit	VWR (Cell viability Incorporated)
Xylol	WALTER CMP GmbH & Co. KG

Consumable plasticwares were bought from Corning Life Sciences, unless specified.

Table 2 – Buffers and composition

Buffer	**Composition**
4% PFA	4% (w/v) PFA in PBS
7H11 agar medium for use	1.9% (w/v) 7H11 agar, 0.5% (v/v) glycerol, 10% (v/v) bovine serum in dH2O
7H9 medium for use	4.7g 7H9 base per 1L broth, 0.2% glycerol v/v, and 0.05% Tween 80 v/v, 10% v/v OADC in H_2O.
complete Roswell Park Memorial Institute medium (cRPMI)	10 % (v/v) Fetal calf serum (heat-inactivated and charcoal filtered), 1% (v/v) L-glutamine, 1% (v/v) HEPES, 1% (v/v) sodium pyruvate, 0.1% (v/v) ß-mercaptoethanol in RPMI 1640 w/o glutamine
Fluorescence assisted cell sorting (FACS) blocking buffer	1% (v/v) rat serum, 1% (v/v) mouse serum, 1% (v/v) hamster serum, 1% (v/v) anti-CD16/32 in FACS-buffer
FACS buffer	3% (v/v) Fetal calf serum (charcoal filtered, heat-inactivated), 0.1% (w/v) NaN3, 2 mM EDTA in 1x PBS
Haematoxylin solution (Mayer) (provided by Histopathology department, in-house at Research Center Borstel)	1g Crystalline Haematoxylin, 50g Chloralhydrate, 1g Citric acid-monohydrate 0.2g Natriumiodide, 50g Kaliumaluminiumsulfate-Dodecahydrate/Alaun, 1000 mL distilled H_2O.
Lung Digestion buffer (DNAase-Librase-RPMI digestion buffer)	50 µg/ml Liberase TL (Stock 2,5 mg/ml), 100 µg/ml DNase I (Stock 10 mg/ml) in RPMI
Organ lysis buffer (for mechanical disintegration of organs)	0.05% v/v Tween 20 in PBS containing a proteinase inhibitor cocktail
Red blood cell (RBC) lysis buffer	155 mM NH_4Cl, 10 mM $KHCO_3$, 0.1 mM EDTA in dH_2O
WTA buffer	1 % Bovine Serum Albumin (w/v), 1 % Tween 80 (v/v) in H_2O

Table 3 - Laboratory equipment

-20 °C Comfort freezer	Liebherr-Hausgeraete GmbH
-80 °C Hera freezer HFU 400 BV	Thermo Fisher Scientific Inc.
-80 °C Revco value plus freezer	Thermo Fisher Scientific Inc.
Autoclave Systec DX-150	Systec GmbH, Germany
BD FACS LSR™II	Becton Dickinson GmbH
Cooling centrifuge Heraeus X1R	Thermo Fisher Scientific Inc.
FastPrep™-24 Classic Bead-Beating device	MP Biomedicals, USA
Fridge	Liebherr-Hausgeräte GmbH
Fridge	Robert Bosch GmbH
Grant bio PMA microplate shaker	Keison Products
HeraeusFresco™ 21 benchtop centrifuge	Thermo Scientific, USA
Herasafe safety cabinet	Heraeus Instruments, Germany
Incubator BD 53	Binder GmbH
Incubator Heratherm	Thermo Fisher Scientific Inc.
Inhalation system Model 099C A4224	Glas-Col®, Terre-Haute
Microtome Leica SM 2000 R	Leica Biosystems
Multi-channel finnpipette (300 µL)	Thermo Fisher Scientific Inc.
Nikon eclipse microscope	Nikon Corporation
Pipettes (10 µL, 100 µL, 200 µL, 1000 µL)	Sarstedt AG & Co. KG
Preparation instruments	Hammer
Rotilabo Glass rods	Carl Roth GmbH & Co. KG
Sterile working bench safe 2020	Thermo Fisher Scientific Inc.
Sunrise™ microplate reader	Tecan Life Sciences
Tissue stainer (H&E)	Tissue Stainer TST 44 C, Medite
Vi-CELL™ XR Counter	Beckman Coulter
Vortexer MS 3 basic	IKA-Werke GmbH & CO. KG
Water Bath Aqualine A5	Lauda Dr. R. Wobserr GmbH & Co. KG

4. Methods

4.1. Microbiological methods

4.1.1. BCG, VPM1002 and BCGΔBCG1419c culture

Culture was started using 1 mL of vial for BCG and VPM1002 (kindly provided by Prof. Dr. Stefan Kaufmann, Berlin) and a colony of BCGΔBCG1419c (kindly provided by Dr. Mario Alberto Flores-Valdez, Mexico). They were grown in 7H9 bacterial culture media supplemented with 0.02% v/v glycerol, 0.05% v/v Tween 80 and 10% v/v OADC until it reached an OD_{600} of 0.8 for BCG and an OD_{600} of 1 for VPM1002 and BCGΔBCG1419c. Stocks were frozen in 0.5 mL or 1 mL screw cap vials. 3 weeks after frozen stocks were made, they were plated on 7H11 plates supplemented with bovine serum to record the stock concentration.

4.1.2. *Mtb* culture

Mtb H37Rv and *Mtb* HN878 were grown in Middlebrook 7H9 broth supplemented with 10% v/v OADC to logarithmic growth phase (OD_{600} 0.2-0.4), aliquots were frozen at -80°C and their stock concentration was determined (grown in-house by Ms. Silvia Maaß, kindly provided by the Molecular and Experimental Mycobacteriology group, Research Center Borstel).

4.1.3. Organ colony forming units (CFUs)

To perform CFU experiments of both vaccine strain proliferation post-vaccination as well as to assess the organ *Mtb* bacterial loads post-infection challenge, LNs, lungs and spleen were harvested as required after mice were sacrificed in CO_2, transferred to Minilysis tubes with beads with 1 mL ice-cold lysis buffer and placed on ice. Lungs were cut to smaller pieces before transfer into lysis tubes. The organs were shredded in FastPrep, 2x45 second in maximum speed setting. The organ lysates are diluted in WTA buffer in deep well plates – and plated further onto 7H11 agar plates. The agar plates were incubated for 3-4 weeks until they were ready for counting.

Lungs were diluted from: 10^{-2} till 10^{-5}, Spleen: 10^{-1} till 10^{-4}, LN: 10^{-1} till 10^{-4}.

All procedures were conducted in BSL-2 or BSL-3 labs as required for vaccine strains and *Mtb* infection, respectively, following sterility guidelines.

4.2. Animal experiments

All animal experiments were approved by the Ethics Committee for Animal Experiments of the Ministry of Energy, Agriculture, Environment, and Rural Areas of the State of Schleswig

Holstein, Germany (approval number 78-9/20). 10–16-week-old female and male C57BL/6j mice, bred in-house in the animal facility of Research Center Borstel under specific pathogen free conditions and maintained under BSL-2 or BSL-3 barrier conditions as required, were used for this study.

4.2.1 Vaccination

Vaccine strains BCG, VPM1002 (both kindly provided by Prof. Dr. Stefan H.E. Kaufmann, Max Planck Institute for Infection Biology, Berlin and Max Planck Institute for Multidisciplinary Sciences, Göttingen, Germany) and BCGΔBCG1419c (kindly provided by Dr. Mario Alberto Flores-Valdez, CIATEJ, Mexico) vials were thawed in 37 °C water bath and resuspended 10 times each with a 27G needle in 1 mL syringe and then with a 1 mL pipette. It was diluted in PBS at room temperature such that 100 µL would have 10^6 CFUs of the vaccine strain. C57BL/6j mice were vaccinated subcutaneously (s.c.) with 100 µL/10^6 CFU of vaccine strain in the scruff of the neck. The final dilution was continuously resuspended and used for mouse vaccinations. All vaccinations were performed in the morning.

4.2.3. Aerosol *Mtb* infection

Mice were challenged with either *Mtb* HN878 strain – a virulent strain of clinical relevance or H37Rv – a lab adapted strain of *Mtb*, via the aerosol route of infection as described before[235]. *Mtb* was applied via the respiratory route by employment of an aerosol chamber (Glas-Col, Terre-Haute). This system allows for lung infections by droplet-borne infectious agents, mimicking the natural route of *Mtb* infection. Mice were infected with an uptake of circa 100 viable bacilli per lung for low-dose infection (H37Rv) or circa 500 bacilli for high-dose infection (HN878), respectively. For aerosol infection, aliquots were thawed and bacteria were separated by resuspension with a 1 mL syringe and 26G cannula. The aliquot was diluted in Braun water to a total volume of 6 mL, from which 5.5 mL were used for aerosol infection. From the residual 0.5 mL, dilutions (10^{-2} up to 10^{-5}) were plated on 7H11 agar plates to assess the bacteria count in the inoculum (as input control). Mice were put in special mesh steel baskets within the aerosol chamber. After completion of the aerosol infection program (900s pre-warming, 2400s nebulizing, 2400s declouding, 900s decontamination), mice were transferred back into their cages.

On day 1 post-challenge, *Mtb* CFUs were assessed in whole lungs from groups of female and male mice, in order to confirm that the infection dose is within expected range. Following

infection all mice were clinically scored until the experiment end-point or at score of 3.5 (using the criteria (Table 4) which takes into account activity, body weight, general condition and behavior), whichever was earlier – when they were euthanized.

4.2.4. Observational study/survival post *Mtb* challenge

For the observational study vaccinated *Mtb*-challenged female and male mice, with unvaccinated controls were observed until they reached a clinical score of 3.5 (Table 4) and humanely sacrificed. Lungs of mice intended for evaluation were perfused and harvested in 4% PFA, fixed for at least 24 hours and moved out of BSL-3 following sterility protocols for Hematoxylin and Eosin staining.

Table 4 - Clinical scoring of *Mtb* infected mice

Score	Activity	Reduction in body weight	Condition of mouse	Behavior
1	Very active	No reduction	Shiny and groomed fur; clear eyes; clean body orifices	Normal
2	Active	Less than 10%	Fur defects (less or excessive grooming)	Mild deviations
3	Less active	10-20%	Dull/greasy and ruffled fur, decreased grooming, body orifices not well cleaned, increased muscle tone	Unusual; impaired motor functions or hyperkinetic
4	Barely active	20-30%	Dirty fur; sticky or damp body orifices; hunched; high muscle tone; dull eyes	Isolation from peers; lethargy; hyperkinetic; stereotypies; coordinative dysfunctions
5	Lethargic	Greater than 30%	Cramps; paralysis (trunk musculature, limbs); respiratory sounds; cold body	Vocalization of pain when grabbing; self-amputation (auto-aggressive behavior)

Clinical score per mouse is calculated by taking the mean of the scores of all 4 parameters.

4.3 Organ harvest and preparation of single-cell suspensions

4.3.1. Lymph Node (LN)

Mice were sacrificed in CO_2/O_2 and LNs were harvested into ice-cold 2 mL cRPMI. The contents were transferred through a 100 µM cell-sieve into a 50 mL falcon. The LN was squashed using the plunger of a 5 mL syringe maintaining sterile protocols. The remaining cells were washed through the sieve with 10 mL ice-cold PBS into the 50 mL falcon, centrifuged at 1500 rpm for 5 min and the supernatant was discarded. The LN pellet was resuspended in 1 mL RBC lysis buffer and incubated for 1 minute 45 second in room temperature. After the incubation time, 10 mL of cRPMI was added and centrifuged at 1500 rpm for 5 min at 4 °C. The supernatant was discarded and the LN cell pellet was resuspended in 1 mL cRPMI and placed at 4 °C for processing. An aliqot was taken at this time for cell counting where required. Live cells were counted using Vi-cell counter (Beckman Coulter). All procedures were performed in BSL-2 or BSL-3 laboratory as required (respectively for vaccine strain or *Mtb* infected mice).

4.3.2. Spleen

Mice were sacrificed in CO_2/O_2 and spleens were harvested into ice-cold 3 mL cRPMI. The contents were transferred through a 100 µM cell-sieve into a 50 mL falcon. The spleen was squashed using the plunger of a 5 mL syringe maintaining sterile protocols. The remaining cells were washed through the sieve with 10 mL ice-cold PBS into a 50 mL falcon and centrifuged at 1500 rpm for 5 min and the supernatant was discarded. The spleen pellet was resuspended in 2 mL RBC lysis buffer and incubated for 1 minute 45 second in room temperature. After the incubation time, 10 mL of cRPMI was added and centrifuged at 1500 rpm for 5 min at 4 °C. The supernatant was discarded and the spleen cell pellet was resuspended in 1 mL cRPMI, transferred once more through a 100 µL cell-sieve into a 50 mL falcon and placed at 4 °C for processing. An aliqot was taken at this time for cell counting where required. Live cells were counted either using Vi-cell counter (Beckman Coulter). All procedures were performed in BSL-2 or BSL-3 conditions as required (respectively for vaccine strains or *Mtb* infected mice).

4.4. Immunological methods

4.4.1. *Ex-vivo* restimulation of lymph nodes (LNs) and spleen using *Mtb* whole-cell lysate

Cell pellets of either LN, lungs or spleen (obtained by centrifugation of single-cell suspensions at 1500 rpm for 5 min at 4 °C) were resuspended in PBS at room temperature such that 1 mL of resuspension would contain $2x10^6$ cells. Cell proliferation dye (CellTrace™ Violet, Thermo

Fisher Scientific) was reconstituted in 20 µL DMSO (provided with the proliferation kit) to give a final concentration of 2.5 mM. The reconstituted proliferation dye was then added to the resuspended cells in PBS, calculating 0.5 mL of the proliferation dye for every 1 mL of cell pellet resuspension, in a 50 mL falcon. It was incubated at 37 °C for 20 minutes. An unstained control was kept to correct for background fluorescence for the initialization of fluorescence cytometry measurements. After incubation, 10 mL PBS with 5% Fetal calf serum was added and it was centrifuged at 1500 rpm for 5 min at 4 °C and the supernatant was discarded. The washing step was repeated once more. The cell proliferation dye tagged cell pellet was resuspended in cRMPI such that 150 µL would have 10^5 cells. The cells were plated in 96 well round-bottom plates, 150 µL per well. The wells are prepared with 50µL of cRMPI (control), ConA (2.5µg/mL) or *Mtb* lysate (50µg/mL), as necessary. The cells are then incubated for 96 hours at 37 °C in an incubator with 5% CO_2.

4.4.2. Fluorescence cytometry-based cell proliferation study

Following 96 hours of incubation, the wells are checked in light microscope and harvested in cRPMI for fluorescence cytometry staining. Briefly, the media in 96 well plates are resuspended to dislodge the cells. It was then centrifuged at 1500 rpm at 4 °C for 5 mins. The supernatant was discarded. The pellet was resuspended in block buffer 50µL/well, incubated for 30 minutes at 4 °C in dark and centrifuged as previously. The supernatant was discarded and the 50µL of antibody-mix (Table 5) were added to the wells, resuspended and incubated for 30 minutes in dark at 4 °C. Then, 180 µL of FACS buffer was added to each well, resuspended, and centrifuged as above. The supernatant was discarded and the cells were fixed in 100 µL of 4% PFA for 1 hour at 4 °C. The cells were again resuspended, centrifuged as previously, and the supernatant is discarded. The cell pellets were washed twice with 200 µL FACS buffer before finally resuspending them in 200 µL FACS buffer, until fluorescence cytometry measurement. All steps were performed in sterile conditions following BSL-2 guidelines (necessary for BCG and BCGΔBCG1419c vaccine strains) and in dark as necessary for proliferation dye and antibody staining. Measurements were performed in BD® LSR II Flow Cytometer (BD Biosciences, USA).

Table 5 - Fluorescent cytometry antibodies and dilutions

Antibody	Clone	Company	Dilution
CD4 PE	RM4-5	BioLegend	1:400
CD8a FITC	53-6.7	BioLegend	1:400
B220 PE Cy7	RA3-6B2	BD Biosciences	1:160
CD90.2 APC	53-2.1	eBioscience	1:2500

4.4.3. *Mtb* specific ELISA

To determine *Mtb*-specific Immunoglobulin (Ig), ELISA plates were coated with *Mtb* whole-cell lysate (20 µg/mL; BEI Resources) at 37°C for 1 hour. The coated plates were blocked with 3% BSA in Tris-buffered saline (TBS) at 4°C overnight. After washing with TBS + 0.1% Tween 20, lung homogenates were added (1:25 dilution in PBS), and the plates were incubated at 37°C for 1 hour. Alkaline Phosphatase-conjugated anti-mouse IgG, IgA, IgM, IgG2a (1:1000 in TBS/1% Bovine Serum Albumin) were added, and the plates were incubated at 37°C for 1 hour. Wells were developed in pNitrophenylphosphate for 20 min at room temperature and stopped by the addition of 1 N NaOH. Absorbance was measured at 405 nm.

4.5. Histology - Hematoxylin and Eosin (H&E) staining

Tissue processing and staining was performed in collaboration with the division of histopathology headed by Prof. Dr. Torsten Goldmann, Research Center Borstel. H&E stain was performed in automatic stainer operated by the division of histopathology. In brief, lungs were fixed in 4% PFA for 24 hours and embedded in paraffin. They were sectioned at 4µm thickness and continued for H&E staining (Table 6).

Table 6 – steps of H&E staining in automatic stainer

	Solution	Incubation time
Step 1	Xylol	1 minute
Step 2	Xylol	1 minute
Step 3	100% Alcohol	1 minute
Step 4	96% Alcohol	1 minute
Step 5	70% Alcohol	1 minute
Step 6	Distilled water	1 minute
Step 7	Haematoxylin (Mayer)	3 minutes
Step 8	Haematoxylin (Mayer)	3 minutes
Step 9	Wash in tap water	1 minute
Step 10	1% Calcium acetate solution	1 minute
Step 11	Wash in tap water	1 minute
Step 12	0.2% Eosin	2 minutes
Step 13	80% Alcohol	15 seconds
Step 14	96% Alcohol	30 seconds
Step 15	100% Alcohol	1 minute
Step 16	100% Alcohol	1 minute
Step 17	Xylol	1 minute
Step 18	Xylol	1 minute

Slides were imaged with BX41 light microscope and cell^B software. The quantitative analysis of lymphoid aggregates was conducted using the software QuPath (open-source platform)[236].

4.6. Data analysis and software

Statistical analysis was performed in GraphPad Prism version 10. Data was checked for normal distribution where necessary. Principal component analysis (PCA) and high-variance feature extraction was performed in BioVinci (version 3.0.9, BioTuring). Histology image quantification was performed in QuPath (open-source)[236]. Fluorescence cytometry data was acquired using FACSDiva™ version 6.0 and was analyzed, including unified manifold approximation and projection (UMAP), in FCS Express version 7 (DeNovo Software). Biorender (Science Suite Inc) was used to create Figure 6 (from data figures obtained from respective analytical tools). Microsoft Word 2016 (Microsoft corporation) was used to write thesis. Digital image

subtraction and superimposition, as well as digital subtraction of superimposed female and male proliferations (to identify proliferating populations unique to each sex) was carried out in Python – code is provided in the supplement (Suppl. Code S3 and Suppl. Code S4, respectively).

5. Results

TB is a disease that disproportionately affects males, with males at least about twice as likely as females to develop active TB[11,27]. The only approved vaccine for TB, BCG, remains variable in its efficacy – leading to the development of several vaccine candidates, including those derived from BCG, which are currently in various stages of development[113,120,160,213,237]. Although sex differences in TB itself have been increasingly described[27,48,105,174], the influence of biological sex on BCG efficacy has been scarcely explored. Here, in my PhD project, the influence of biological sex on the protective efficacy of BCG against TB – as well as the ability of newer recombinant derivatives of BCG to ameliorate any potential male specific vulnerability in BCG efficacy is investigated.

5.1. Sex of the individual determine the protective efficacy of vaccination against TB in C57BL/6 mice

In order to establish the role of biologic sex in vaccine mediated immune responses against TB and in the protective effect of different vaccine (candidates), groups of female and male C57BL/6 mice were vaccinated with BCG and two recombinant derivatives of BCG – VPM1002 and BCGΔBCG1419c. VPM1002 and BCGΔBCG1419c are also referred to as recombinant Bacillus Calmette-Guérin (rBCG). 90 days post-vaccination, they were challenged with *Mtb* strain HN878, a virulent strain of *Mtb*, and their disease progression was observed (Figure 1A). Mice reaching the pre-defined humane end-point were sacrificed and the time-point was recorded as the end point of survival for that individual mouse.

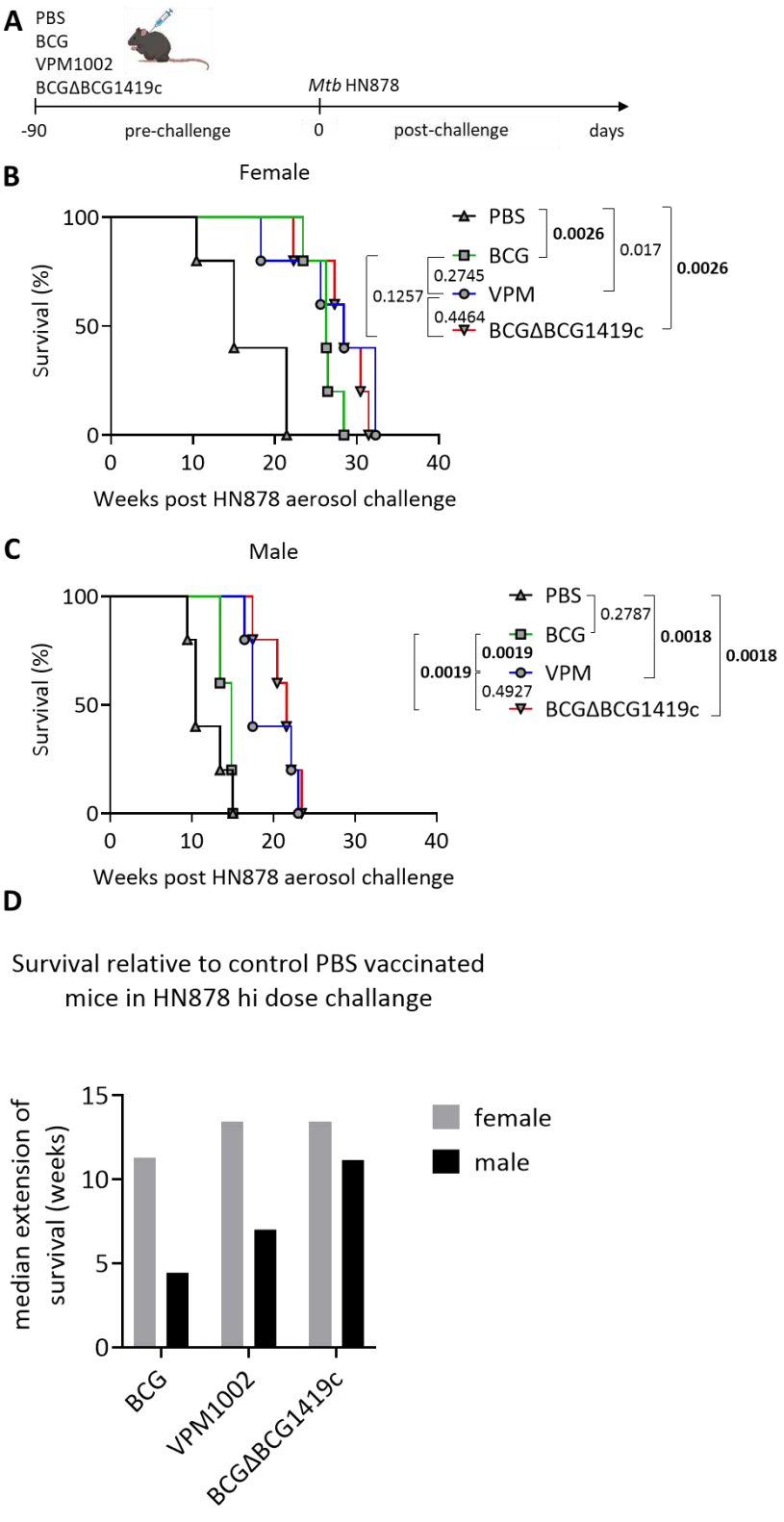

Figure 1: Survival of vaccinated female and male mice after *Mtb* HN878 aerosol challenge. A) Experimental outline: Male and female C57BL/6 mice were vaccinated s.c. with 10^6 CFUs of BCG, VPM1002, BCGΔBCG1419c, or PBS only (unvaccinated control), respectively, and challenged with HN878 via the aerosol route 90 days later. Survival of females **B)** or males **C)** post HN878 challenge. **D)** The median extension of survival in weeks offered by each vaccine after *Mtb* challenge relative to unvaccinated controls (sex matched PBS group). n = 5 mice per group of 1 experiment; Log-Rank test was performed sex-wise to compare each vaccine group against each other, with Bonferroni correction for error inflation due to multiple testing. Corrected p value threshold for significance is 0.0083 (data A, B, C from preprint Harikumar Parvathy et.al., 2024[238]).

Male mice vaccinated with BCG show no significant difference in survival over PBS, while female mice are significantly protected. BCG vaccination – the only vaccine approved for clinical use, which has been in use for over 100 years[107,239] – demonstrates a male specific vulnerability in its protective efficacy. Next, the protective efficacy of newer recombinant variations of BCG were compared in order to observe if the male specific vulnerability of BCG was maintained for these rBCGs or whether rBCGs offer enhanced protection against *Mtb* challenge. rBCGs demonstrated a significant protective efficacy in males, in contrast to the inefficacy of BCG, over the PBS control group as well as the BCG vaccinated males. In females, however, rBCGs did not significantly improve protection over BCG in survival (Figure 1B and 1C). Overall, although females have higher median extension of survival than males relative to the survival of sex-matched PBS controls in all groups analyzed (Figure 1D), rBCGs partially ameliorate the male specific vulnerability of BCG vaccine mediated protection, with BCGΔBCG1419c demonstrating the best efficacy in terms of median survival. However, the survival differences between VPM1002 and BCGΔBCG1419c vaccinated groups do not reach statistical significance either for females or males – and both of the rBCGs offered enhanced protection over BCG in males.

Next, it was sought to determine whether the differences in survival upon vaccination between females and males, as well as, between different vaccine candidates correspond to differences in actual bacterial loads following aerosol infection challenge. For this purpose, groups of female and male mice were vaccinated with BCG, VPM1002 and BCGΔBCG1419c. 90 days later, they were challenged with *Mtb* HN878 via the natural aerosol route of infection and their lung and spleen CFUs were analyzed at days 28 and 77 post aerosol *Mtb* challenge.

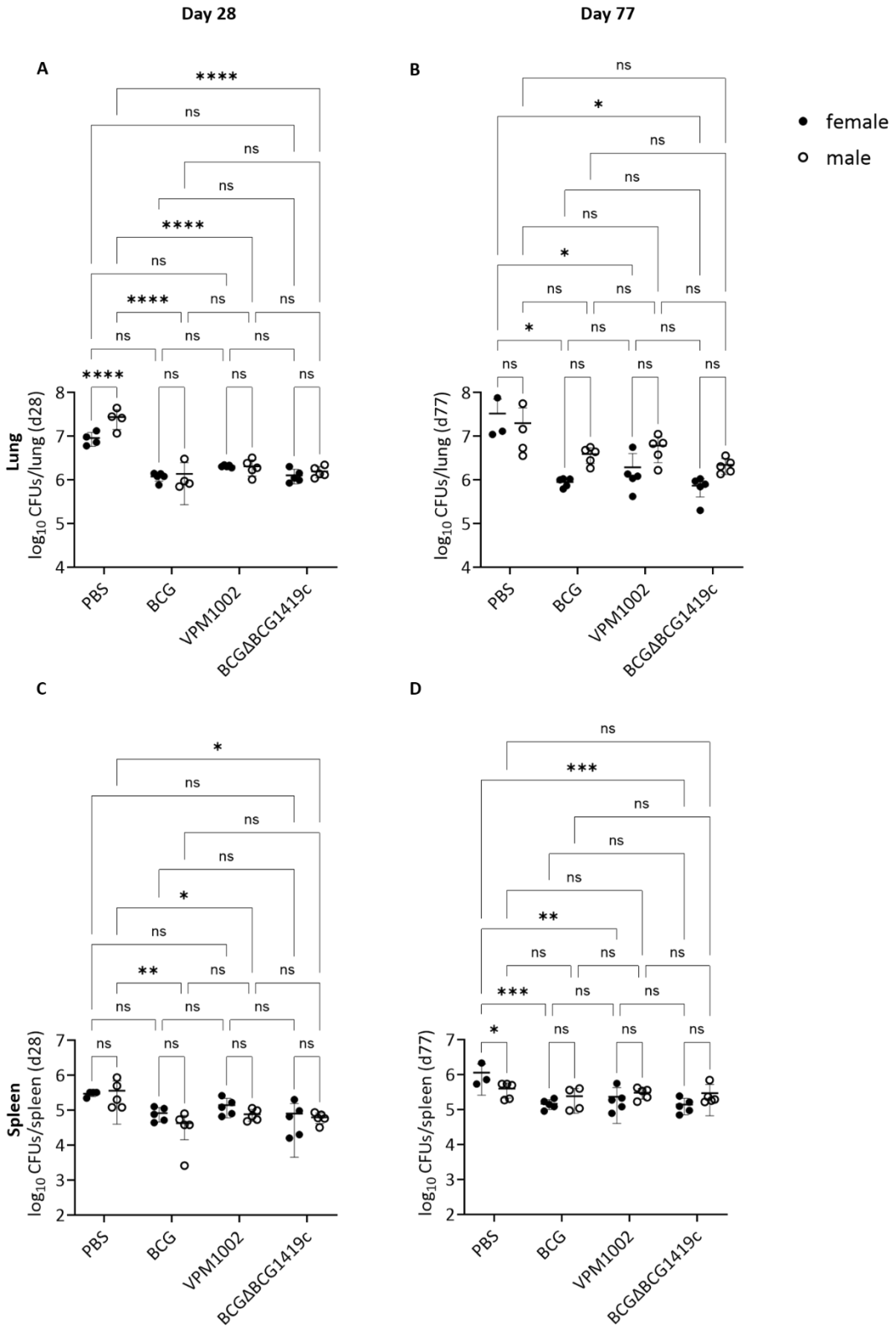

Figure 2: Lung and spleen CFUs following *Mtb* HN878 aerosol infection challenge after vaccination. Female and male C57BL/6 mice were vaccinated s.c. with 10^6 CFUs of BCG, VPM1002, or BCGΔBCG1419c, respectively, and *Mtb* HN878 CFUs were determined in lungs and spleen at days 28 **(A and C)** and 77 **(B and D)** following aerosol *Mtb* challenge (n = 3-5 mice per group of 1 experiment). Two-way ANOVA with Tukey's multiple comparison test with adjusted p values *p ≤ 0.05; **p ≤ 0.01; ***p ≤ 0.001; ****p ≤ 0.0001. Error bars represent SD from Mean (data from preprint Harikumar Parvathy et.al., 2024[238]).

At 28 days post *Mtb* infection challenge, the mean CFUs in lung were decreased in vaccinated male and female mice compared to PBS mice, for all vaccinated groups irrespective of vaccine choice – although these differences were only significant for males, possibly due to higher CFUs in PBS males as compared to PBS females (Figure 2A). No significant differences among sex-matched individual vaccine groups or between females and males of any vaccinated group was observed at this time-point. Likewise, males had a significant decrease in their CFUs following vaccination in the spleen (Figure 2C), although here no significant differences were observed between PBS females and males. Similar to lung CFUs at day 28 post *Mtb* infection challenge, there were no significant differences among sex-matched individual vaccine groups or between sexes for any one vaccine candidate at this time-point in spleen.

At day 77 after *Mtb* challenge, the reduction in CFUs by vaccination was less pronounced in males compared to the earlier time-point and was not statistically significant, in contrast to their female counterparts for both lungs and spleen (Figure 2B and 2D). In spleen, PBS control males had significantly reduced *Mtb* CFUs compared to PBS control females at day 77 after *Mtb* challenge. However, *Mtb* CFUs showed no significant difference between sexes for any vaccinated group or among sex-matched individual vaccine groups.

That is, no significant difference in *Mtb* CFUs among the various vaccines tested were observed, either among sex-matched individual vaccine groups themselves or between sexes for any particular vaccine for both time-points. However, particular vaccinated groups showed significant reduction in CFUs compared to PBS controls at various time-points.

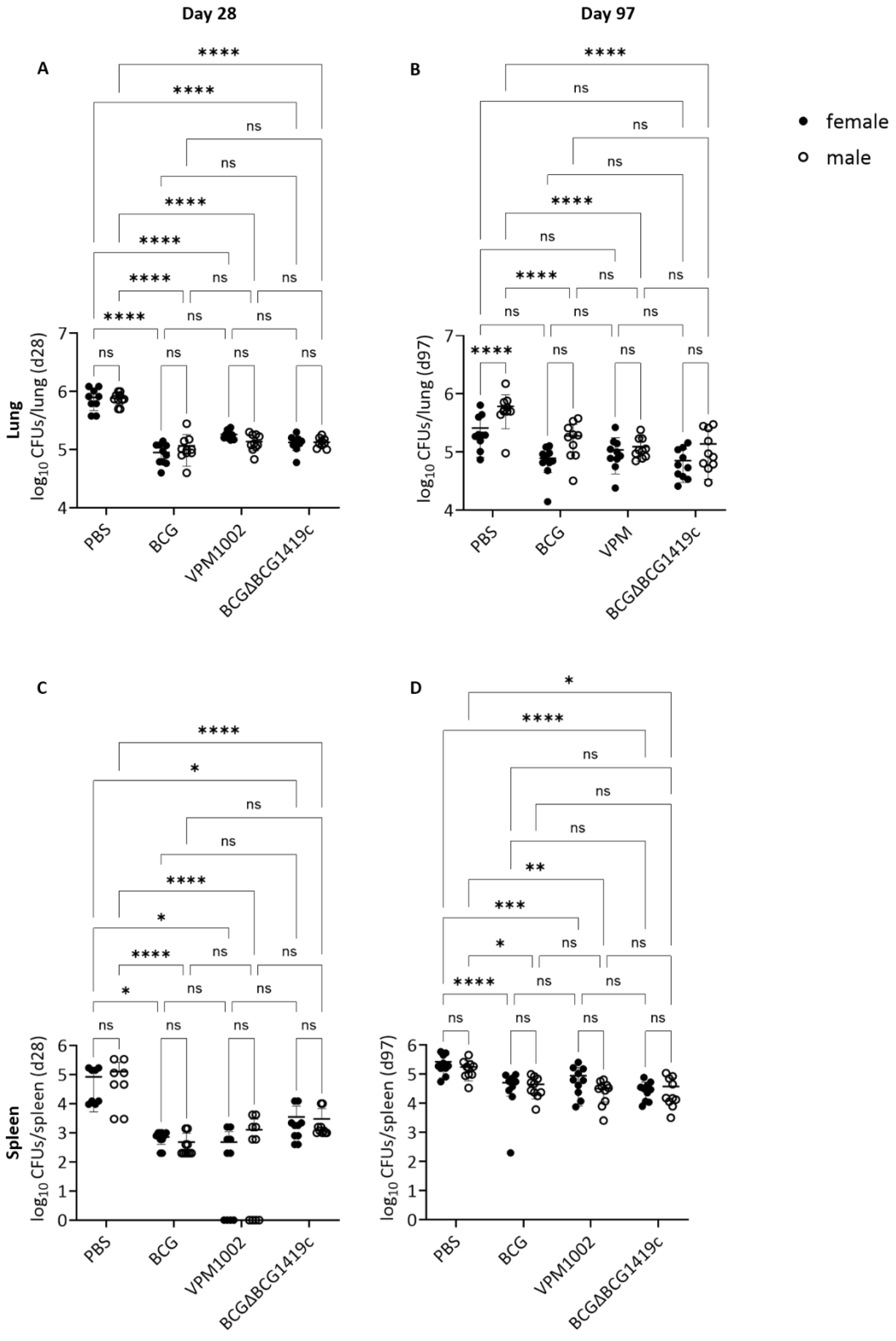

Figure 3: Lung and spleen CFUs following *Mtb* H37Rv aerosol infection challenge after vaccination. Female and male C57BL/6 mice were vaccinated s.c. with 10^6 CFUs of BCG, VPM1002, or BCGΔBCG1419c, respectively, and *Mtb* H37Rv CFUs were determined in lung and spleen at days 28 **(A and C)** and 97 **(B and D)** following aerosol *Mtb* H37Rv challenge (n = 8-10 mice per group; data pooled from 2 experiments). Two-way ANOVA with Tukey's multiple comparison test with adjusted p values *p ≤ 0.05; **p ≤ 0.01; ***p ≤ 0.001; ****p ≤ 0.0001; ns – not significant. Error bars represent SD from mean (data from preprint Harikumar Parvathy et.al., 2024[238]).

Previously published data has shown TB pathology may not be directly associated with bacterial loads – which has been confirmed at least in the case of BCGΔBCG1419c in a previous study[113,240]. Nevertheless, it was sought to confirm the findings obtained with *Mtb* HN878 strain with a different, H37Rv strain of *Mtb* at a lower dose of infection than used for HN878 strain in the survival observation and CFU studies.

At day 28 post *Mtb* H37Rv challenge, all vaccines significantly reduced lung and spleen CFUs in mice irrespective of sex, relative to PBS controls (Figure 3A and 3C). However, at day 97 post *Mtb* H37Rv challenge, the lung CFUs were significantly reduced only for males, although the mean was reduced for both sexes (Figure 3B). This might be due to the significantly higher lung CFUs in PBS male controls relative to female control mice at day 97 post-H37Rv challenge. At day 97, spleen CFUs showed significant reduction for both sexes for all vaccine groups, relative to PBS controls (Figure 3D). The dramatic reductions seen in the CFUs of spleen for a subpopulation of VPM1002 vaccinated mice at day 28 is not replicated at the later time-point of day 97 post-H37Rv challenge. However, lung and spleen H37Rv CFUs at days 28 and 97 post *Mtb* challenge of vaccinated mice demonstrated no significant differences between females and males of any particular vaccinated group or among different sex-matched vaccinated groups relative to each other.

Thus, these results demonstrate that the absence of significant difference in *Mtb* CFUs between sexes for any particular vaccine candidate or among sex-matched groups of vaccinated mice themselves is not unique to one particular strain of *Mtb*. Therefore, it was speculated that the strong differences in survival which have been identified between rBCGs and BCG vaccinated males upon *Mtb* HN878 infection challenge should, at least partially be, associated with specific differences in the host response to vaccination aiding in disease control and the immune-pathology of *Mtb* infection (following vaccination) – and not overwhelmingly associated with *Mtb* load in lungs and spleen at the time-points tested.

Results 5.1. Summary:

1. In contrast to females, BCG vaccination offers no protection in males over PBS controls following *Mtb* challenge – demonstrating its male specific vulnerability.

2. The two rBCGs – VPM1002 and BCGΔBCG1419c – provide significantly improved survival advantage in males, over both PBS controls as well as BCG vaccination.

3. Lung and spleen bacterial loads following *Mtb* challenge neither show significant differences between sexes of any vaccinated group nor among sex-matched vaccinated groups themselves.

5.2. Histology of lungs from the survival group shows increased organization of lymphoid aggregates in BCGΔBCG1419c vaccinated males following *Mtb* challenge relative to PBS control

To better understand the effect of BCGΔBCG1419c in male mice, which is the best performing vaccine in males in terms of median survival post *Mtb* challenge, those lungs which were available from certain mouse groups following the survival study were processed for Hematoxylin and Eosin (H&E) staining and the area of organized lymphoid aggregates were quantified using QuPath[236] – an open-source platform for image analysis. The lymphoid aggregates were identified as clusters of small cells with intense hematoxylin-stained nucleus having a thin rim of cytoplasm. BCGΔBCG1419c vaccine candidate was chosen to represent the rBCGs as it demonstrated the highest median survival for males, although it was not statistically significant over VPM1002 vaccinated males. Because lungs were harvested at the humane endpoint of each individual mouse, they were very comparable in their disease severity at the time of harvest. Therefore, the differences in the area of organized lymphoid aggregates in the lungs, identified by their morphology in H&E staining and as has been previously described in the lungs of *Mtb* infected mice for its role in controlling lung infections including TB[48,241,242], is unlikely to be due to differences in overall disease stages at the time of harvest.

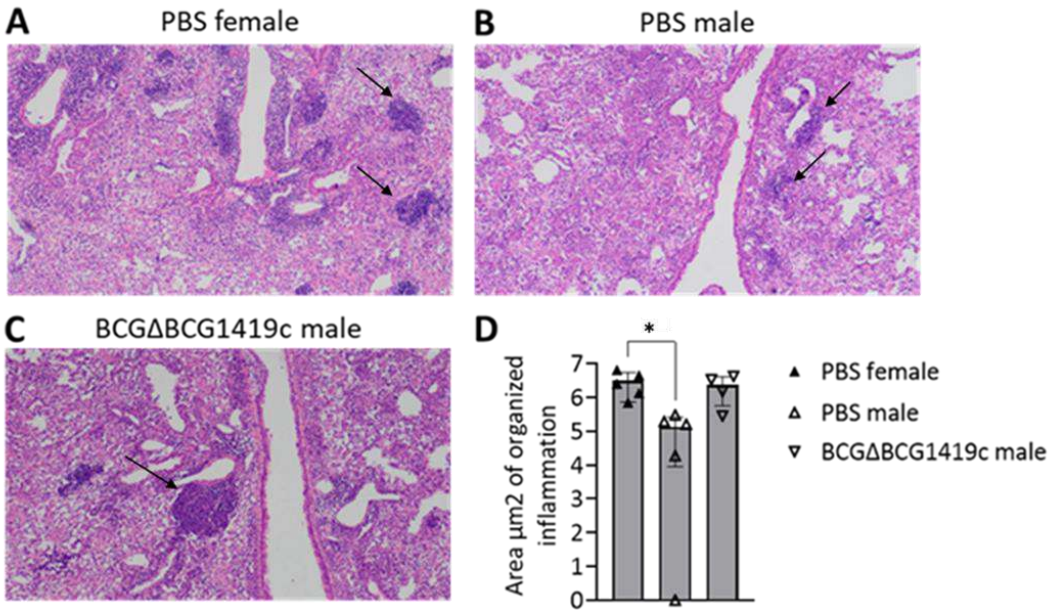

Figure 4: Hematoxylin and Eosin staining of lung sections following survival study. Female and male C57BL/6 mice were vaccinated s.c. with either PBS or 10^6 CFUs of BCGΔBCG1419c (available for male mice only) and challenged with HN878 strain of *Mtb*. At their humane endpoints, their lungs were processed for histology. **A)-C)** Shows representative images of staining from lung sections as indicated **D)** Their area of organized (lymphoid) aggregates, mean of 4 random areas from lung section representing each mouse, were quantified in QuPath open-source software (n = 4-5 mice per group of 1 experiment). Area is represented in log scale. One-way ANOVA with Tukey's multiple comparison test with adjusted p values *p ≤ 0.05; **p ≤ 0.01; ***p ≤ 0.001; ****p ≤ 0.0001. Error bars represent SD from mean (data from preprint Harikumar Parvathy et.al., 2024[238]).

In control mice, it was observed that females had significantly greater area of organized lymphoid aggregates as compared to unvaccinated males (Figure 4A and 4B), in line with increased median survival of PBS vaccinated females relative to their male counterparts in the survival study. Formation of lymphoid aggregates in lung has been shown to have a positive association with disease outcome in recent studies of TB as well as at other sites for chronic diseases such as cancer[48,104,241–243]. Vaccination of male mice with BCGΔBCG1419c was associated with an increase in the area of organized lymphoid aggregates compared to unvaccinated males (Figure 4C). Although, this increase per se was not significant, it made BCGΔBCG1419c vaccinated group of males comparable to their female counterparts (Figure 4D) and overcame the significant reduction in area of organized lymphoid aggregates observed in unvaccinated males relative to unvaccinated females.

Results 5.2. Summary:

1. Without vaccination, male mice have significantly decreased area of organized lymphoid aggregates as compared to females.

2. BCGΔBCG1419c vaccination in male mice results in an increase in area of organized lymphoid aggregates, now becoming comparable to unvaccinated females.

5.3. The vaccine strain proliferation in draining lymph nodes (LNs) show a sex and vaccine specific pattern

Because BCG and its recombinant derivatives are live vaccines, they proliferate in the draining LNs and spleen post-vaccination. It has been speculated that some degree of vaccine strain proliferation is required for its efficacy. Nevertheless, the nature of relationship between vaccine strain proliferation and protection remains very vague. Further the sex specific nature of this relationship has never been explored in a resistant model of TB, to the best of my knowledge. This is also true for the recombinant derivatives of BCG. Therefore, it was proposed to delineate the influence of sex on vaccine strain proliferation of BCG and the two rBCGs.

For this purpose, groups of female and male mice were vaccinated either with BCG, VPM1002 or BCGΔBCG1419c vaccine candidates. At different time-points the draining LNs were harvested and plated independently. Because the vaccination was administered on the scruff of the neck, visually the cervical LNs were the ones most consistently enlarged at day 7 and 14 following vaccination from among the cervical, mandibular and axillary groups of LNs observed visually. Therefore, the cervical group of LNs were primarily considered as the draining LNs in this vaccine model, used for the current study.

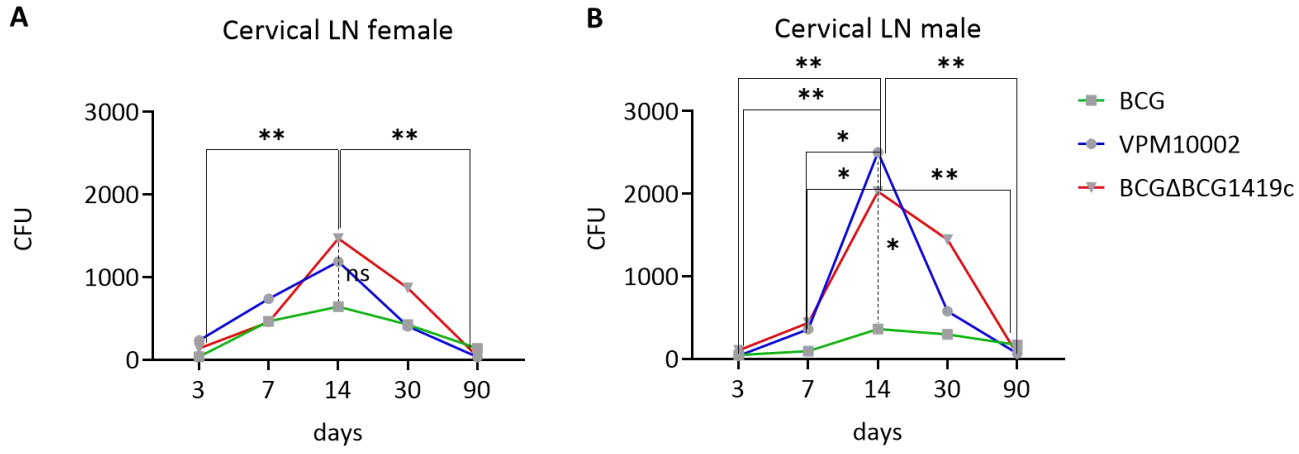

Figure 5: Time-kinetics of vaccine strain CFUs in female and male cervical lymph nodes. Female **A)** and male **B)** C57BL/6 mice were vaccinated s.c. with 10^6 CFUs of BCG, VPM1002, or BCGΔBCG1419c, respectively, and CFUs in cervical LN were determined at various time-points post-vaccination (n = 4-8 mice per group from 2 experiments). Two-way ANOVA with Tukey's multiple comparison test with adjusted p values *p ≤ 0.05; **p ≤ 0.01; ***p ≤ 0.001; ****p ≤ 0.0001; ns – not significant (data from preprint Harikumar Parvathy et.al., 2024[238]).

The vaccine strain CFUs peaked at day 14 post-vaccination, in both females and males (Figure 5A and 5B). In females, the vaccine CFUs among BCG, VPM1002 and BCGΔBCG1419c show no remarkable differences in their peaking at day 14 post-vaccination. However, in males, VPM1002 and BCGΔBCG1419c show a much higher mean peak at day 14 compared to BCG. This corresponds to the survival advantage offered by VPM1002 and BCGΔBCG1419c specifically in males following *Mtb* challenge as described in the earlier section.

Result 5.3. Summary:

1. Vaccine strain CFUs, peaking at day 14 in both sexes, shows sex specific variability.
2. VPM1002 and BCGΔBCG1419c show higher mean peaks as compared to BCG in males. No such difference is observed in females.

5.4. Specific proliferative responses following vaccination correlate with enhanced protection during *Mtb* infection

It was hypothesized that especially in the late time-point following vaccination, when the LN vaccine strain CFUs have approached zero, restimulation with *Mtb* whole-cell lysate would trigger proliferation of memory B and/or T cells. Among them, CD8 T cells have a well-defined role in containing TB as delineated by multiple studies over the years [114,123,199,200,244], with an acknowledged role for CD4 T cells[205,245] and an ever-increasing appreciation of the role of B cells[104,246]. CD8 T cell responses have also been implicated in the efficacy of BCGΔBCG1419c[114] as well as that of VPM1002[111,120]. As such, it was sought to determine if those responses show a sex specific difference in BCG (which performs poorly in males) and rBCGs. For the following experiments BCGΔBCG1419c was used as a representative of rBCGs.

Groups of female and male mice were vaccinated either with BCG or BCGΔBCG1419c along with PBS controls (Figure 6). At days 28 and 90 following vaccination, their draining LNs were harvested and was made into single-cell suspensions, tagged with CellTrace™ Violet (a proliferation marker) and the co-culture of the draining LNs was restimulated with *Mtb* whole-cell lysate *ex-vivo*. The co-culture provides a platform to form aggregates of B and T cells as well. After 96 hours of restimulation, when such aggregates could also be routinely visualized by light microscopy, the cells were harvested and stained with markers for B and T cells. The proliferation patterns of B, CD4 T and CD8 T cells across PBS, BCG and BCGΔBCG1419c vaccinated groups for both sexes were analyzed by fluorescence cytometry (gating strategy in Suppl. Fig. S1).

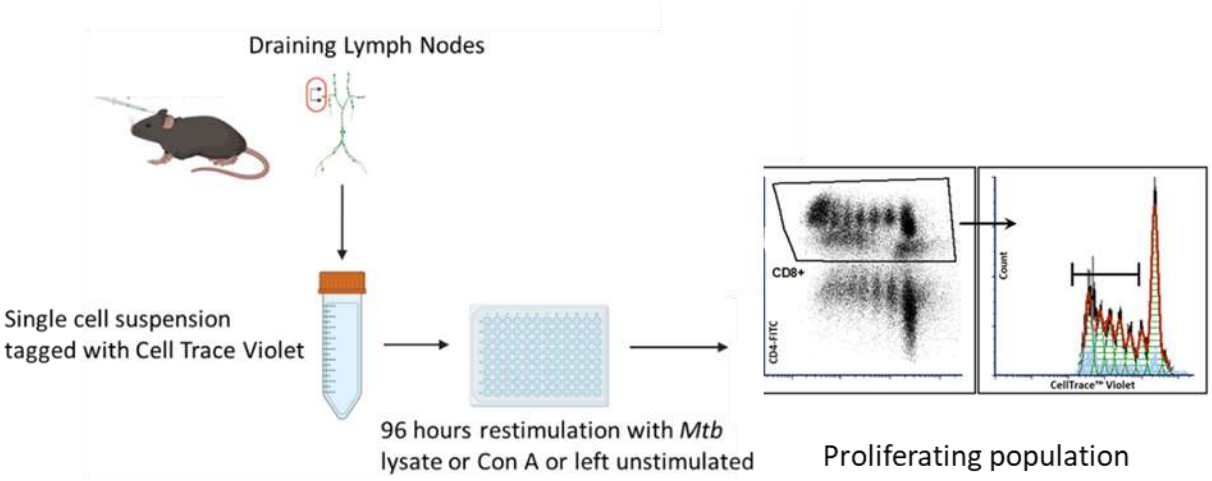

Figure 6: Schema of proliferation study of draining lymph nodes following vaccination. Draining lymph nodes from female and male mice s.c. vaccinated with either 10^6 CFUs of BCG or BCGΔBCG1419c (representing rBCG), along with PBS controls were harvested, tagged with CellTrace™ Violet and restimulated *ex-vivo* with *Mtb* whole-cell lysate for 96 hours. Negative control of proliferation is unstimulated sample and positive control of proliferation is ConA.

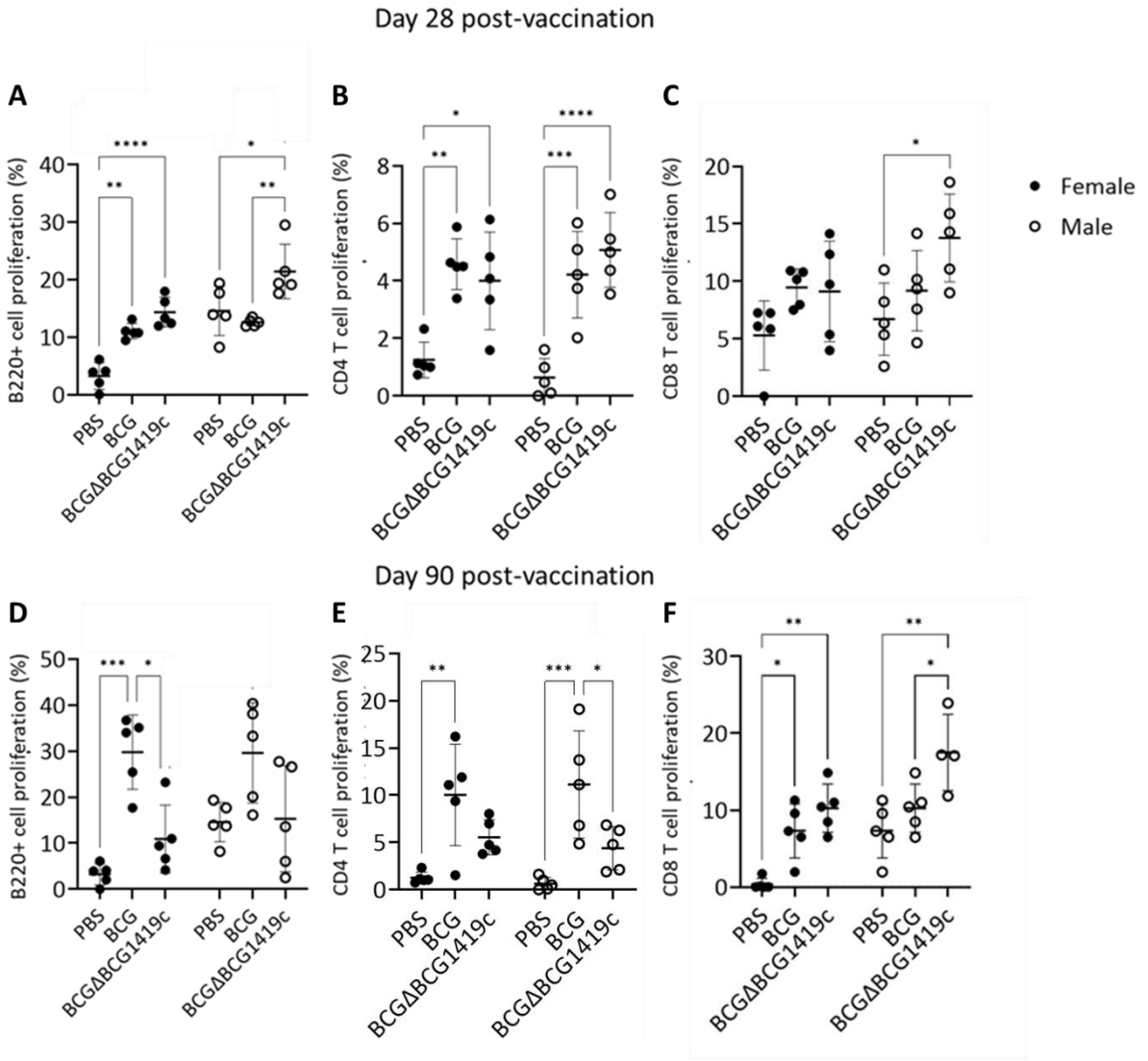

Figure 7: Lymph node T and B cell proliferation in response to *ex-vivo* restimulation with *Mtb* whole-cell lysate. Single-cell suspensions of lymph nodes at days 28 and 90 post-vaccination were restimulated with *Mtb* whole-cell lysate for 96 hours and stained for CD8 T, CD4 T and B cells (gating strategy Suppl. Fig. S1). Proliferating populations were measured by fluorescence cytometry. **A)** B220+ B cell **B)** CD4+ T cell and **C)** CD8+ T cell proliferations at day 28 post-vaccination. Corresponding data at day 90 post-vaccination are shown in **D)**, **E)** and **F)**. Data are shown as mean ± SD (n = 4-5, from 1 of 2 experiments). *p ≤ 0.05; **p ≤ 0.01; ***p ≤ 0.001; ****p ≤ 0.0001 determined by 2-way ANOVA followed by Tukey's multiple-comparison test. Sex-wise significant differences are shown for comparison (data from Harikumar Parvathy et.al., 2024[238]).

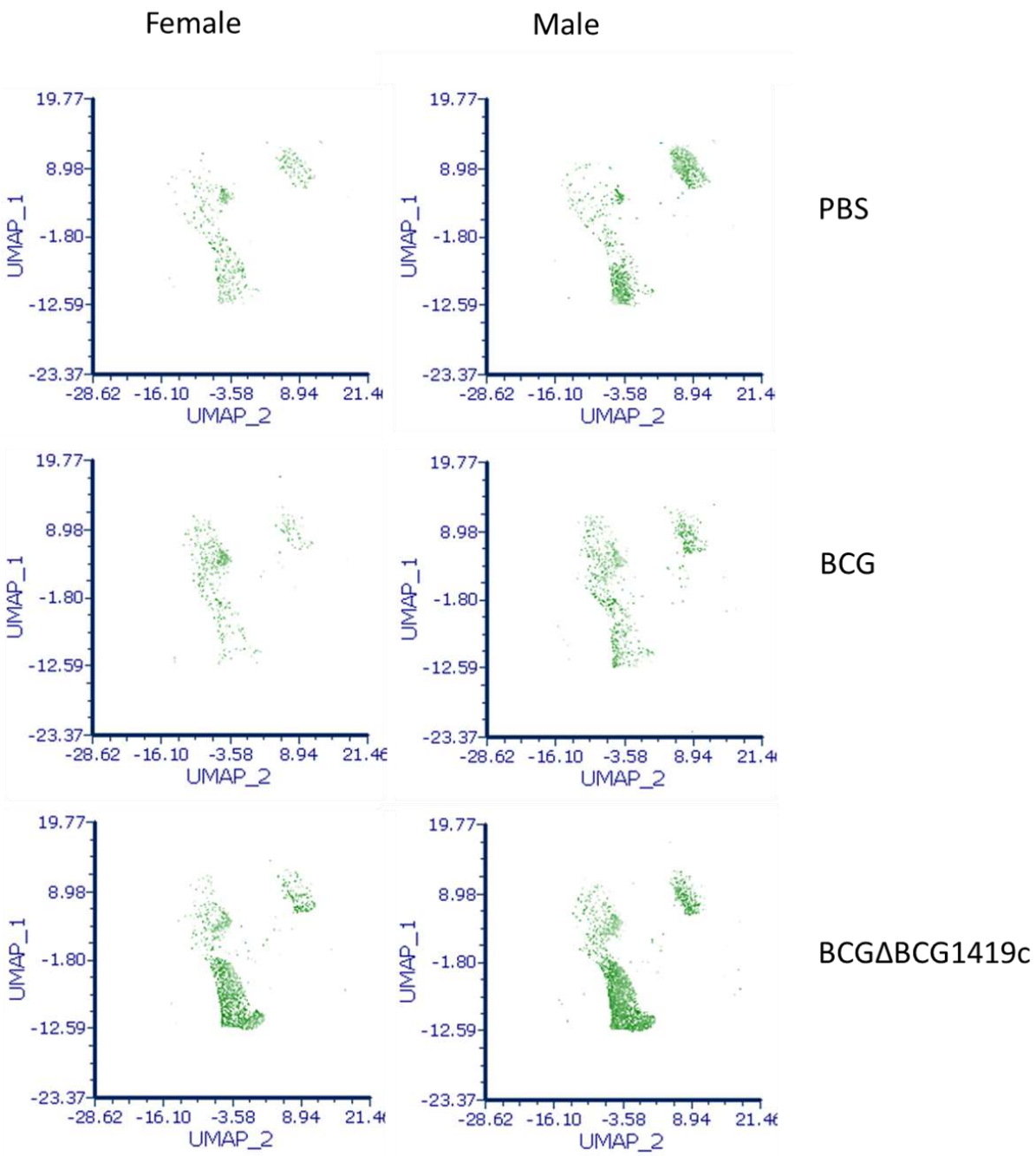

Figure 8: UMAP visualization of CD8 T cell proliferative response at day 90 following vaccination. Female and male C57BL/6 mice were vaccinated s.c. with 10^6 CFUs of BCG or BCGΔBCG1419c, respectively, and T and B cell proliferative responses to *ex-vivo* restimulation with *Mtb* whole-cell lysate were determined at day 90 post-vaccination, measured by fluorescence cytometry (n = 9-10 mice per group from 2 experiments for UMAP plots; reanalyzed data from preprint Harikumar Parvathy et.al., 2024[238]).

At day 28 post-vaccination, both BCG and BCGΔBCG1419c demonstrated significantly higher CD4 T cell proliferative response in both females and males over PBS controls, with BCGΔBCG1419c showing a greater mean increase and significance than BCG, specifically in males (females p value 0.0021 for BCG and 0.0138 for BCGΔBCG1419c; male p value 0.0009 for BCG and less than 0.0001 for BCGΔBCG1419c; Figure 7B). B cell proliferation also showed

significant increase for both sexes over PBS controls except for BCG males, with BCGΔBCG1419c demonstrating the highest mean increase for both sexes (female p value 0.0053 for BCG and less than 0.0001 for BCGΔBCG1419c; male p value 0.8939 for BCG and 0.0172 for BCGΔBCG1419c; Figure 7A). In addition, B cell proliferation in BCGΔBCG1419c vaccinated males were significantly higher relative to their BCG vaccinated male counterparts (p value 0.0013).

At day 28 post-vaccination, CD8 T cell proliferation remained non-significant over baseline PBS controls, except for BCGΔBCG1419c vaccinated males (p value 0.0296; Figure 7C) – where it started to increase significantly over PBS controls - the increase became even more statistically significant at day 90. However, there was no significant difference in CD8 T cell proliferation between BCG and BCGΔBCG1419c vaccinated males at this time-point.

At day 90 post-vaccination, CD4 T cell and B cell proliferation in BCGΔBCG1419c group showed no significant difference over PBS group for both sexes, while for BCG they both showed significant increase over PBS at this time-point (p value CD4 T female 0.0056, CD4 T male 0.0016 and B cell female 0.0003; Figure 7D and 7E) except for B cell proliferation in BCG males, where the higher mean did not reach significance over PBS group (p value 0.0710). Female mice demonstrated remarkable CD8 T cell proliferative response upon *Mtb* whole-cell lysate restimulation for both BCG and BCGΔBCG1419c vaccinated groups (Figure 7F), relative to PBS control group (p value 0.0325 and 0.0012, respectively). In contrast however, in males, BCG group showed no significant increase in CD8 T cell proliferation over PBS controls (p value 0.7314), while BCGΔBCG1419c group showed significant increase in CD8 T cell proliferation relative to both PBS control group and BCG vaccination group (p values 0.0017 and 0.0367, respectively).

Further, visualizing the day 90 post-vaccination data for CD8 T cell proliferation in unified manifold approximation and projection (UMAP) demonstrated the ability of BCGΔBCG1419c to increase CD8 T cell proliferation upon restimulation with *Mtb* whole-cell lysate over certain population clusters (Figure 8), although its increase over BCG became significant only for males.

These findings of day 90 CD8 T cell proliferation correspond to the survival study which demonstrates no significant differences between BCG and rBCGs for females, while rBCGs promote a significant male specific improvement in survival relative to both PBS control group

and BCG vaccination group. These findings are also in agreement with the implicated role of CD8 T cell response in the efficacy of the two newer TB vaccine candidates that were tested as well as a recent study demonstrating the ability of androgens to adversely affect CD8 T cell response in tumors[35,111,114,120,203].

Results 5.4. Summary:

1. At day 28 post-vaccination, both CD4 T cell and B cell proliferation in BCGΔBCG1419c vaccinated males showed a greater mean increase and higher statistical significance, as compared to that of BCG males, over PBS control.

2. BCG vaccinated males – unlike females - have no significant CD8 T cell proliferative response over PBS controls 90 days after vaccination.

3. The deficiency of day 90 post-vaccination CD8 T cell proliferative response of BCG vaccinated males is ameliorated by BCGΔBCG1419c vaccine.

5.5. Integration of multiple datasets using Principal Component Analysis showed grouping patterns mirroring the efficacy profile of vaccines

In order to understand the combined influence of the measured parameters on PBS, BCG and BCGΔBCG1419c vaccinated groups of both sexes, the multi-parametric dataset was combined into Principal Component Analysis (PCA). All data were standardized and integrated into PCA using a machine-learning aided analysis and visualization platform, BioVinci (version 3.0.9, BioTuring).

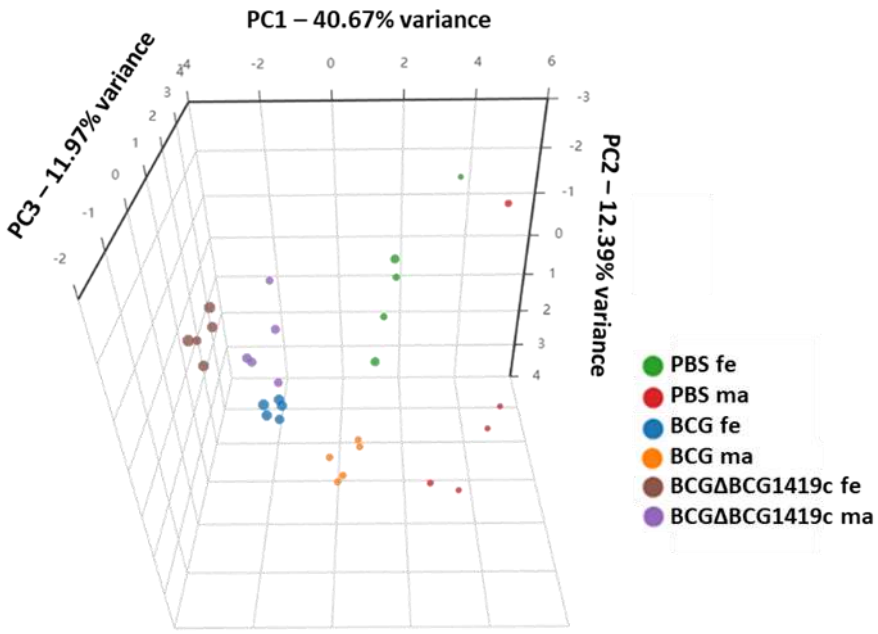

Figure 9: PCA of integrated dataset. Datasets containing *Mtb* CFUs, vaccine strain CFUs, lymph node proliferation data for CD4 T cells, CD8 T cells, B cells, survival data and *Mtb* specific antibody responses post infection challenge (Suppl. Fig. S2) were standardized using the default algorithm in BioVinci and integrated together into a PCA plot (n=5 for each group). PC1, PC2 and PC3 captures 40.67%, 12.39% and 11.97% of the variance respectively. The dot sizes represent survival. fe – females, ma –males (data from preprint Harikumar Parvathy et.al., 2024[238]).

The PCA components 1, 2 and 3 together captured 65.03% of the variance in the datasets. The best performing vaccine groups for each sex – BCG females, BCGΔBCG1419c females and BCGΔBCG1419c males grouped close to each other - with BCGΔBCG1419c females, the best performing group overall, grouping further separately. The rest - PBS females, PBS males, BCG males – all different from each other either in-terms of vaccination status or response to *Mtb* infection including survival post *Mtb* challenge – grouped separately (Figure 9).

Because the PCA grouping also reflected the functional or interventional status of the experimental groups (survival and vaccination, respectively), the top 5 high-variance features

of principal component 1 (PC1) were extracted using BioVinci (as described for PCA). Day 28 post-vaccination CD4 T cell proliferation, day 90 CD8 T cell proliferation, survival post *Mtb* challenge, day 28 post-vaccination B cell proliferation and day 28 lung CFUs following *Mtb* HN878 challenge were identified as the top 5 factors influencing the PCA grouping. Further, a PCA biplot was created to delineate the vectors of these top 5 features (Figure 10). Here, day 28 post-vaccination CD4 T cell and B cell proliferation as well as day 90 post-vaccination CD8 T cell proliferation was identified to be closely associated with survival – with comparable length and direction of these vectors, together with survival, pointing to a positive correlation with each other. Nevertheless, day 28 CD4 T and B cell proliferation vectors, as well as day 90 CD8 T cell proliferation and survival vectors were the pairs most closely associated with each other. The day 28 HN878 lung CFU vector is represented in a different quadrant as that of survival and other top 5 factors, pointing to a largely negative correlation between lung *Mtb* load and survival, as well as between lung *Mtb* CFUs and T and B cell proliferative responses. However, none of their relationships with lung bacterial load reached statistical significance in this model, as will be described later, in line with the findings that *Mtb* CFUs do not significantly differ between various vaccine groups, analyzed sex-wise (Figure 2, Figure 3 and Figure 11 described next).

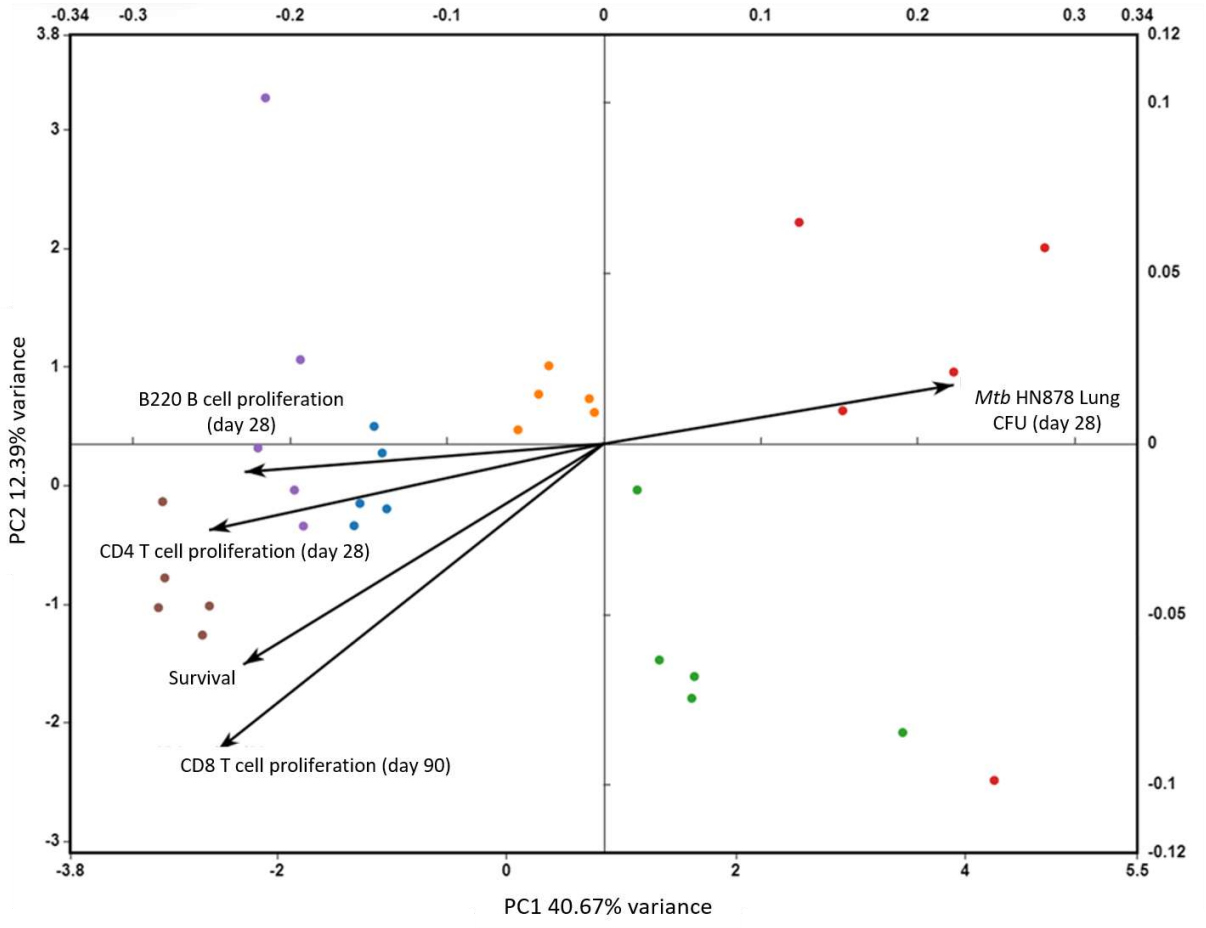

Figure 10: Top 5 high-variance features in PCA. Top 5 high-variance PCA features were delineated using BioVinci, a machine-learning aided analysis platform. Time-points represent days post-vaccination, while survival represent the time taken by the experimental groups challenged with *Mtb* HN878 to reach their humane end-points; effect of all experimental groups are analyzed together (data from preprint Harikumar Parvathy et.al., 2024)[238].

The specific role of CD4 T cells to aid the transition of CD8 T cell exhausted progenitors to a CD8 T cell effector-like functional state and away from a terminally exhausted state was recently published[90,205]. Likewise, the role of B cells to direct interactions between CD4 T and CD8 T cells in B cell follicles has also been published[104,247]. Therefore, it was investigated whether the CD4 T cell and B cell proliferation at early time-point following vaccination correlate with CD8 T cell memory responses, as measured by its proliferation following *ex-vivo* restimulation of draining LNs with *Mtb* whole-cell lysate 90 days post-vaccination. It was also sought to explore the association of day 90 CD8 T cell proliferation with survival post *Mtb* HN878 challenge. To do so, a Spearman's rank correlation matrix for all the top 5 high-variance factors associated with PCA grouping was created (Figure 11A and corresponding p values in 11B). Spearman's correlation coefficient showed a perfect relationship between CD8 T cell proliferation in response to *Mtb* whole-cell lysate 90 days after vaccination and survival post

Mtb challenge (p value 2.7 x 10^{-3}) – in line with the known and established role of CD8 T cell responses being required for protection against TB[202,203,248].

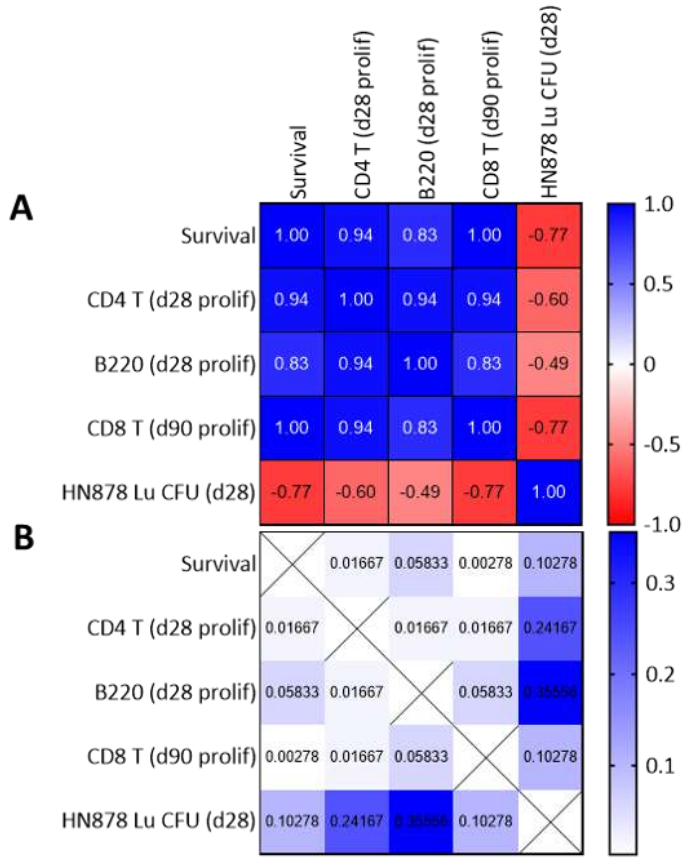

Figure 11: Spearman's rank correlation coefficients for the top 5 high-variance features in PCA. A) Spearman's correlation matrix. **B)** p-value of each corresponding correlation coefficient of pooled PBS, BCG and BCGΔBCG1419c vaccinated mice of both sexes (n=6). 2-tailed p-values are reported (data from preprint Harikumar Parvathy et.al., 2024)[238].

Early CD4 T cell proliferation also showed a significant highly positive correlation with late CD8 T cell response (correlation coefficient 0.94, p value 1.6 x 10^{-2}) as well as with survival post *Mtb* challenge (correlation coefficient 0.94, p value 1.6 x 10^{-2}). Early B cell proliferation also demonstrated significant positive correlation with CD4 T cells (correlation coefficient 0.94, p value 1.6 x 10^{-2}). However, the positive relationship between B cell proliferation directly with survival was not statistically significant in this model (correlation coefficient 0.83, p value 5.8 x 10^{-2}).

Results 5.5. Summary:

1. 3-dimensional PCA shows clustering of experimental groups mirroring their vaccine efficacy against TB or their vaccination status (control groups).

2. The best performing vaccine groups, irrespective of sex (BCG females, BCGΔBCG1419c females and males) cluster close to each other, while the remaining groups cluster separately.

3. Extraction of high-variance features in PC1 identified:
    - day 28 post-vaccination proliferations of CD4 T cell (in response to restimulation)
    - day 28 post-vaccination proliferations of B cell (in response to restimulation)
    - day 90 post-vaccination CD8 T cell proliferation (in response to restimulation)
    - survival post *Mtb* HN878 challenge
    - day 28 lung bacterial loads following *Mtb* HN878 challenge

    as the top 5 features influencing PCA.

4. Spearman's rank correlation of high-variance features identified significant positive correlation of both day 90 CD8 T cell responses and day 28 CD4 T cell responses post-vaccination with survival post *Mtb* HN878 challenge.

5.6. Male mice lack specific subpopulations of CD8 T cells in spleen, compared to females following vaccination and restimulation

When it was initially identified that males consistently fare poorly compared to females across all vaccine groups and with subsequent identification of defects in late CD8 T cell proliferative responses in male draining LNs following vaccination particularly with BCG, it was sought to investigate if there is a global shift in the pattern of CD8 T cell responses in males as compared to females. For this purpose, splenocytes of both sexes were tagged with CellTrace™ Violet (a proliferation marker dye) 28 days after vaccination with either BCG or BCGΔBCG1419c, along with PBS controls. Their co-cultures were subsequently restimulated with *Mtb* whole-cell lysate, as already described for LNs. The 28-day time-point was chosen, because after 90 days, the difference between the high background proliferation in spleen and the restimulated proliferation population is not significant in most situations to be identified by the fluorescence cytometry panel that was used, probably due to the low number of *Mtb* specific memory cells circulating through the spleen at a very late time-point that respond to restimulation and the broadness of the staining panel.

Because of the high background proliferation of splenic CD8 T cells, the 96 hour *ex-vivo* homeostatic proliferation of CD8 T cells of all groups (PBS, BCG and BCGΔBCG1419c) were digitally subtracted from their respective 96-hour CD8 T cell proliferation following *Mtb* whole-cell lysate restimulation, for both sexes (Figure 12A; representative figure of BCG female group made from intermediate steps in processing workflow for method description). Thereafter, the images of all 3 groups were superimposed sex-wise (Figure 12B; corrected UMAP images of each group obtained by subtracting homeostatic proliferation from ex-vivo restimulation; workflow made from intermediate steps in processing for method description). The distribution of CD8 T cells proliferating in response to *Mtb* whole-cell lysate in males were compared relative to females using the sex-wise superimposed images.

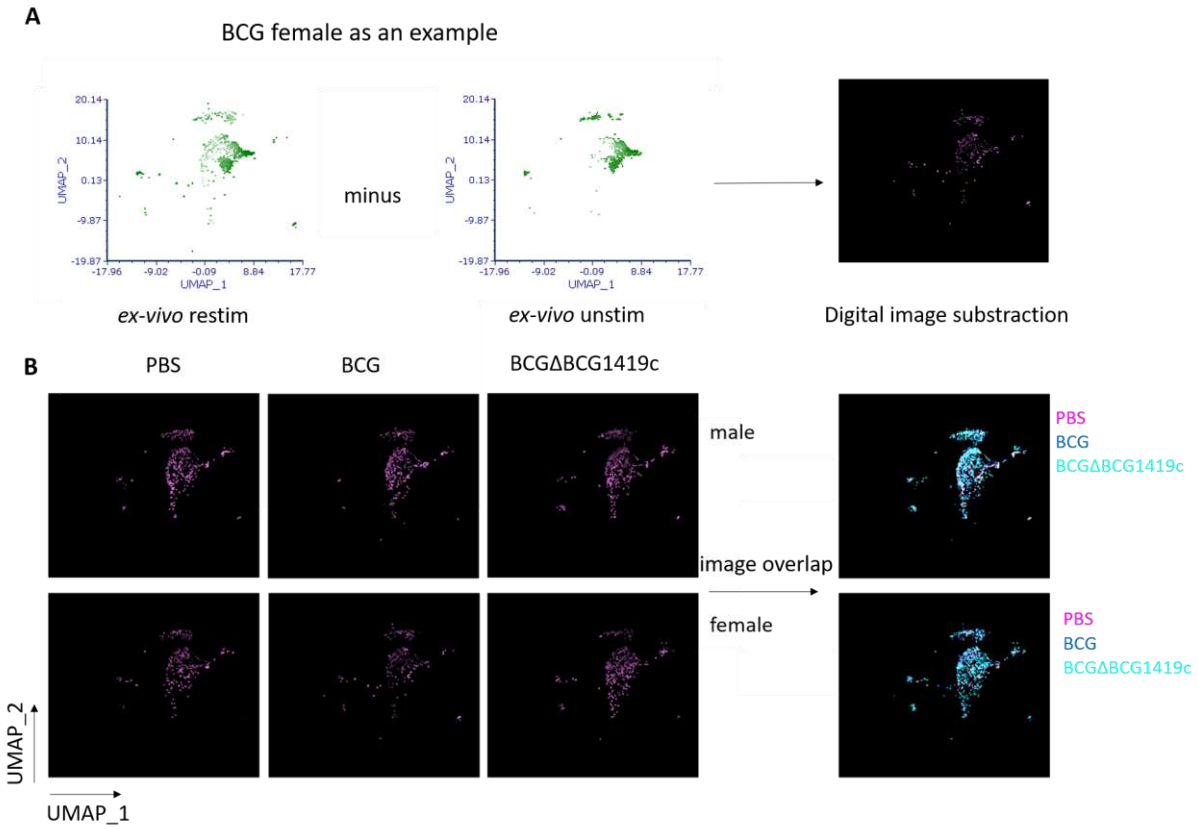

Figure 12: CD8 T cell proliferation in spleen in the presence or absence of *ex-vivo* restimulation with *Mtb* whole-cell lysate. A) Background homeostatic proliferation in *ex-vivo* unstimulated condition is subtracted from CD8 T cell proliferation in response to specific *Mtb* whole-cell lysate restimulation. Representative images made from intermediate steps in processing for method description **B)** Subtracted images from A) for all vaccine groups are superimposed over each other, separately for both sexes; workflow shown for method description. White color denotes areas where pixels precisely overlap. (n=9-10, for each vaccine group or control per sex; data pooled from 2 experiments; data from preprint Harikumar Parvathy et.al., 2024)[238].

In tune with male specific deficiencies identified in vaccine efficacy across all groups relative to females, specific differences were identified in the distribution of proliferating CD8 T cell populations responding to *Mtb* whole-cell lysate restimulation in male splenocyte co-culture across all vaccine groups tested, relative to their female counterparts (Figure 13A and 13B). By digitally subtracting the superimposed images of females and males from each other, the populations unique to females and males were visualized, with sex-wise consideration of all experimental groups. Thus, CD8 T cell proliferating populations that differed between females and males, irrespective of vaccine choice were identified (Figure 13C and 13D). Multiple CD8 T cell populations show differences in global distribution patterns, across sexes regardless of vaccine choice or vaccination status. Due to limitations in the current analytical software and programming resources, the differing clusters in the superimposed images between sexes could not be quantitatively determined. Nevertheless, these visually apparent differences in

the distribution of proliferating CD8 T cells in male spleen as compared to female spleen, deserve further study.

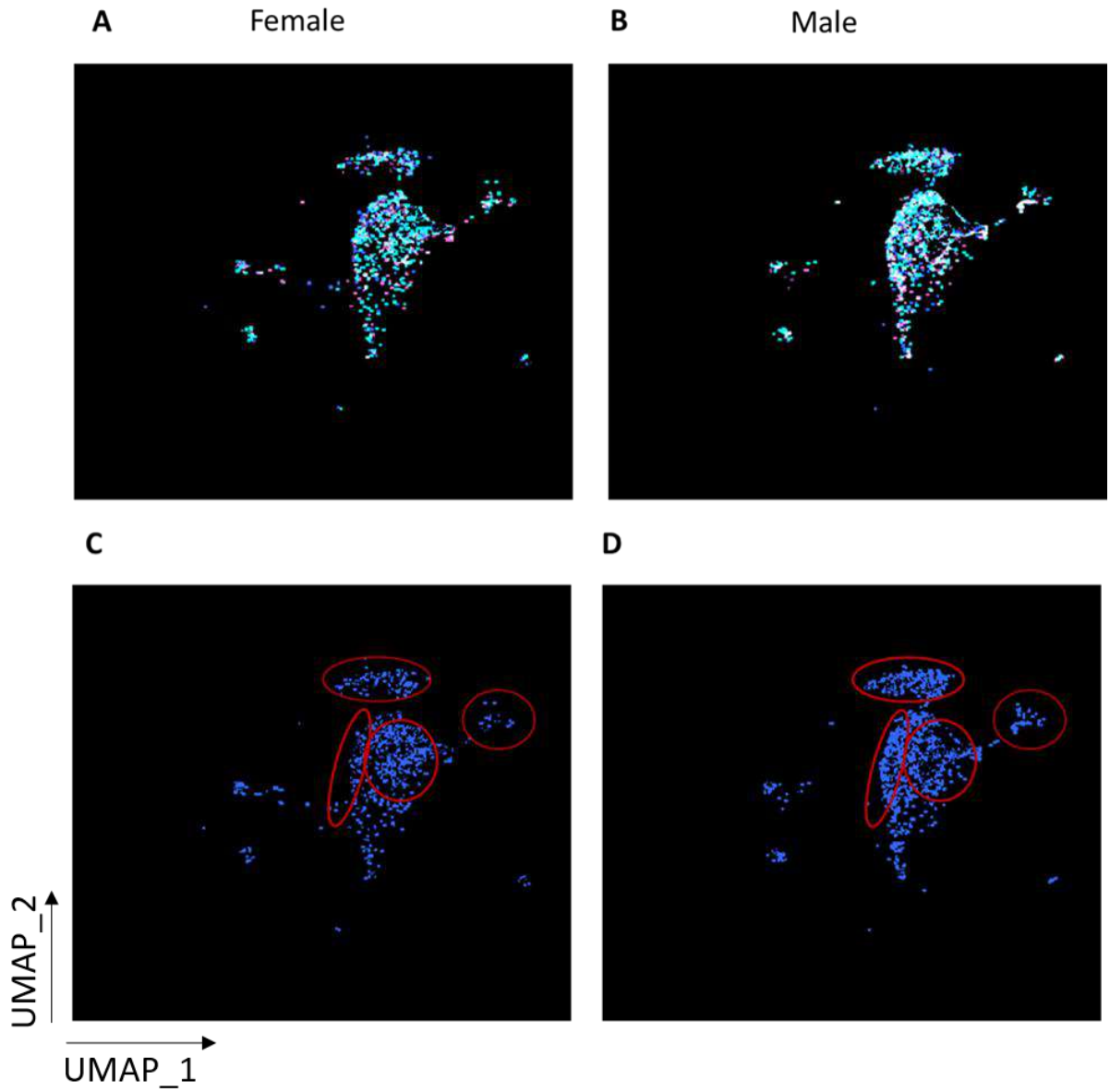

Figure 13: Distribution pattern of CD8 T cell proliferation in spleen upon *ex-vivo* restimulation with *Mtb* whole-cell lysate for females and males. A) and B) Digitally superimposed UMAP plots of CD8 T cell proliferation in PBS, BCG, BCGΔBCG1419c groups of female and male mice. **C) and D)** Superimposed images in A) and B) were subtracted from each other to obtain A-B or B-A. Thus, populations unique to either females or males are respectively shown in C) and D). Red circle denotes area of differences in CD8 T cell distribution identified manually (n=9-10, for each vaccine group or control per sex; data pooled from 2 experiments; data A) and B) from preprint Harikumar Parvathy et.al., 2024)[238].

Further studies involving a more detailed fluorescence cytometry panel and newly emerging machine learning platforms for fluorescence cytometry data analysis would help narrow down these population clusters in more resolution. Newer spectral sorting platforms would enable their precise sorting, making it possible to study them using proteomic or transcriptomic

approaches, in order to exactly define the clusters that are specifically differing across sexes. Coupled with functional experiments, this would aid to identify whether such differences are consequential or is a coincidental finding in the current model.

Results 5.6. Summary:

1. Male splenocytes show a global difference in specific clusters of CD8 T cells responding to *Mtb* whole-cell lysate restimulation relative to females.

2. These differences are present irrespective of vaccine choice.

6. Discussion

Despite BCG being in use for over 100 years as the only clinically available vaccine against TB, it remains remarkably variable in its efficacy[108,237]. Although, beneficial in preventing TB meningitis in children[249], BCG offers little protection from adult pulmonary TB in endemic regions of the world[237]. Here, for the first time (to the best of my knowledge), the contribution of biological sex in BCG efficacy in a resistant mouse model of TB vaccination is investigated. Although a recent study investigated the biology of sex differences in the context of BCG vaccination, their study was performed in a susceptible model of disease[229]. In the current study, a resistant model was chosen so as not to amplify those differences that might be inconsequential while having an immune system that is able to relatively resist the infection challenge following vaccination. Nevertheless, the recent study in a susceptible model is also of significance as TB is a disease that is often fatal in immunocompromised patients – as the world has particularly witnessed during co-infections with Human Immuno-deficiency Virus and *Mtb*[250,251] – and as such, delineating the mechanistic underpinnings of TB vaccination in susceptible conditions is necessary. Nevertheless, BCG itself is not indicated for immunocompromised patients because of its ability to cause disseminated disease in that population[252,253].

The current study also compares sex differences between BCG and two of its recombinant derivatives (rBCGs) – VPM1002 which is already in phase 3 clinical trials and an even newer BCGΔBCG1419c vaccine candidate currently in pre-clinical studies, demonstrating for the first time, to the best of my knowledge, the ability of newer derivatives of BCG to ameliorate the male specific inefficacy of BCG vaccine. Functional responses such as survival post *Mtb* challenge, bacterial loads in lungs and spleen, T and B cell memory responses as analyzed by their ability to proliferate following restimulation with *Mtb* whole-cell lysate 90 days after vaccination, as well as data analysis using varied analytical and machine learning tools were used in order to gain an insight into the sex specific efficacy and immune responses afforded by the vaccine (candidates).

6.1. Biological sex influences TB vaccine efficacy in a manner largely independent of lung *Mtb* load

In the first section, the protective efficacy of BCG and its two recombinant derivatives (rBCGs) – VPM1002 and BCGΔBCG1419c – with biological sex as a variable were investigated. In line

with previous results showing male vulnerability in TB disease development and male specific vulnerability of BCG described recently in a susceptible mouse model of TB[229], it was identified that BCG vaccination offers no significant improvement in protection against *Mtb* challenge compared to PBS controls specifically in males in the resistant mouse model of TB. This finding, together with previously published work in a susceptible model of TB[229], point to male specific deficiencies of BCG across different genetic backgrounds (in different models) and *Mtb* strains – pointing to an underlying male specific defect in the immune response to BCG vaccination. Newer recombinant derivatives of BCG, however, provided significant protection for males relative to sex-matched PBS controls as well as to that of BCG vaccination. Nevertheless, such a lack of protective efficacy for BCG was not apparent in female mice – where both BCG and rBCGs performed comparably. Females also had overall higher median survival in all groups tested relative to their male counterparts.

Of note, the two rBCGs that were tested – VPM1002 and BCGΔBCG1419c – enhance CD8 T cell responses[114,244], a feature that may directly benefit males considering the propensity of males to have enhanced T cell exhaustion in chronic diseases [30,35,207]. Females have been shown to have enhanced expression of genes related to lymphocyte proliferation, with estradiol also been shown to positively influence T cell[29,254,255] and B cell responses[29,48,256]. As such, even a vaccine with relatively low efficacy could potentially prime the physiologically enhanced adaptive immune phenotype of females. Males, although exhibiting the phenotype of enhanced innate immune memory[257], have lower expression of genes related to lymphocyte proliferation[28], lower expression of AID in germinal centers and lower antibody titers as compared to females[176,258,259]. Such differences could particularly impact TB vaccination in ways different to other vaccinations for infectious diseases where higher antigen specific antibody titers correlate with protective efficacy. B cells or high affinity antibody titers alone are insufficient to offer significant protection from TB, although their contributory role is becoming increasingly apparent[246,260,261]. TB disease control, as described classically for a long time, requires CD8 T cell mediated immunity[109,114,123,180,181,200–203], aided by CD4 T cells, B cells and other diverse members of the immune system[29,78,204–206,245,246,262,263]. Although the details have evolved in recent years, the role of CD8 T cells in TB control remains prominent[114,120,200,203]. Considering the sex specific peculiarities of the innate and adaptive immune system, it is conceivable that the different vaccines – with varying abilities to initiate

particular immune responses, including CD8 T cell responses - might perform differently in females and males.

In agreement with such a reasoning of vaccines potentially performing differently in females and males, as well as of the male specific vulnerability of BCG in the recently published susceptible mouse model of TB[229], BCG performs poorly in males with no survival benefit provided by BCG vaccine in males over PBS controls in the current study. Both VPM1002 and BCGΔBCG1419c, in contrast, provide significant survival advantage over both PBS controls and BCG vaccination in males. However, in line with physiologically enhanced adaptive immune response of females[27,29,48,105,264], even BCG which is performing poorly in males, is able to provide a median survival comparable to both VPM1002 and BCGΔBCG1419c in females. Also, in line with the physiologically augmented adaptive immune memory in females[28,177,233], all female groups in this survival study perform better than their male counterparts in terms of median survival following *Mtb* challenge.

Further, upon enumerating lung and spleen *Mtb* loads, no significant difference in *Mtb* CFUs at days 28 and 77 post *Mtb* HN878 challenge that uniformly mirror the survival data across all groups were found. This is similar to previous findings of BCGΔBCG1419c vaccine where decrease in lung pathology was not associated with corresponding decreases in lung bacterial loads[113,114]. However previous studies with VPM1002 demonstrate variable differences in lung bacterial loads compared to BCG (differing across studies)[112,212,265]. These studies with VPM1002 used different time-points, where differences in CFUs first became apparent only at day 150 post H37Rv infection, different *Mtb* strains and different mouse models (BALB/C) depending on the studies - whereas, the current study was performed in a resistant C57BL/6 mouse model of TB. This finding was not unique to a particular *Mtb* strain, as an infection challenge with H37Rv strain of *Mtb* also demonstrated no apparent sex specific differences in lung *Mtb* load between vaccine candidates, followed up to 97 days post-H37Rv challenge. This would point to the established role of immune responses, educated by vaccination, to efficiently control disease progression without a drastic reduction in *Mtb* bacterial loads as being necessary, as previously described by independent studies for both TB disease[240,266] and BCGΔBCG1419c vaccination[113,114].

Although some mice in the VPM1002 group of both sexes showed no bacterial spread to the spleen at day 28 post *Mtb* challenge while still showing CFUs in lungs, it is largely in line with

a previous finding in one study where VPM1002 showed nearly 1000-fold reduction in CFUs in a BALB/c mouse model of TB[120,212]. C57BL/6 mice with its increased propensity to develop a Th1 response[267], unlike the Th2 skewing in BALB/c mice[268], would presumably be able to resist TB growth and dissemination even further – especially when challenged with a lab adapted H37Rv isolate of *Mtb* at a low dose of infection of about 100 CFUs per mouse, in contrast to the virulent HN878 strain at a high dose of about 500 CFUs per mouse where no such drastic decrease was apparent. However, because the subsequent day 97 time-point did not replicate the finding of a proportion of mice with no dissemination in the spleen when vaccinated with VPM1002, it was hypothesized that these mice that showed an apparent absence of *Mtb* dissemination in spleen at day 28 post-H37Rv challenge had such small CFU loads that could not be detected within the dilution range of CFU plating – rather than pointing at a complete absence of dissemination to the spleen for the VPM1002 vaccinated group. However, with time, no vaccinated mouse group show dramatic reductions in CFUs, either in lung or spleen, relative to other vaccinated groups for the time-points analyzed.

6.2. BCGΔBCG1419c vaccination enhances the organization of lymphoid aggregates in males and makes it comparable to unvaccinated female controls

Because females performed better than their male counterparts in all experimental groups – including PBS controls - in terms of median survival, it was hypothesized that females would have a background host response that promotes better infection control than males. In order to identify any such features in their lung morphology during severe disease, as well as, how the best performing vaccine in males would approximate those possible male specific deficiencies, H&E staining of lung sections from PBS control females and males, together with BCGΔBCG1419c males were undertaken. Image quantification uncovered that the area of organized lymphoid aggregates, as identified from their morphological features and previously shown to be composed of B cell follicles[48,105], differed significantly between PBS control females and males.

These organized lymphoid structures, have been associated with better disease outcome in chronic diseases such as cancer as well as in infections such as TB[48,104,269,270] – including in TB vaccination[102,271]. It is also a possible site for B cell, CD4 T cell and CD8 T cell interaction[104,272,273]. Chronic diseases such as cancer and chronic infections such as TB share overlapping immune landscapes of CD8 T cell exhaustion[84,85,172] and males, in general, have an

immune landscape permissive to T cell exhaustion compared to their female counterparts[31,175]. Acknowledging these peculiarities, it was hypothesized that a possible area of interaction between CD4 T cells, B cells and CD8 T cells or CD8 T exhausted progenitors could be within these organized lymphoid structures. Such an interaction, as described previously[90,198,205,273], would have the potential to aid the transition of CD8 T exhausted progenitors to CD8 T effector like state – away from their otherwise terminally exhausted fate[90]. Mature tertiary lymphoid structures also have mature dendritic cells in addition to B cells and T cells[270]. Therefore, it could provide a site for both the calibration of dendritic cells via CD4 T cells together with interferon alpha and beta, as well as for the interactions between these calibrated dendritic cells and CD8 T cells, guiding CD8 T cell responses[198,270].

Broadly supporting such a hypothesis, this study identified increased organization of lymphoid structures in BCGΔBCG1419c males, now becoming comparable to unvaccinated females. However, the detailed composition of these structures, its relationship with CD8 T cell response and its mechanistic underpinnings in vaccine mediated protective immune responses during *Mtb* challenge require further study. Such a study would conclusively describe the extent of such associations with protective immunity and whether such increase in organization of lymphoid aggregates also contribute to the known ability of BCGΔBCG1419c to restrict T cell exhaustion as compared to BCG[110].

6.3. Specific cellular (recall) responses following vaccination correlates with enhanced protection during *Mtb* infection

Because of the well-established role for CD8 T cell responses[114,120,248], along with the well acknowledged role of CD4 T cells and the role of B cells that is becoming increasingly apparent in *Mtb* protection[48,205,245,246], it was decided to probe the efficacy of vaccination to promote those responses. The hypothesis about possible sex specific differences was further strengthened by the findings of male specific peaking of rBCG (VPM1002 and BCGΔBCG1419c) vaccine strain CFUs following vaccination, which led to reason that they would generate potentially different immune (memory) responses as compared to BCG, specifically in males. An increased antigen load, in general, has been shown to grant a male specific benefit, as in the case of influenza vaccine, where males require double the dose as compared to females to induce comparable levels of antibody response in influenza vaccine[178].

Therefore, any potential sex specific difference in B and T cell proliferative responses were probed upon *ex-vivo* restimulation with *Mtb* whole-cell lysate at days 28 and 90 after vaccination. The time-point of 90 days post-vaccination has also been recently used in a human study of BCG vaccine to decipher the memory responses post-vaccination[274] – in line with the reasoning that B and T cell response to restimulation at this time-point would largely be derived from memory populations. Agreeing with the hypothesis, CD8 T cell proliferative response in LN to *ex-vivo* restimulation with *Mtb* whole-cell lysate at day 90 post-vaccination mirrored the survival advantage provided by BCG and BCGΔBCG1419c in a sex specific way. While the median survival of BCG and BCGΔBCG1419c vaccinated mice were comparable post *Mtb* challenge in females, with both providing statistically significant survival advantage for females – BCGΔBCG1419c and not BCG provided a survival advantage for male mice - a result that is mirrored by day 90 post-vaccination CD8 T cell proliferative response. This is in line with established literature demonstrating the role of CD8 T cell response in protection against *Mtb* in both VPM1002 and BCGΔBCG1419c[114,120,213].

At day 28 post-vaccination, increased proliferation of both CD4 T cells and B cells were observed in BCGΔBCG1419c vaccinated males compared to their BCG vaccinated counterparts – with BCGΔBCG1419c demonstrating a higher mean as well as a greater statistical significance over PBS control males in both cases, compared to BCG vaccination.

CD4 T cells are essential to prime naïve CD8 T cells in both sexes and contribute to the quality as well as magnitude of CD8 T cell response[198,205,262,275,276]. B cells have also been shown to direct T follicular like helper cells into lymphoid follicles enabling *Mtb* control in a murine model of the disease[104]. A known site of CD4 T cell and CD8 T cell interaction is in the areas surrounding the B cell regions in germinal centers of LNs - lymphoid follicles being their counterparts in non-lymphoid tissue[277,278]. Therefore, it is presumable that such interactions at an early time-point in draining LNs following vaccination could, hypothetically, affect the quality of CD8 T cell memory response. Moreover, sex differences determining the fate of CD8 T cell during the priming process are largely extrinsic to the CD8 T cell and related to other factors such as antigen presentation - events estradiol has been known to influence[29,216]. However, sex differences in the effector functions of CD8 T cells are known to be cell intrinsic[29,32]. In this context, it must be noted that the 96 hour *ex-vivo* restimulation protocol in this study did not have added sex hormones. Therefore, the sex specific picture that have

been captured during *ex-vivo* restimulation are those likely due to cell intrinsic nature of sex differences – imprinted either in their genome or epigenome or those imprints driven by sex steroids before LN harvest. Therefore, the LN harvest at day 28 post-vaccination and their subsequent co-culture without added sex hormones may not have fully captured the sex specific effects of cell-cell interactions and antigen presentation occurring under the direct influence of sex steroids prominently. However, because these events would have continually occurred before day 28 post-vaccination as well, it could be hypothesized that some information would also be revealed at day 28 *ex-vivo* restimulation of LN with *Mtb* whole-cell lysate – as shown from the relationship between day 28 CD4 T cell and day 90 CD8 T cell proliferation as well as between day 28 CD4 T and B cell proliferation during correlation analysis.

Males are also known to have increased T cell exhaustion during chronic conditions[30,35,175], along with lower CD4/CD8 T cell ratio[28]. CD8 T exhausted progenitors could be redirected from their terminally exhausted fate to a partially functional effector-like exhausted fate with CD4 T cell help[90,205], as well as with a less defined role for B cell help[279]. Hypothetically, females should have no such remarkable deficiency in CD8 T cell responses following vaccination with either vaccine and exposure to *Mtb* antigens, as BCG is comparable in its efficacy to rBCGs in females. Even following vaccination, females have been shown to develop more efficient CD8 T cell responses relative to their male counterparts[280,281]. However, such an additional help from CD4 T cells to CD8 T cells during the priming phase would be particularly relevant for males. It could hypothetically drive CD8 T cell memory phenotype, stemming from a better functional population of CD8 T cells, during the contraction phase of the acute response to vaccination. Thus, effecting the sex specific memory responses indicated by CD8 T cell proliferation upon restimulation at day 90 post-vaccination. CD8 T cell exhaustion has also been described as one of the reasons for the waning efficacy of BCG vaccination, both in the context of TB as well as in its use for bladder cancer treatment[173,248].

In broad agreement with such a reasoning, in BCGΔBCG1419c vaccinated males at day 28 post-vaccination, CD4 T cell proliferation was significantly enhanced over male PBS controls – with a higher mean and greater significance than that provided by BCG over PBS, specifically in males. Similarly, at this time-point, B cell proliferation was significantly increased in BCGΔBCG1419c vaccinated males but not in BCG vaccinated males over PBS control. However,

in females both vaccines significantly increased B cell proliferation at this time-point, although BCGΔBCG1419c showed higher mean and greater significance than BCG over PBS control. Additionally, in agreement with published data showing the importance of CD8 T cell response in *Mtb* control and the demonstrated association of BCGΔBCG1419c to enhance CD8 T cell responses[114,200], statistically significant correlation was observed between CD8 T cell proliferation upon *Mtb* whole-cell lysate restimulation *ex-vivo* at day 90 post-vaccination and survival post *Mtb* challenge.

Further, it was reasoned that if there were specific benefits offered by CD4 T or B cells, such as in overcoming the exhausted CD8 T cell landscape as is known to be more prevalent in TB, even more so in males generally[30,93,282], CD4 T cell and/or B cell proliferation during the early (day 28 post-vaccination) phase would have an association with CD8 T cell memory responses at the late (day 90 post-vaccination) phase. A recent study in a lung cancer model identified tumor associated CD4 T cell - identified to be T follicular helper cells in single-cell ribonucleic acid sequencing (scRNA sequencing) - and germinal center B cell help as being required for effective CD8 T cell response against tumor neoantigens[247]. Similarly, CD4 T cell help – especially IL-21 produced by CD4 T follicular helper cells, which are located in LNs and tertiary lymphoid follicles[283] – is required for robust CD8 T cell responses in models of chronic infection and vaccination, thereby enhancing CD8 T cell responses and development of CD8 T cell memory post-vaccination[262,284]. CD4 T cells have also been shown to direct CD8 T exhausted progenitors away from a terminally exhausted fate, and instead towards a CD8 T effector like fate – retaining many of the effector functions[90].

In line with expectations, those were among the top 5 high-variance features identified in PCA analysis. Further, Spearman's ranked correlation analysis found a significant positive correlation between day 28 post-vaccination CD4 T proliferation and survival as well as with that of day 90 CD8 T cell proliferation following restimulation. CD8 T cell proliferation at day 90 post-vaccination also demonstrated significant positive correlation with survival post *Mtb* challenge. Day 28 B cell proliferation had a significant positive correlation with day 28 CD4 T cell response, in line with reciprocating help provided by CD4 T cells and B cells during the priming phase[285–287]. However, in the current study model, the correlations of early (day 28) B cell responses with survival post *Mtb* challenge as well as with late (day 90) CD8 T cell responses did not reach significance. It might be due to technical limitations rather than an

absolute absence of relationship – that could be potentially identified by further subtyping of B and T cells using a spectral fluorescence cytometry platform or by scRNA sequencing analysis.

Nevertheless, the analysis from this study points to a potential role for CD4 T cells and B cells early in the draining LNs (day 28 time-point of analysis), during acute response to vaccination. Whether this would play a causal role in the higher CD8 T cell proliferative responses in both sexes – and whether newer rBCGs such as BCGΔBCG1419c direct at least part of their improved efficacy in males through enhanced CD4 T cell and/or B cell responses, as the case maybe for individual vaccine candidates early during vaccination, which in turn directs CD8 T cell memory formation that is better protective against a subsequent pathogen encounter remains to be elucidated. Further studies will delineate whether such a mechanistic relationship exist – and if so, their extent and also the vaccine features that enable such an immune response. The knowledge from such future studies is useful beyond developing TB vaccination, particularly in other conditions where chronic exposure to antigen(s) and T cell exhaustion adversely affects disease outcome as in several cancers.

6.4. Male mice lack specific subpopulations of CD8 T cells in spleen compared to females following vaccination and restimulation

Because males performed poorly compared to females even with BCGΔBCG1419c vaccination – that ameliorates the male specific vulnerability of BCG – combined with the sex and vaccine specific nature of CD8 T cell proliferation that was uncovered in the present study, it was inquired whether these differences that were observed would also translate into systemic differences in CD8 T cell responses. Spleen was chosen as an organ to assess these systemic responses as spleen has high blood flow and is a secondary lymphoid organ. Therefore, it was reasoned that spleen would provide the possibility to capture some of the very few circulating memory T cells, following vaccination. Although the day 90 post-vaccination time-point was the focus for detailing of the memory CD8 T cell responses in LNs, the day 28 post-vaccination time-point was chosen to detail CD8 T cell responses in spleen. It is because at day 90 post-vaccination, CD8 T cell proliferation in spleen is similar between *Mtb* whole-cell lysate restimulation and homeostatic proliferation as captured in the experiments of this study. However, more than pointing to an absence of circulating memory CD8 T cells at the day 90 time-point, it might point to limitations in the technique and the broadness of the fluorescence

cytometry panel which is limited in the required depth to extract the very few circulating central memory population from the overall CD8 T cell population – and to also differentiate it from those responding non-specifically to *Mtb* whole-cell lysate in the background including via innate activation of memory T cells independent of cognate antigen[288–290]. More powerful methods delving into detailed transcriptional state of individual cells, such as scRNA sequencing, would probably identify the contracted population of circulating memory T cells even at the late time-point of day 90 post-vaccination.

Nevertheless, from the *Mtb* whole-cell lysate restimulation of splenocyte co-culture from spleens harvested at day 28 post-vaccination, specific clusters of proliferating CD8 T cells that showed differences between sexes irrespective of vaccine choice were identified. Future studies, with a detailed fluorescence cytometry panel for CD8 T cells coupled with dedicated algorithms to quantify such differences, would help to identify the precise phenotype and extent of these differences. Further, they can be sorted by newer spectral fluorescence cytometry-based sorting platforms and analyzed via RNA sequencing or proteomics methods to gain a deeper insight into those populations specifically present in females and absent in males and vice-versa. Functional studies would determine whether the differing populations are associated with reduced protection of males against *Mtb* challenge as compared to their respective female counterparts, both in vaccination and control groups. scRNA sequencing would also help determine whether these populations are “helped” or “unhelped” CD8 T cells, with regard to the help received from CD4 T cells particularly through CD4 T cell interaction with antigen presenting cells[198] – or directly by CD4 T cells when they are CD8 T exhaustion progenitors, in aiding them to differentiate to CD8 T effector like fate[90]. Helped CD8 T cells have been shown to have a better functionality to offer protection in infection models[198,205].

6.5. Implications of the current study and its limitations

Despite the established influence of biological sex in TB, the underlying biological basis of which is being increasingly delineated in multiple studies[27,48,105], the role of biological sex in BCG and emerging vaccine candidates against TB is scarcely explored. The present study, for the first time to the best of my knowledge, investigates the underlying biology of male specific deficiency in BCG vaccine mediated protection in a resistant mouse model of TB, broadly in line with most of the human population being able to resist an encounter with *Mtb*[291]. Further, for the very first time also to the best of my knowledge, a role for newer derivatives of BCG to

ameliorate the male specific vulnerability in BCG mediated protection was identified. Further, specific features such as CD8 T cell response in draining LN co-culture from LNs harvested 90 days post-vaccination were shown to be correlated with survival following *Mtb* challenge. Also, specific populations of proliferating CD8 T cells in spleen co-culture post-vaccination that are differing across sexes irrespective of vaccine choice were elucidated. However, the role of these specific CD8 T cell clusters in mediating vaccine efficacy, their causal relationship and whether they are more important for one sex over another deserve further study.

Moreover, being one of the first-in-class studies to investigate the underlying biology of sex differences in BCG vaccination in relation to newer rBCGs, the current study was driven by broad hypothetical questions to investigate whether such a male specific vulnerability exist for BCG efficacy in a resistant mouse model of TB and if so, the ability of newer rBCGs to ameliorate the male specific vulnerability of BCG - as well as to uncover pointers of the biological basis of this male specific vulnerability. As such, a deep characterization of cell populations of interest identified in the current study could not be performed within its scope. The scope of the current study was to identify any potential differences specific to sex in broad cell populations following BCG vaccination such as CD8 T cell response, which has also been implicated in the efficacy of both VPM1002 and BCGΔBCG1419c vaccine candidates. Future studies, using more comprehensive approaches involving platforms such as proteomics, sequencing and spectral fluorescence cytometry will help to specifically characterize these identified populations of interest, as well as to extensively evaluate the subtypes of those broad cell populations in a sex specific manner.

6.6. Some final thoughts on the field of TB vaccination

Vaccination remains the corner-stone for prevention of many infectious diseases in communities across the world. Diseases such as smallpox, polio, tetanus, diphtheria among others, have seen dramatic reductions in incidence up to total eradication following vaccine development, with vaccines being 97-100% effective in prevention of these diseases that are mentioned, except for smallpox where it has been about 95% historically[292–296]. Certain other diseases prevented by appropriate vaccination nearly 100% of the time, although a little less common, have very high mortality – sometimes nearing 100% fatality once symptoms develop as is the case in rabies[297].

Nevertheless, development of effective vaccines against (obligate) intracellular bacteria have largely remained as a challenge for the field. Although some vaccines are approved for bacteria requiring an intracellular life-cycle, such as *Salmonella typhi* (the causative agent of Typhoid), they remain relatively poor in efficacy, at about 45% in the case of Typhoid fever[298]. It is also the case with BCG in prevention of pulmonary TB in adults with an efficacy 0-80%, which is widely variable[299]. One of the compounding factors for the slow development of vaccines in this category is the difficulty in describing clear correlates of protection for many of these diseases – a situation that is expounded in TB, with its complex landscape of immune response spanning acute, chronic and latent phases of infection – whose implications in TB disease and vaccination are still being actively investigated[133,300]. Currently, to the best of my knowledge, no TB vaccine candidate claim sterilizing immunity as an end-point in pre-clinical models, although two vaccine modalities have demonstrated sterilizing immunity for a subpopulation of infected group in animal models[301–303]. Nevertheless, very few of the TB vaccine candidates have reached advanced stages of human clinical trials. The recent recognition and funding obtained from International AIDS vaccine initiative (IAVI) for further development of MTBVAC, the only vaccine candidate made from attenuated *Mtb* itself to be currently in the pipeline, showcases the urgency for an effective vaccine[304,305]. Although it significantly reduced lung pathology and disease scores compared to unvaccinated control and BCG in animal models, at least in one major study it did not provide a clear statistically significant survival advantage over either BCG or unvaccinated controls in an animal model of TB, although a trend was apparent[306]. Nevertheless, vaccines that halt disease development and progression itself has been projected to contribute to hundreds of billions of dollars in saved costs by 2050[307], thereby potentially allowing the population in the most vulnerable regions of the world to develop socio-economically. Indeed, reducing extreme poverty has been projected to reduce TB disease burden by about 33% by 2035[308]. However, this does not take into account the disruption inflicted by the SARS-CoV-2 pandemic, further emphasizing the urgency for the development of effective strategies to contain TB. Because TB is spread over wide geographical areas and populations, vaccination using the actual human causative agent might provide a broader spectrum of antigens that is able to accommodate the diversity in MHC haplotypes across human populations.

On the other hand, VPM1002 which is currently in phase 3 clinical trials, was concluded to be less “immunogenic” as compared to BCG in a phase 2 study outcome in infants that was

recently published[117]. However, this study has not comprehensively analyzed the long-term infection risk, as well as those in immune-compromised populations where BCG use is contra-indicated. In the absence of clear correlates of protection, the very interpretation of "immunogenic" - whatever parameters that definition may include - as a surrogate for disease protection becomes challenging. This further points to the urgent need to mechanistically understand the immune landscape of TB in the context of both disease and vaccination.

6.7. Concluding remarks

TB is a disease that shows a strong male preponderance in disease development, with males at least two-fold as likely as females to develop TB[27] – and TB vaccine (candidates) including BCG, VPM1002 and BCGΔBCG1419c demonstrate sex specific (dis)advantages in the survival study upon *Mtb* challenge conducted in the current project. Therefore, the investigation of its immune landscape without considering biological sex and its increasingly recognized role in the immune response would further preclude a clear delineation of parameters conferring disease protection or encouraging progression. Any successful vaccination strategy should address the groups most vulnerable to disease in a population. With males being at least two-fold more likely than females to develop TB, any strategy that do not address the specific disease vulnerability of males would be limited in its impact in arresting TB. However, many studies on TB, including vaccination, do not assertively address the influence of sex[27] – the effect of which is illustrated by the result from this study showing BCG to be significantly effective against TB over PBS controls in female mice, while BCG provides no statistically significant survival advantage over PBS controls in male mice; a finding that is also replicated using another *Mtb* strain in a susceptible mouse model of TB[229].

Future investigations aimed at delineating the immune-landscape of both females and males in TB disease and vaccination – aiming to delineate why females are better protected when males have a stark vulnerability to TB disease development – would help understand and describe sex specific reasons for immunity and vulnerability to TB. In addition to informing vaccination and treatment strategies that ameliorate sex specific vulnerabilities of male sex in TB disease development, the general concepts of sex specific immunity would provide hope for the development of disruptive therapeutic and preventive vaccinations for chronic diseases characterized by a landscape of immune insufficiency and exhaustion in the future. It could take advantage of current developments in mathematical modelling, computer science and

technology, such as in fluorescence cytometry, imaging, proteomics and sequencing platforms among others, to harness and analyze necessary data, as well as to identify patterns within the heavily networked immune-landscape that could not be investigated until now – all the while continually embracing newer vaccine platforms that are gaining approval for medical use.

References

1. CDCTB. World TB Day History. *Centers for Disease Control and Prevention* https://www.cdc.gov/tb/worldtbday/history.htm (2023).
2. Tuberculosis deaths and disease increase during the COVID-19 pandemic. https://www.who.int/news/item/27-10-2022-tuberculosis-deaths-and-disease-increase-during-the-covid-19-pandemic.
3. Shariq, M. *et al.* COVID-19 and tuberculosis: the double whammy of respiratory pathogens. *Eur. Respir. Rev.* **31**, (2022).
4. Trajman, A. The social drivers of tuberculosis, reconfirmed. *Lancet Infect. Dis.* **24**, 5–6 (2024).
5. Kirby, T. Global tuberculosis progress reversed by COVID-19 pandemic. *Lancet Respir. Med.* **9**, e118–e119 (2021).
6. Dheda, K. *et al.* The intersecting pandemics of tuberculosis and COVID-19: population-level and patient-level impact, clinical presentation, and corrective interventions. *Lancet Respir. Med.* **10**, 603–622 (2022).
7. Xue, Y. *et al.* Burden of tuberculosis and its association with socio-economic development status in 204 countries and territories, 1990–2019. *Front. Med.* **9**, (2022).
8. Global Burden of Disease Collaborative Network. Global Burden of Disease Study 2019 (GBD 2019) Socio-Demographic Index (SDI) 1950–2019. [object Object] https://doi.org/10.6069/D8QB-JK35 (2020).
9. Paulson, T. Epidemiology: A mortal foe. *Nature* **502**, S2–S3 (2013).
10. 2.2 TB mortality. https://www.who.int/teams/global-tuberculosis-programme/tb-reports/global-tuberculosis-report-2022/tb-disease-burden/2-2-tb-mortality.
11. RKI - Infectious Diseases in Germany - Report on the Epidemiology of Tuberculosis in Germany - 2021. https://www.rki.de/EN/Content/infections/epidemiology/inf_dis_Germany/TB/summary_2021.html.
12. Peer, V., Schwartz, N. & Green, M. S. Gender differences in tuberculosis incidence rates—A pooled analysis of data from seven high-income countries by age group and time period. *Front. Public Health* **10**, (2023).
13. Global Gender Gap Report 2023. *World Economic Forum* https://www.weforum.org/publications/global-gender-gap-report-2023/in-full/benchmarking-gender-gaps-2023/.
14. Pisitkun, P. *et al.* Autoreactive B Cell Responses to RNA-Related Antigens Due to TLR7 Gene Duplication. *Science* **312**, 1669–1672 (2006).
15. Berghöfer, B. *et al.* TLR7 Ligands Induce Higher IFN-α Production in Females1. *J. Immunol.* **177**, 2088–2096 (2006).
16. Klein, S. L., Jedlicka, A. & Pekosz, A. The Xs and Y of immune responses to viral vaccines. *Lancet Infect. Dis.* **10**, 338–349 (2010).
17. Torcia, M. G. *et al.* Sex Differences in the Response to Viral Infections: TLR8 and TLR9 Ligand Stimulation Induce Higher IL10 Production in Males. *PLOS ONE* **7**, e39853 (2012).
18. Migliore, L., Nicolì, V. & Stoccoro, A. Gender Specific Differences in Disease Susceptibility: The Role of Epigenetics. *Biomedicines* **9**, 652 (2021).
19. Hoffmann, J. P., Liu, J. A., Seddu, K. & Klein, S. L. Sex hormone signaling and regulation of immune function. *Immunity* **56**, 2472–2491 (2023).
20. Potluri, T. *et al.* Age-associated changes in the impact of sex steroids on influenza vaccine responses in males and females. *Npj Vaccines* **4**, 1–12 (2019).
21. Demonbreun, A. R. *et al.* COVID-19 mRNA Vaccination Generates Greater Immunoglobulin G Levels in Women Compared to Men. *J. Infect. Dis.* **224**, 793–797 (2021).
22. Yoshida, Y., Wang, J. & Zu, Y. Sex differences in comorbidities and COVID-19 mortality–Report from the real-world data. *Front. Public Health* **10**, (2022).

23. Kaplan Marshall M. & Gershwin M. Eric. Primary Biliary Cirrhosis. *N. Engl. J. Med.* **353**, 1261–1273 (2005).
24. Kaul, A. *et al.* Systemic lupus erythematosus. *Nat. Rev. Dis. Primer* **2**, 1–21 (2016).
25. Forsyth, K. S., Jiwrajka, N., Lovell, C. D., Toothacre, N. E. & Anguera, M. C. The conneXion between sex and immune responses. *Nat. Rev. Immunol.* 1–16 (2024) doi:10.1038/s41577-024-00996-9.
26. Government of Canada, C. I. of H. R. What is gender? What is sex? - CIHR. https://cihr-irsc.gc.ca/e/48642.html (2014).
27. Hertz, D. & Schneider, B. Sex differences in tuberculosis. *Semin. Immunopathol.* **41**, 225–237 (2019).
28. Klein, S. L. & Flanagan, K. L. Sex differences in immune responses. *Nat. Rev. Immunol.* **16**, 626–638 (2016).
29. Dunn, S. E., Perry, W. A. & Klein, S. L. Mechanisms and consequences of sex differences in immune responses. *Nat. Rev. Nephrol.* **20**, 37–55 (2024).
30. Kwon, H. *et al.* Androgen conspires with the CD8+ T cell exhaustion program and contributes to sex bias in cancer. *Sci. Immunol.* **7**, eabq2630 (2022).
31. Tournant, F. Immunological sex differences in glioblastoma. *Nat. Cancer* **4**, 1636–1636 (2023).
32. Yee Mon, K. J. *et al.* Differential Sensitivity to IL-12 Drives Sex-Specific Differences in the CD8+ T Cell Response to Infection. *ImmunoHorizons* **3**, 121–132 (2019).
33. Fischinger, S., Boudreau, C. M., Butler, A. L., Streeck, H. & Alter, G. Sex differences in vaccine-induced humoral immunity. *Semin. Immunopathol.* **41**, 239–249 (2019).
34. Spiering, A. E. & de Vries, T. J. Why Females Do Better: The X Chromosomal TLR7 Gene-Dose Effect in COVID-19. *Front. Immunol.* **12**, (2021).
35. Yang, C. *et al.* Androgen receptor-mediated CD8+ T cell stemness programs drive sex differences in antitumor immunity. *Immunity* **55**, 1268-1283.e9 (2022).
36. Wikby, A., Månsson, I. A., Johansson, B., Strindhall, J. & Nilsson, S. E. The immune risk profile is associated with age and gender: findings from three Swedish population studies of individuals 20–100 years of age. *Biogerontology* **9**, 299–308 (2008).
37. Huang, Z. *et al.* Effects of sex and aging on the immune cell landscape as assessed by single-cell transcriptomic analysis. *Proc. Natl. Acad. Sci.* **118**, e2023216118 (2021).
38. Abdullah, M. *et al.* Gender effect on *in vitro* lymphocyte subset levels of healthy individuals. *Cell. Immunol.* **272**, 214–219 (2012).
39. Melzer, S. *et al.* Reference intervals for leukocyte subsets in adults: Results from a population-based study using 10-color flow cytometry. *Cytometry B Clin. Cytom.* **88**, 270–281 (2015).
40. Patin, E. *et al.* Natural variation in the parameters of innate immune cells is preferentially driven by genetic factors. *Nat. Immunol.* **19**, 302–314 (2018).
41. Bustamante, J. *et al.* Germline CYBB mutations that selectively affect macrophages in kindreds with X-linked predisposition to tuberculous mycobacterial disease. *Nat. Immunol.* **12**, 213–221 (2011).
42. Cheng, M. I. *et al.* The X-linked epigenetic regulator UTX controls NK cell-intrinsic sex differences. *Nat. Immunol.* **24**, 780–791 (2023).
43. Szappanos, D. *et al.* The RNA helicase DDX3X is an essential mediator of innate antimicrobial immunity. *PLOS Pathog.* **14**, e1007397 (2018).
44. Soulat, D. *et al.* The DEAD-box helicase DDX3X is a critical component of the TANK-binding kinase 1-dependent innate immune response. *EMBO J.* **27**, 2135–2146 (2008).
45. Filipe-Santos, O. *et al.* Inborn errors of IL-12/23- and IFN-γ-mediated immunity: molecular, cellular, and clinical features. *Semin. Immunol.* **18**, 347–361 (2006).
46. Greenfield, A. *et al.* The UTX Gene Escapes X Inactivation in Mice and Humans. *Hum. Mol. Genet.* **7**, 737–742 (1998).
47. Rothwarf, D. M., Zandi, E., Natoli, G. & Karin, M. IKK-γ is an essential regulatory subunit of the IκB kinase complex. *Nature* **395**, 297–300 (1998).

48. Hertz, D., Dibbern, J., Eggers, L., von Borstel, L. & Schneider, B. E. Increased male susceptibility to Mycobacterium tuberculosis infection is associated with smaller B cell follicles in the lungs. *Sci. Rep.* **10**, 5142 (2020).
49. Fink, A. L., Engle, K., Ursin, R. L., Tang, W.-Y. & Klein, S. L. Biological sex affects vaccine efficacy and protection against influenza in mice. *Proc. Natl. Acad. Sci.* **115**, 12477–12482 (2018).
50. Khoury, D. S. *et al.* Neutralizing antibody levels are highly predictive of immune protection from symptomatic SARS-CoV-2 infection. *Nat. Med.* **27**, 1205–1211 (2021).
51. Setiabudiawan, T. P. *et al.* Protection against tuberculosis by Bacillus Calmette-Guérin (BCG) vaccination: A historical perspective. *Med* **3**, 6–24 (2022).
52. Hayman, J. MYCOBACTERIUM ULCERANS: AN INFECTION FROM JURASSIC TIME? *The Lancet* **324**, 1015–1016 (1984).
53. World Population Clock: 8.1 Billion People (LIVE, 2024) - Worldometer. https://www.worldometers.info/world-population/.
54. Barberis, I., Bragazzi, N. L., Galluzzo, L. & Martini, M. The history of tuberculosis: from the first historical records to the isolation of Koch's bacillus. *J. Prev. Med. Hyg.* **58**, E9–E12 (2017).
55. Brown, L. *The Story of Clinical Pulmonary Tuberculosis*. (Williams & Wilkins, Baltimore, 1941).
56. Tuberculosis (TB). https://www.who.int/news-room/fact-sheets/detail/tuberculosis.
57. Mycobacterium Tuberculosis - an overview | ScienceDirect Topics. https://www.sciencedirect.com/topics/medicine-and-dentistry/mycobacterium-tuberculosis.
58. Zhai, W., Wu, F., Zhang, Y., Fu, Y. & Liu, Z. The Immune Escape Mechanisms of Mycobacterium Tuberculosis. *Int. J. Mol. Sci.* **20**, 340 (2019).
59. Yihao, D., Hongyun, H. & Maodan, T. Latency-associated protein Rv2660c of Mycobacterium tuberculosis augments expression of proinflammatory cytokines in human macrophages by interacting with TLR2. *Infect. Dis.* **47**, 168–177 (2015).
60. Faridgohar, M. & Nikoueinejad, H. New findings of Toll-like receptors involved in Mycobacterium tuberculosis infection. *Pathog. Glob. Health* **111**, 256–264 (2017).
61. Mohareer, K., Medikonda, J., Vadankula, G. R. & Banerjee, S. Mycobacterial Control of Host Mitochondria: Bioenergetic and Metabolic Changes Shaping Cell Fate and Infection Outcome. *Front. Cell. Infect. Microbiol.* **10**, (2020).
62. Nisa, A. *et al.* Different modalities of host cell death and their impact on Mycobacterium tuberculosis infection. *Am. J. Physiol.-Cell Physiol.* **323**, C1444–C1474 (2022).
63. Chandra, P. *et al.* Mycobacterium tuberculosis Inhibits RAB7 Recruitment to Selectively Modulate Autophagy Flux in Macrophages. *Sci. Rep.* **5**, 16320 (2015).
64. Fernandez-Soto, P., Bruce, A. J. E., Fielding, A. J., Cavet, J. S. & Tabernero, L. Mechanism of catalysis and inhibition of Mycobacterium tuberculosis SapM, implications for the development of novel antivirulence drugs. *Sci. Rep.* **9**, 10315 (2019).
65. Zhang, Q., Ma, S., Li, P. & Xie, J. The dynamics of *Mycobacterium tuberculosis* phagosome and the fate of infection. *Cell. Signal.* **108**, 110715 (2023).
66. Upadhyay, S., Mittal, E. & Philips, J. A. Tuberculosis and the art of macrophage manipulation. *Pathog. Dis.* **76**, fty037 (2018).
67. Mishra, R. *et al.* Mechanopathology of biofilm-like *Mycobacterium tuberculosis* cords. *Cell* **186**, 5135-5150.e28 (2023).
68. Churchyard, G. *et al.* What We Know About Tuberculosis Transmission: An Overview. *J. Infect. Dis.* **216**, S629–S635 (2017).
69. Silva, S., Arinaminpathy, N., Atun, R., Goosby, E. & Reid, M. Economic impact of tuberculosis mortality in 120 countries and the cost of not achieving the Sustainable Development Goals tuberculosis targets: a full-income analysis. *Lancet Glob. Health* **9**, e1372–e1379 (2021).
70. Glassman, I. *et al.* Pathogenesis, Diagnostic Challenges, and Risk Factors of Pott's Disease. *Clin. Pract.* **13**, 155–165 (2023).
71. Elango, S. *et al.* Unusual manifestations of extra-pulmonary tuberculosis: a pictorial essay. *Pol. J. Radiol.* **87**, 79–86 (2022).

72. Lee, S.-A. *et al.* A New Scoring System for the Differential Diagnosis between Tuberculous Meningitis and Viral Meningitis. *J. Korean Med. Sci.* **33**, (2018).
73. New TB Vaccine Research. https://www.who.int/teams/global-tuberculosis-programme/research-innovation/vaccines.
74. Chakaya, J. *et al.* Global Tuberculosis Report 2020 – Reflections on the Global TB burden, treatment and prevention efforts. *Int. J. Infect. Dis.* **113**, S7–S12 (2021).
75. Cronan, M. R. In the Thick of It: Formation of the Tuberculous Granuloma and Its Effects on Host and Therapeutic Responses. *Front. Immunol.* **13**, (2022).
76. Ramakrishnan, L. Revisiting the role of the granuloma in tuberculosis. *Nat. Rev. Immunol.* **12**, 352–366 (2012).
77. Pagán, A. J. & Ramakrishnan, L. The Formation and Function of Granulomas. *Annu. Rev. Immunol.* **36**, 639–665 (2018).
78. Pagán, A. J. & Ramakrishnan, L. Immunity and Immunopathology in the Tuberculous Granuloma. *Cold Spring Harb. Perspect. Med.* **5**, a018499 (2015).
79. Wolf, A. J. *et al.* Initiation of the adaptive immune response to Mycobacterium tuberculosis depends on antigen production in the local lymph node, not the lungs. *J. Exp. Med.* **205**, 105–115 (2007).
80. Polena, H. *et al.* Mycobacterium tuberculosis exploits the formation of new blood vessels for its dissemination. *Sci. Rep.* **6**, 33162 (2016).
81. Lenaerts, A., Barry III, C. E. & Dartois, V. Heterogeneity in tuberculosis pathology, microenvironments and therapeutic responses. *Immunol. Rev.* **264**, 288–307 (2015).
82. Subbian, S. *et al.* Lesion-Specific Immune Response in Granulomas of Patients with Pulmonary Tuberculosis: A Pilot Study. *PLOS ONE* **10**, e0132249 (2015).
83. Ingersoll, M. A. Does immune cell exhaustion lie at the heart of BCG-unresponsive disease? *Nat. Rev. Urol.* **20**, 201–202 (2023).
84. Lombardi, A., Villa, S., Castelli, V., Bandera, A. & Gori, A. T-Cell Exhaustion in Mycobacterium tuberculosis and Nontuberculous Mycobacteria Infection: Pathophysiology and Therapeutic Perspectives. *Microorganisms* **9**, 2460 (2021).
85. Pauken, K. E. & Wherry, E. J. Overcoming T cell exhaustion in infection and cancer. *Trends Immunol.* **36**, 265–276 (2015).
86. Kaminski, H., Lemoine, M. & Pradeu, T. Immunological exhaustion: How to make a disparate concept operational? *PLOS Pathog.* **17**, e1009892 (2021).
87. Definition of T-cell exhaustion - NCI Dictionary of Cancer Terms - NCI. https://www.cancer.gov/publications/dictionaries/cancer-terms/def/t-cell-exhaustion (2011).
88. Peng, S. & Bao, Y. A narrative review of immune checkpoint mechanisms and current immune checkpoint therapy. *Ann. Blood* **7**, (2022).
89. McCaffrey, E. F. *et al.* The immunoregulatory landscape of human tuberculosis granulomas. *Nat. Immunol.* **23**, 318–329 (2022).
90. Lan, X., Zebley, C. C. & Youngblood, B. Cellular and molecular waypoints along the path of T cell exhaustion. *Sci. Immunol.* **8**, eadg3868 (2023).
91. Alahdal, M. & Elkord, E. Exhaustion and over-activation of immune cells in COVID-19: Challenges and therapeutic opportunities. *Clin. Immunol.* **245**, 109177 (2022).
92. Brunell, A. E., Lahesmaa, R., Autio, A. & Thotakura, A. K. Exhausted T cells hijacking the cancer-immunity cycle: Assets and liabilities. *Front. Immunol.* **14**, (2023).
93. Jayaraman, P. *et al.* TIM3 Mediates T Cell Exhaustion during Mycobacterium tuberculosis Infection. *PLOS Pathog.* **12**, e1005490 (2016).
94. Rath, M., Müller, I., Kropf, P., Closs, E. I. & Munder, M. Metabolism via Arginase or Nitric Oxide Synthase: Two Competing Arginine Pathways in Macrophages. *Front. Immunol.* **5**, (2014).
95. Pessanha, A. P., Martins, R. A. P., Mattos-Guaraldi, A. L., Vianna, A. & Moreira, L. O. Arginase-1 expression in granulomas of tuberculosis patients. *FEMS Immunol. Med. Microbiol.* **66**, 265–268 (2012).

96. Au, F. C., Webber, B. & Rosenberg, S. A. Pulmonary granulomas induced by BCG. *Cancer* **41**, 2209–2214 (1978).
97. Verreck, F. A. W. *et al.* Human IL-23-producing type 1 macrophages promote but IL-10-producing type 2 macrophages subvert immunity to (myco)bacteria. *Proc. Natl. Acad. Sci.* **101**, 4560–4565 (2004).
98. Ashenafi, S. & Brighenti, S. Reinventing the human tuberculosis (TB) granuloma: Learning from the cancer field. *Front. Immunol.* **13**, (2022).
99. Kc, Y. *et al.* Systemic Bacillus Calmette-Guerin Infection One Year After Intravesical Immunotherapy Mimicking Sarcoidosis. *Cureus* **14**, (2022).
100. Di Caro, G. *et al.* Occurrence of Tertiary Lymphoid Tissue Is Associated with T-Cell Infiltration and Predicts Better Prognosis in Early-Stage Colorectal Cancers. *Clin. Cancer Res.* **20**, 2147–2158 (2014).
101. Perdomo, C. *et al.* Mucosal BCG Vaccination Induces Protective Lung-Resident Memory T Cell Populations against Tuberculosis. *mBio* **7**, 10.1128/mbio.01686-16 (2016).
102. Kaushal, D. *et al.* Mucosal vaccination with attenuated Mycobacterium tuberculosis induces strong central memory responses and protects against tuberculosis. *Nat. Commun.* **6**, 8533 (2015).
103. Aguilo, N. *et al.* Pulmonary but Not Subcutaneous Delivery of BCG Vaccine Confers Protection to Tuberculosis-Susceptible Mice by an Interleukin 17–Dependent Mechanism. *J. Infect. Dis.* **213**, 831–839 (2016).
104. Swanson, R. V. *et al.* Antigen-specific B cells direct T follicular-like helper cells into lymphoid follicles to mediate Mycobacterium tuberculosis control. *Nat. Immunol.* **24**, 855–868 (2023).
105. Dibbern, J., Eggers, L. & Schneider, B. E. Sex differences in the C57BL/6 model of Mycobacterium tuberculosis infection. *Sci. Rep.* **7**, 10957 (2017).
106. Slight, S. R. *et al.* $CXCR5^+$ T helper cells mediate protective immunity against tuberculosis. *J. Clin. Invest.* **123**, 712–726 (2013).
107. Lobo, N. *et al.* 100 years of Bacillus Calmette–Guérin immunotherapy: from cattle to COVID-19. *Nat. Rev. Urol.* **18**, 611–622 (2021).
108. Santos, P. C. P. dos *et al.* Effect of BCG vaccination against Mycobacterium tuberculosis infection in adult Brazilian health-care workers: a nested clinical trial. *Lancet Infect. Dis.* **0**, (2024).
109. Mittrücker, H.-W. *et al.* Poor correlation between BCG vaccination-induced T cell responses and protection against tuberculosis. *Proc. Natl. Acad. Sci.* **104**, 12434–12439 (2007).
110. Gunasena, M. *et al.* Evaluation of early innate and adaptive immune responses to the TB vaccine Mycobacterium bovis BCG and vaccine candidate BCGΔBCG1419c. *Sci. Rep.* **12**, 12377 (2022).
111. Kaufmann, S. H. *et al.* The BCG replacement vaccine VPM1002: from drawing board to clinical trial. *Expert Rev. Vaccines* **13**, 619–630 (2014).
112. Desel, C. *et al.* Recombinant BCG ΔureC hly+ Induces Superior Protection Over Parental BCG by Stimulating a Balanced Combination of Type 1 and Type 17 Cytokine Responses. *J. Infect. Dis.* **204**, 1573–1584 (2011).
113. Flores-Valdez, M. A. *et al.* The BCGΔBCG1419c Vaccine Candidate Reduces Lung Pathology, IL-6, TNF-α, and IL-10 During Chronic TB Infection. *Front. Microbiol.* **9**, (2018).
114. Kwon, K. W. *et al.* BCGΔBCG1419c increased memory CD8+ T cell-associated immunogenicity and mitigated pulmonary inflammation compared with BCG in a model of chronic tuberculosis. *Sci. Rep.* **12**, 15824 (2022).
115. Pedroza-Roldán, C. *et al.* The BCGΔBCG1419c strain, which produces more pellicle *in vitro*, improves control of chronic tuberculosis *in vivo*. *Vaccine* **34**, 4763–4770 (2016).
116. Tuberkulose-Impfstoff besteht Sicherheitstest. https://www.mpg.de/19038856/0801-bich-tuberkulose-impfstoff-kandidat-vpm1002-bei-hiv-und-nicht-hiv-exponierten-neugeborenen-in-studie-sicher-17216463-x.
117. Cotton, M. F. *et al.* Safety and immunogenicity of VPM1002 versus BCG in South African newborn babies: a randomised, phase 2 non-inferiority double-blind controlled trial. *Lancet Infect. Dis.* **22**, 1472–1483 (2022).

118. Grode, L. *et al.* Safety and immunogenicity of the recombinant BCG vaccine VPM1002 in a phase 1 open-label randomized clinical trial. *Vaccine* **31**, 1340–1348 (2013).
119. Hamon, M. A., Ribet, D., Stavru, F. & Cossart, P. Listeriolysin O: the Swiss army knife of Listeria. *Trends Microbiol.* **20**, 360–368 (2012).
120. Nieuwenhuizen, N. E. *et al.* The Recombinant Bacille Calmette–Guérin Vaccine VPM1002: Ready for Clinical Efficacy Testing. *Front. Immunol.* **8**, (2017).
121. Farinacci, M., Weber, S. & Kaufmann, S. H. E. The recombinant tuberculosis vaccine rBCG Δ*ureC::hly*+ induces apoptotic vesicles for improved priming of CD4+ and CD8+ T cells. *Vaccine* **30**, 7608–7614 (2012).
122. Zheng, W. *et al.* Mycobacterium tuberculosis resides in lysosome-poor monocyte-derived lung cells during chronic infection. *PLOS Pathog.* **20**, e1012205 (2024).
123. Sathkumara, H. D. *et al.* BCG Vaccination Prevents Reactivation of Latent Lymphatic Murine Tuberculosis Independently of CD4+ T Cells. *Front. Immunol.* **10**, (2019).
124. Scordo, J. M. *et al.* The human lung mucosa drives differential Mycobacterium tuberculosis infection outcome in the alveolar epithelium. *Mucosal Immunol.* **12**, 795–804 (2019).
125. Moliva, J. I. *et al.* Molecular composition of the alveolar lining fluid in the aging lung. *AGE* **36**, 1187–1199 (2014).
126. Viklund, E. *et al.* Current smoking alters phospholipid- and surfactant protein A levels in small airway lining fluid: An explorative study on exhaled breath. *PLOS ONE* **16**, e0253825 (2021).
127. Wang, E. Y., Arrazola, R. A., Mathema, B., Ahluwalia, I. B. & Mase, S. R. The impact of smoking on tuberculosis treatment outcomes: a meta-analysis. *Int. J. Tuberc. Lung Dis.* **24**, 170–175 (2020).
128. Chroneos, Z. C., Midde, K., Sever-Chroneos, Z. & Jagannath, C. Pulmonary surfactant and tuberculosis. *Tuberculosis* **89**, S10–S14 (2009).
129. Bussi, C. & Gutierrez, M. G. Mycobacterium tuberculosis infection of host cells in space and time. *FEMS Microbiol. Rev.* **43**, 341–361 (2019).
130. Mai, D. *et al.* Exposure to Mycobacterium remodels alveolar macrophages and the early innate response to Mycobacterium tuberculosis infection. *PLOS Pathog.* **20**, e1011871 (2024).
131. Scordo, J. M., Knoell, D. L. & Torrelles, J. B. Alveolar Epithelial Cells in Mycobacterium tuberculosis Infection: Active Players or Innocent Bystanders? *J. Innate Immun.* **8**, 3–14 (2015).
132. Woo, M. *et al.* Mycobacterium tuberculosis Infection and Innate Responses in a New Model of Lung Alveolar Macrophages. *Front. Immunol.* **9**, (2018).
133. Chandra, P., Grigsby, S. J. & Philips, J. A. Immune evasion and provocation by Mycobacterium tuberculosis. *Nat. Rev. Microbiol.* **20**, 750–766 (2022).
134. Rothchild, A. C. *et al.* Alveolar macrophages generate a noncanonical NRF2-driven transcriptional response to Mycobacterium tuberculosis in vivo. *Sci. Immunol.* **4**, eaaw6693 (2019).
135. Cohen, S. B. *et al.* Alveolar Macrophages Provide an Early Mycobacterium tuberculosis Niche and Initiate Dissemination. *Cell Host Microbe* **24**, 439-446.e4 (2018).
136. Leemans, J. C. *et al.* Depletion of Alveolar Macrophages Exerts Protective Effects in Pulmonary Tuberculosis in Mice1. *J. Immunol.* **166**, 4604–4611 (2001).
137. Huang, L., Nazarova, E. V., Tan, S., Liu, Y. & Russell, D. G. Growth of Mycobacterium tuberculosis in vivo segregates with host macrophage metabolism and ontogeny. *J. Exp. Med.* **215**, 1135–1152 (2018).
138. Kovats, S. Estrogen receptors regulate innate immune cells and signaling pathways. *Cell. Immunol.* **294**, 63–69 (2015).
139. Manuel, R. S. J. & Liang, Y. Sexual dimorphism in immunometabolism and autoimmunity: Impact on personalized medicine. *Autoimmun. Rev.* **20**, 102775 (2021).
140. Yang, Q. *et al.* Sex hormone influence on female-biased autoimmune diseases hints at puberty as an important factor in pathogenesis. *Front. Pediatr.* **11**, (2023).
141. Bonafè, M. *et al.* Inflamm-aging: Why older men are the most susceptible to SARS-CoV-2 complicated outcomes. *Cytokine Growth Factor Rev.* **53**, 33–37 (2020).
142. Gubbels Bupp, M. R., Potluri, T., Fink, A. L. & Klein, S. L. The Confluence of Sex Hormones and Aging on Immunity. *Front. Immunol.* **9**, (2018).

143. Karasawa, T. & Takahashi, M. Role of NLRP3 Inflammasomes in Atherosclerosis. *J. Atheroscler. Thromb.* **24**, 443–451 (2017).
144. Anagnostis, P., Lambrinoudaki, I., Stevenson, J. C. & Goulis, D. G. Menopause-associated risk of cardiovascular disease. *Endocr. Connect.* **11**, (2022).
145. Hodis, H. N. & Mack, W. J. Menopausal Hormone Replacement Therapy and Reduction of All-Cause Mortality and Cardiovascular Disease: It Is About Time and Timing. *Cancer J.* **28**, 208 (2022).
146. Ernst, J. D. The immunological life cycle of tuberculosis. *Nat. Rev. Immunol.* **12**, 581–591 (2012).
147. Srivastava, S., Grace, P. S. & Ernst, J. D. Antigen Export Reduces Antigen Presentation and Limits T Cell Control of M. tuberculosis. *Cell Host Microbe* **19**, 44–54 (2016).
148. Rastogi, S., Ellinwood, S., Augenstreich, J., Mayer-Barber, K. D. & Briken, V. Mycobacterium tuberculosis inhibits the NLRP3 inflammasome activation via its phosphokinase PknF. *PLOS Pathog.* **17**, e1009712 (2021).
149. Chai, Q., Wang, L., Liu, C. H. & Ge, B. New insights into the evasion of host innate immunity by Mycobacterium tuberculosis. *Cell. Mol. Immunol.* **17**, 901–913 (2020).
150. Miller, J. L., Velmurugan, K., Cowan, M. J. & Briken, V. The Type I NADH Dehydrogenase of Mycobacterium tuberculosis Counters Phagosomal NOX2 Activity to Inhibit TNF-α-Mediated Host Cell Apoptosis. *PLOS Pathog.* **6**, e1000864 (2010).
151. Vergne, I. *et al.* Mycobacterium tuberculosis Phagosome Maturation Arrest: Mycobacterial Phosphatidylinositol Analog Phosphatidylinositol Mannoside Stimulates Early Endosomal Fusion. *Mol. Biol. Cell* **15**, 751–760 (2004).
152. Ehrt, S. & Schnappinger, D. Mycobacterial survival strategies in the phagosome: defence against host stresses. *Cell. Microbiol.* **11**, 1170–1178 (2009).
153. Portal-Celhay, C. *et al.* Mycobacterium tuberculosis EsxH inhibits ESCRT-dependent CD4+ T-cell activation. *Nat. Microbiol.* **2**, 1–9 (2016).
154. Mittal, E. *et al.* Mycobacterium tuberculosis Type VII Secretion System Effectors Differentially Impact the ESCRT Endomembrane Damage Response. *mBio* **9**, e01765-18 (2018).
155. Sutiwisesak, R. *et al.* A natural polymorphism of Mycobacterium tuberculosis in the esxH gene disrupts immunodomination by the TB10.4-specific CD8 T cell response. *PLOS Pathog.* **16**, e1009000 (2020).
156. Srivastava, S. & Ernst, J. D. Cell-to-Cell Transfer of *M. tuberculosis* Antigens Optimizes CD4 T Cell Priming. *Cell Host Microbe* **15**, 741–752 (2014).
157. Griffiths, K. L. *et al.* Targeting dendritic cells to accelerate T-cell activation overcomes a bottleneck in tuberculosis vaccine efficacy. *Nat. Commun.* **7**, 13894 (2016).
158. Moliva, J. I., Turner, J. & Torrelles, J. B. Immune Responses to Bacillus Calmette–Guérin Vaccination: Why Do They Fail to Protect against Mycobacterium tuberculosis? *Front. Immunol.* **8**, (2017).
159. Bakhru, P. *et al.* BCG vaccine mediated reduction in the MHC-II expression of macrophages and dendritic cells is reversed by activation of Toll-like receptors 7 and 9. *Cell. Immunol.* **287**, 53–61 (2014).
160. Brandt, L. *et al.* Failure of the Mycobacterium bovis BCG Vaccine: Some Species of Environmental Mycobacteria Block Multiplication of BCG and Induction of Protective Immunity to Tuberculosis. *Infect. Immun.* **70**, 672–678 (2002).
161. LUCA, S. & MIHAESCU, T. History of BCG Vaccine. *Mædica* **8**, 53–58 (2013).
162. Yang, J. D. *et al.* Mycobacterium tuberculosis-specific CD4+ and CD8+ T cells differ in their capacity to recognize infected macrophages. *PLOS Pathog.* **14**, e1007060 (2018).
163. Moguche, A. O. *et al.* Antigen Availability Shapes T Cell Differentiation and Function during Tuberculosis. *Cell Host Microbe* **21**, 695-706.e5 (2017).
164. Woodworth, J. S. *et al.* Protective CD4 T Cells Targeting Cryptic Epitopes of Mycobacterium tuberculosis Resist Infection-Driven Terminal Differentiation. *J. Immunol.* **192**, 3247–3258 (2014).
165. Urdahl, K. B. Understanding and overcoming the barriers to T cell-mediated immunity against tuberculosis. *Semin. Immunol.* **26**, 578–587 (2014).

166. Kerns, P. W., Ackhart, D. F., Basaraba, R. J., Leid, J. G. & Shirtliff, M. E. Mycobacterium tuberculosis pellicles express unique proteins recognized by the host humoral response. *Pathog. Dis.* **70**, 347–358 (2014).
167. Flores-Valdez, M. A. *et al.* The cyclic di-GMP phosphodiesterase gene Rv1357c/BCG1419c affects BCG Pellicle production and In Vivo maintenance. *IUBMB Life* **67**, 129–138 (2015).
168. Liu, X. *et al.* IL-2 Restores T-Cell Dysfunction Induced by Persistent Mycobacterium tuberculosis Antigen Stimulation. *Front. Immunol.* **10**, (2019).
169. Khan, N., Vidyarthi, A., Amir, M., Mushtaq, K. & Agrewala, J. N. T-cell exhaustion in tuberculosis: pitfalls and prospects. *Crit. Rev. Microbiol.* **43**, 133–141 (2017).
170. Nandakumar, S., Kannanganat, S., Posey, J. E., Amara, R. R. & Sable, S. B. Attrition of T-Cell Functions and Simultaneous Upregulation of Inhibitory Markers Correspond with the Waning of BCG-Induced Protection against Tuberculosis in Mice. *PLOS ONE* **9**, e113951 (2014).
171. Liu, X., Li, H., Li, S., Yuan, J. & Pang, Y. Maintenance and recall of memory T cell populations against tuberculosis: Implications for vaccine design. *Front. Immunol.* **14**, (2023).
172. Bickett, T. E. & Karam, S. D. Tuberculosis–Cancer Parallels in Immune Response Regulation. *Int. J. Mol. Sci.* **21**, 6136 (2020).
173. Strandgaard, T. *et al.* Elevated T-cell Exhaustion and Urinary Tumor DNA Levels Are Associated with Bacillus Calmette-Guérin Failure in Patients with Non–muscle-invasive Bladder Cancer. *Eur. Urol.* **82**, 646–656 (2022).
174. Gupta, M., Srikrishna, G., Klein, S. L. & Bishai, W. R. Genetic and hormonal mechanisms underlying sex-specific immune responses in tuberculosis. *Trends Immunol.* **43**, 640–656 (2022).
175. Lee, J. *et al.* Sex-Biased T-cell Exhaustion Drives Differential Immune Responses in Glioblastoma. *Cancer Discov.* **13**, 2090–2105 (2023).
176. Mai, T. *et al.* Estrogen Receptors Bind to and Activate the *HOXC4/HoxC4* Promoter to Potentiate HoxC4-mediated Activation-induced Cytosine Deaminase Induction, Immunoglobulin Class Switch DNA Recombination, and Somatic Hypermutation*. *J. Biol. Chem.* **285**, 37797–37810 (2010).
177. Ursin, R. L. *et al.* Greater Breadth of Vaccine-Induced Immunity in Females than Males Is Mediated by Increased Antibody Diversity in Germinal Center B Cells. *mBio* **13**, e01839-22 (2022).
178. Engler, R. J. M. *et al.* Half- vs Full-Dose Trivalent Inactivated Influenza Vaccine (2004-2005): Age, Dose, and Sex Effects on Immune Responses. *Arch. Intern. Med.* **168**, 2405–2414 (2008).
179. Zhang, N. & Bevan, M. J. CD8+ T Cells: Foot Soldiers of the Immune System. *Immunity* **35**, 161–168 (2011).
180. Winau, F. *et al.* Apoptotic Vesicles Crossprime CD8 T Cells and Protect against Tuberculosis. *Immunity* **24**, 105–117 (2006).
181. Lin, P. L. & Flynn, J. L. CD8 T cells and Mycobacterium tuberculosis infection. *Semin. Immunopathol.* **37**, 239–249 (2015).
182. Segura, E. & Villadangos, J. A. Antigen presentation by dendritic cells *in vivo*. *Curr. Opin. Immunol.* **21**, 105–110 (2009).
183. Ni, H. *et al.* Extracellular mRNA Induces Dendritic Cell Activation by Stimulating Tumor Necrosis Factor-α Secretion and Signaling through a Nucleotide Receptor∗. *J. Biol. Chem.* **277**, 12689–12696 (2002).
184. Keijzer, C., Van Der Zee, R., Van Eden, W. & Broere, F. Treg Inducing Adjuvants for Therapeutic Vaccination Against Chronic Inflammatory Diseases. *Front. Immunol.* **4**, (2013).
185. Cifuentes-Rius, A., Desai, A., Yuen, D., Johnston, A. P. R. & Voelcker, N. H. Inducing immune tolerance with dendritic cell-targeting nanomedicines. *Nat. Nanotechnol.* **16**, 37–46 (2021).
186. Krienke, C. *et al.* A noninflammatory mRNA vaccine for treatment of experimental autoimmune encephalomyelitis. *Science* **371**, 145–153 (2021).
187. Van Brussel, I. *et al.* Tolerogenic dendritic cell vaccines to treat autoimmune diseases: Can the unattainable dream turn into reality? *Autoimmun. Rev.* **13**, 138–150 (2014).
188. Amsen, D. *et al.* Instruction of Distinct CD4 T Helper Cell Fates by Different Notch Ligands on Antigen-Presenting Cells. *Cell* **117**, 515–526 (2004).

189. Curtsinger, J. M. & Mescher, M. F. Inflammatory cytokines as a third signal for T cell activation. *Curr. Opin. Immunol.* **22**, 333–340 (2010).
190. Viola, A., Schroeder, S., Sakakibara, Y. & Lanzavecchia, A. T Lymphocyte Costimulation Mediated by Reorganization of Membrane Microdomains. *Science* **283**, 680–682 (1999).
191. Sallusto, F. & Lanzavecchia, A. The instructive role of dendritic cells on T-cell responses. *Arthritis Res. Ther.* **4**, S127 (2002).
192. Hasegawa, H. & Matsumoto, T. Mechanisms of Tolerance Induction by Dendritic Cells In Vivo. *Front. Immunol.* **9**, (2018).
193. Enk, A. H., Jonuleit, H., Saloga, J. & Knop, J. Dendritic cells as mediators of tumor-induced tolerance in metastatic melanoma. *Int. J. Cancer* **73**, 309–316 (1997).
194. Steinman, R. M. & Nussenzweig, M. C. Avoiding horror autotoxicus: The importance of dendritic cells in peripheral T cell tolerance. *Proc. Natl. Acad. Sci.* **99**, 351–358 (2002).
195. Esterházy, D. *et al.* Classical dendritic cells are required for dietary antigen–mediated induction of peripheral Treg cells and tolerance. *Nat. Immunol.* **17**, 545–555 (2016).
196. Kraus, T. A. *et al.* Induction of mucosal tolerance in Peyer's patch—deficient, ligated small bowel loops. *J. Clin. Invest.* **115**, 2234–2243 (2005).
197. Mazzini, E., Massimiliano, L., Penna, G. & Rescigno, M. Oral Tolerance Can Be Established via Gap Junction Transfer of Fed Antigens from CX3CR1+ Macrophages to CD103+ Dendritic Cells. *Immunity* **40**, 248–261 (2014).
198. Gressier, E. *et al.* CD4+ T cell calibration of antigen-presenting cells optimizes antiviral CD8+ T cell immunity. *Nat. Immunol.* **24**, 979–990 (2023).
199. Silva, Bonato, Lima, Faccioli, & Leão. Characterization of the memory/activated T cells that mediate the long-lived host response against tuberculosis after bacillus Calmette–Guérin or DNA vaccination. *Immunology* **97**, 573–581 (1999).
200. van Pinxteren, L. A. H., Cassidy, J. P., Smedegaard, B. H. C., Agger, E. M. & Andersen, P. Control of latent Mycobacterium tuberculosis infection is dependent on CD8 T cells. *Eur. J. Immunol.* **30**, 3689–3698 (2000).
201. Müller, I., Cobbold, S. P., Waldmann, H. & Kaufmann, S. H. Impaired resistance to Mycobacterium tuberculosis infection after selective in vivo depletion of L3T4+ and Lyt-2+ T cells. *Infect. Immun.* **55**, 2037–2041 (1987).
202. Winchell, C. G. *et al.* CD8+ lymphocytes are critical for early control of tuberculosis in macaques. *J. Exp. Med.* **220**, e20230707 (2023).
203. Wang, J., Santosuosso, M., Ngai, P., Zganiacz, A. & Xing, Z. Activation of CD8 T Cells by Mycobacterial Vaccination Protects against Pulmonary Tuberculosis in the Absence of CD4 T Cells1. *J. Immunol.* **173**, 4590–4597 (2004).
204. McShane, H., Behboudi, S., Goonetilleke, N., Brookes, R. & Hill, A. V. S. Protective Immunity against Mycobacterium tuberculosis Induced by Dendritic Cells Pulsed with both CD8+- and CD4+-T-Cell Epitopes from Antigen 85A. *Infect. Immun.* **70**, 1623–1626 (2002).
205. Lu, Y.-J. *et al.* CD4 T cell help prevents CD8 T cell exhaustion and promotes control of *Mycobacterium tuberculosis* infection. *Cell Rep.* **36**, 109696 (2021).
206. Lewinsohn, D. A., Lewinsohn, D. M. & Scriba, T. J. Polyfunctional CD4+ T Cells As Targets for Tuberculosis Vaccination. *Front. Immunol.* **8**, (2017).
207. Guan, X. *et al.* Androgen receptor activity in T cells limits checkpoint blockade efficacy. *Nature* **606**, 791–796 (2022).
208. Szulc-Dąbrowska, L., Bossowska-Nowicka, M., Struzik, J. & Toka, F. N. Cathepsins in Bacteria-Macrophage Interaction: Defenders or Victims of Circumstance? *Front. Cell. Infect. Microbiol.* **10**, (2020).
209. Frontiers | A century of BCG vaccination: Immune mechanisms, animal models, non-traditional routes and implications for COVID-19. https://www.frontiersin.org/journals/immunology/articles/10.3389/fimmu.2022.959656/full.
210. Urdahl, K. B., Shafiani, S. & Ernst, J. D. Initiation and regulation of T-cell responses in tuberculosis. *Mucosal Immunol.* **4**, 288–293 (2011).

211. Rajaram, M. V. S. *et al.* M. tuberculosis-Initiated Human Mannose Receptor Signaling Regulates Macrophage Recognition and Vesicle Trafficking by FcRγ-Chain, Grb2, and SHP-1. *Cell Rep.* **21**, 126–140 (2017).
212. Grode, L. *et al.* Increased vaccine efficacy against tuberculosis of recombinant *Mycobacterium bovis* bacille Calmette-Guérin mutants that secrete listeriolysin. *J. Clin. Invest.* **115**, 2472–2479 (2005).
213. Dockrell, H. M. A next generation BCG vaccine moves forward. *Lancet Infect. Dis.* **22**, 1404–1406 (2022).
214. Nalbandian, G. & Kovats, S. Understanding sex biases in immunity. *Immunol. Res.* **31**, 91–106 (2005).
215. Douin-Echinard, V. *et al.* Estrogen Receptor α, but Not β, Is Required for Optimal Dendritic Cell Differentiation and CD40-Induced Cytokine Production1. *J. Immunol.* **180**, 3661–3669 (2008).
216. Kovats, S. Estrogen receptors regulate an inflammatory pathway of dendritic cell differentiation: Mechanisms and implications for immunity. *Horm. Behav.* **62**, 254–262 (2012).
217. Mousavi, M. J., Mahmoudi, M. & Ghotloo, S. Escape from X chromosome inactivation and female bias of autoimmune diseases. *Mol. Med.* **26**, 127 (2020).
218. Seillet, C. *et al.* The TLR-mediated response of plasmacytoid dendritic cells is positively regulated by estradiol in vivo through cell-intrinsic estrogen receptor α signaling. *Blood* **119**, 454–464 (2012).
219. González-Navajas, J. M., Lee, J., David, M. & Raz, E. Immunomodulatory functions of type I interferons. *Nat. Rev. Immunol.* **12**, 125–135 (2012).
220. He, F., Furones, A. R., Landegren, N., Fuxe, J. & Sarhan, D. Sex dimorphism in the tumor microenvironment – From bench to bedside and back. *Semin. Cancer Biol.* **86**, 166–179 (2022).
221. Thompson, M., Watkins, S. & Hurwitz, A. A. Abstract LB-322: Synergistic effects of FOXO3 and AR to increase tolerogenicity of tumor associated dendritic cells. *Cancer Res.* **73**, LB-322 (2013).
222. Shin, K.-S. *et al.* Monocyte-Derived Dendritic Cells Dictate the Memory Differentiation of CD8+ T Cells During Acute Infection. *Front. Immunol.* **10**, (2019).
223. Komi, J. & Lassila, O. Nonsteroidal anti-estrogens inhibit the functional differentiation of human monocyte-derived dendritic cells. *Blood* **95**, 2875–2882 (2000).
224. Carreras, E. *et al.* Estrogen receptor signaling promotes dendritic cell differentiation by increasing expression of the transcription factor IRF4. *Blood* **115**, 238–246 (2010).
225. Laffont, S., Seillet, C. & Guéry, J.-C. Estrogen Receptor-Dependent Regulation of Dendritic Cell Development and Function. *Front. Immunol.* **8**, (2017).
226. Morotti, M. *et al.* PGE2 inhibits TIL expansion by disrupting IL-2 signalling and mitochondrial function. *Nature* 1–9 (2024) doi:10.1038/s41586-024-07352-w.
227. Lacher, S. B. *et al.* PGE2 limits effector expansion of tumour-infiltrating stem-like CD8+ T cells. *Nature* **629**, 417–425 (2024).
228. Miyagi, M., Morishita, M. & Iwamoto, Y. Effects of Sex Hormones on Production of Prostaglandin E2 by Human Peripheral Monocytes. *J. Periodontol.* **64**, 1075–1078 (1993).
229. Nieuwenhuizen, N. E. *et al.* Weaker protection against tuberculosis in BCG-vaccinated male 129 S2 mice compared to females. *Vaccine* **39**, 7253–7264 (2021).
230. Vance, R. E., Eichberg, M. J., Portnoy, D. A. & Raulet, D. H. Listening to each other: Infectious disease and cancer immunology. *Sci. Immunol.* **2**, eaai9339 (2017).
231. Preda, M. *et al.* The Bidirectional Relationship between Pulmonary Tuberculosis and Lung Cancer. *Int. J. Environ. Res. Public. Health* **20**, 1282 (2023).
232. Luczynski, P., Poulin, P., Romanowski, K. & Johnston, J. C. Tuberculosis and risk of cancer: A systematic review and meta-analysis. *PLOS ONE* **17**, e0278661 (2022).
233. Dhakal, S. *et al.* Estradiol mediates greater germinal center responses to influenza vaccination in female than male mice. *mBio* **15**, e00326-24 (2024).
234. Menzies, N. A. *et al.* Time Since Infection and Risks of Future Disease for Individuals with Mycobacterium tuberculosis Infection in the United States. *Epidemiology* **32**, 70 (2021).

235. Mueller, A.-K., Behrends, J., Blank, J., Schaible, U. E. & Schneider, B. E. An Experimental Model to Study Tuberculosis-Malaria Coinfection upon Natural Transmission of Mycobacterium tuberculosis and Plasmodium berghei. *J. Vis. Exp. JoVE* 50829 (2014) doi:10.3791/50829.
236. Bankhead, P. *et al.* QuPath: Open source software for digital pathology image analysis. *Sci. Rep.* **7**, 16878 (2017).
237. Kumar, P. A Perspective on the Success and Failure of BCG. *Front. Immunol.* **12**, (2021).
238. Gishnu Harikumar Parvathy *et al.* Sex differences in vaccine induced immunity and protection against Mycobacterium tuberculosis. *bioRxiv* 2024.04.20.590403 (2024) doi:10.1101/2024.04.20.590403.
239. Tagliabue, A., Boraschi, D., Leite, L. C. C. & Kaufmann, S. H. E. 100 Years of BCG Immunization: Past, Present, and Future. *Vaccines* **10**, 1743 (2022).
240. Lyadova, I. V. *et al.* In Mice, Tuberculosis Progression Is Associated with Intensive Inflammatory Response and the Accumulation of Gr-1dim Cells in the Lungs. *PLOS ONE* **5**, e10469 (2010).
241. Foo, S. Y. & Phipps, S. Regulation of inducible BALT formation and contribution to immunity and pathology. *Mucosal Immunol.* **3**, 537–544 (2010).
242. Gao, X., Liu, C. & Wang, S. Mucosal immune responses in the lung during respiratory infection: The organization and regulation of iBALT structure. *hLife* **1**, 71–82 (2023).
243. Sun, H. *et al.* Prognostic value of tertiary lymphoid structures (TLS) in digestive system cancers: a systematic review and meta-analysis. *BMC Cancer* **23**, 1248 (2023).
244. Loxton, A. G. *et al.* Safety and Immunogenicity of the Recombinant Mycobacterium bovis BCG Vaccine VPM1002 in HIV-Unexposed Newborn Infants in South Africa. *Clin. Vaccine Immunol.* **24**, e00439-16 (2017).
245. Du Bruyn, E. *et al.* Mycobacterium tuberculosis-specific CD4 T cells expressing CD153 inversely associate with bacterial load and disease severity in human tuberculosis. *Mucosal Immunol.* **14**, 491–499 (2021).
246. Stewart, P. *et al.* Role of B Cells in Mycobacterium Tuberculosis Infection. *Vaccines* **11**, 955 (2023).
247. Cui, C. *et al.* Neoantigen-driven B cell and CD4 T follicular helper cell collaboration promotes anti-tumor CD8 T cell responses. *Cell* **184**, 6101-6118.e13 (2021).
248. Sud, D., Bigbee, C., Flynn, J. L. & Kirschner, D. E. Contribution of CD8+ T cells to control of Mycobacterium tuberculosis infection. *J. Immunol. Baltim. Md* **176**, 4296–4314 (2006).
249. Thilothammal, N., Krishnamurthy, P. V., Runyan, D. K. & Banu, K. Does BCG vaccine prevent tuberculous meningitis? *Arch. Dis. Child.* **74**, 144–147 (1996).
250. TB and HIV - the co-epidemic. https://www.who.int/news/item/03-12-2007-tb-and-hiv---the-co-epidemic.
251. The untold story: new report reveals 7000 additional TB deaths during COVID-19 pandemic. https://www.ecdc.europa.eu/en/news-events/untold-story-new-report-reveals-7000-additional-tb-deaths-during-covid-19-pandemic (2024).
252. Bernatowska, E. A. *et al.* Disseminated Bacillus Calmette-Guérin Infection and Immunodeficiency - Volume 13, Number 5—May 2007 - Emerging Infectious Diseases journal - CDC. doi:10.3201/eid1305.060865.
253. Fact Sheets | Infection Control & Prevention | Fact Sheet - BCG Vaccine | TB | CDC. https://www.cdc.gov/tb/publications/factsheets/prevention/bcg.htm (2022).
254. Yuan, B. *et al.* Estrogen receptor beta signaling in CD8+ T cells boosts T cell receptor activation and antitumor immunity through a phosphotyrosine switch. *J. Immunother. Cancer* **9**, e001932 (2021).
255. Maret, A. *et al.* Estradiol enhances primary antigen-specific CD4 T cell responses and Th1 development in vivo. Essential role of estrogen receptor α expression in hematopoietic cells. *Eur. J. Immunol.* **33**, 512–521 (2003).
256. Fink, A. L. & Klein, S. L. The evolution of greater humoral immunity in females than males: implications for vaccine efficacy. *Curr. Opin. Physiol.* **6**, 16–20 (2018).
257. Earhart, A. P. *et al.* Lower female survival from an opportunistic infection reveals progesterone-driven sex bias in trained immunity. *Cell Rep.* **42**, (2023).

258. Park, S.-R. *et al.* HoxC4 binds to the promoter of the cytidine deaminase AID gene to induce AID expression, class-switch DNA recombination and somatic hypermutation. *Nat. Immunol.* **10**, 540–550 (2009).
259. Dodd, K. C. & Menon, M. Sex bias in lymphocytes: Implications for autoimmune diseases. *Front. Immunol.* **13**, (2022).
260. Divangahi, M., Javid, B. & Kaufmann, E. 100 years of antibody solitude in TB. *Nat. Immunol.* **22**, 1470–1471 (2021).
261. Lu, L. L. *et al.* A Functional Role for Antibodies in Tuberculosis. *Cell* **167**, 433-443.e14 (2016).
262. Laidlaw, B. J., Craft, J. E. & Kaech, S. M. The multifaceted role of CD4+ T cells in CD8+ T cell memory. *Nat. Rev. Immunol.* **16**, 102–111 (2016).
263. Joosten, S. A. *et al.* Patients with Tuberculosis Have a Dysfunctional Circulating B-Cell Compartment, Which Normalizes following Successful Treatment. *PLOS Pathog.* **12**, e1005687 (2016).
264. Brown, M. A. & Su, M. A. An Inconvenient Variable: Sex Hormones and Their Impact on T Cell Responses. *J. Immunol.* **202**, 1927–1933 (2019).
265. Gengenbacher, M. *et al.* Deletion of nuoG from the Vaccine Candidate Mycobacterium bovis BCG ΔureC::hly Improves Protection against Tuberculosis. *mBio* **7**, 10.1128/mbio.00679-16 (2016).
266. Divangahi, M., Khan, N. & Kaufmann, E. Beyond Killing Mycobacterium tuberculosis: Disease Tolerance. *Front. Immunol.* **9**, (2018).
267. Watanabe, H., Numata, K., Ito, T., Takagi, K. & Matsukawa, A. INNATE IMMUNE RESPONSE IN TH1- AND TH2-DOMINANT MOUSE STRAINS. *Shock* **22**, 460 (2004).
268. Gorham, J. D. *et al.* Genetic mapping of a murine locus controlling development of T helper 1/T helper 2 type responses. *Proc. Natl. Acad. Sci. U. S. A.* **93**, 12467–12472 (1996).
269. Wang, Q. *et al.* Tertiary lymphoid structures predict survival and response to neoadjuvant therapy in locally advanced rectal cancer. *Npj Precis. Oncol.* **8**, 1–10 (2024).
270. Fridman, W. H. *et al.* Tertiary lymphoid structures and B cells: An intratumoral immunity cycle. *Immunity* **56**, 2254–2269 (2023).
271. Kaushal, D. *et al.* Prevention of TB in nonhuman primates by a stress-response deficient mutant of Mycobacterium tuberculosis via induction of classical T cell immunity. Preprint at https://doi.org/10.21203/rs.3.rs-4355037/v1 (2024).
272. Chen, Y., Wu, Y., Yan, G. & Zhang, G. Tertiary lymphoid structures in cancer: maturation and induction. *Front. Immunol.* **15**, (2024).
273. Helmink, B. A. *et al.* B cells and tertiary lymphoid structures promote immunotherapy response. *Nature* **577**, 549–555 (2020).
274. Moorlag, S. J. C. F. M. *et al.* Multi-omics analysis of innate and adaptive responses to BCG vaccination reveals epigenetic cell states that predict trained immunity. *Immunity* **57**, 171-187.e14 (2024).
275. Ferris, S. T. *et al.* cDC1 prime and are licensed by CD4+ T cells to induce anti-tumour immunity. *Nature* **584**, 624–629 (2020).
276. Topchyan, P., Lin, S. & Cui, W. The Role of CD4 T Cell Help in CD8 T Cell Differentiation and Function During Chronic Infection and Cancer. *Immune Netw.* **23**, (2023).
277. Castellino, F. & Germain, R. N. COOPERATION BETWEEN CD4+ AND CD8+ T CELLS: When, Where, and How*. *Annu. Rev. Immunol.* **24**, 519–540 (2006).
278. De Silva, N. S. & Klein, U. Dynamics of B cells in germinal centres. *Nat. Rev. Immunol.* **15**, 137–148 (2015).
279. Van Meerhaeghe, T., Néel, A., Brouard, S. & Degauque, N. Regulation of CD8 T cell by B-cells: A narrative review. *Front. Immunol.* **14**, (2023).
280. Chen, Z. & John Wherry, E. T cell responses in patients with COVID-19. *Nat. Rev. Immunol.* **20**, 529–536 (2020).
281. Brasu, N. *et al.* Memory CD8+ T cell diversity and B cell responses correlate with protection against SARS-CoV-2 following mRNA vaccination. *Nat. Immunol.* **23**, 1445–1456 (2022).

282. Russell, S. L. *et al.* Compromised Metabolic Reprogramming Is an Early Indicator of CD8+ T Cell Dysfunction during Chronic Mycobacterium tuberculosis Infection. *Cell Rep.* **29**, 3564-3579.e5 (2019).
283. Fazilleau, N., Mark, L., McHeyzer-Williams, L. J. & McHeyzer-Williams, M. G. Follicular Helper T Cells: Lineage and Location. *Immunity* **30**, 324–335 (2009).
284. Zander, R. *et al.* Tfh-cell-derived interleukin 21 sustains effector CD8+ T cell responses during chronic viral infection. *Immunity* **55**, 475-493.e5 (2022).
285. Castiglioni, P., Gerloni, M., Cortez-Gonzalez, X. & Zanetti, M. CD8 T cell priming by B lymphocytes is CD4 help dependent. *Eur. J. Immunol.* **35**, 1360–1370 (2005).
286. Kroeger, D. R., Rudulier, C. D. & Bretscher, P. A. Antigen Presenting B Cells Facilitate CD4 T Cell Cooperation Resulting in Enhanced Generation of Effector and Memory CD4 T Cells. *PLOS ONE* **8**, e77346 (2013).
287. Akkaya, M., Kwak, K. & Pierce, S. K. B cell memory: building two walls of protection against pathogens. *Nat. Rev. Immunol.* **20**, 229–238 (2020).
288. Arkatkar, T. *et al.* Memory T cells possess an innate-like function in local protection from mucosal infection. *J. Clin. Invest.* **133**, (2023).
289. Tough, D. F., Borrow, P. & Sprent, J. Induction of Bystander T Cell Proliferation by Viruses and Type I Interferon in Vivo. *Science* **272**, 1947–1950 (1996).
290. Maurice, N. J., Taber, A. K. & Prlic, M. The Ugly Duckling Turned to Swan: A Change in Perception of Bystander-Activated Memory CD8 T Cells. *J. Immunol.* **206**, 455–462 (2021).
291. Tuberculosis. https://www.who.int/health-topics/tuberculosis.
292. Pollard, A. J. & Bijker, E. M. A guide to vaccinology: from basic principles to new developments. *Nat. Rev. Immunol.* **21**, 83–100 (2021).
293. Montero, D. A. *et al.* Two centuries of vaccination: historical and conceptual approach and future perspectives. *Front. Public Health* **11**, (2024).
294. About Diphtheria, Tetanus, and Pertussis Vaccination | CDC. https://www.cdc.gov/vaccines/vpd/dtap-tdap-td/hcp/about-vaccine.html (2024).
295. Polio Vaccine Effectiveness and Duration of Protection | CDC. https://www.cdc.gov/vaccines/vpd/polio/hcp/effectiveness-duration-protection.html (2022).
296. Vaccine Basics | Smallpox | CDC. https://www.cdc.gov/smallpox/vaccine-basics/index.html (2022).
297. Rabies: 100 per cent fatal, 100 per cent preventable. https://www.who.int/publications/i/item/vr-148.
298. Batool, R. *et al.* Efficacy of typhoid vaccines against culture-confirmed Salmonella Typhi in typhoid endemic countries: a systematic review and meta-analysis. *Lancet Glob. Health* **12**, e589–e598 (2024).
299. Andersen, P. & Doherty, T. M. The success and failure of BCG — implications for a novel tuberculosis vaccine. *Nat. Rev. Microbiol.* **3**, 656–662 (2005).
300. Gupta, N. *et al.* Future Path Toward TB Vaccine Development: Boosting BCG or Re-educating by a New Subunit Vaccine. *Front. Immunol.* **9**, (2018).
301. Darrah, P. A. *et al.* Prevention of tuberculosis in macaques after intravenous BCG immunization. *Nature* **577**, 95–102 (2020).
302. Lai, R., Ogunsola, A. F., Rakib, T. & Behar, S. M. Key advances in vaccine development for tuberculosis—success and challenges. *Npj Vaccines* **8**, 1–10 (2023).
303. Hansen, S. G. *et al.* Prevention of tuberculosis in rhesus macaques by a cytomegalovirus-based vaccine. *Nat. Med.* **24**, 130–143 (2018).
304. Germany issues award to IAVI to support development of the MTBVAC tuberculosis vaccine candidate. *IAVI* https://www.iavi.org/press-release/germany-issues-award-to-iavi-to-support-development-of-the-mtbvac-tuberculosis-vaccine-candidate/.
305. Lacámara, S. & Martin, C. MTBVAC: A Tuberculosis Vaccine Candidate Advancing Towards Clinical Efficacy Trials in TB Prevention. *Arch. Bronconeumol.* **59**, 821–828 (2023).

306. White, A. D. *et al.* MTBVAC vaccination protects rhesus macaques against aerosol challenge with M. tuberculosis and induces immune signatures analogous to those observed in clinical studies. *Npj Vaccines* **6**, 1–10 (2021).
307. Portnoy, A. *et al.* The cost and cost-effectiveness of novel tuberculosis vaccines in low- and middle-income countries: A modeling study. *PLOS Med.* **20**, e1004155 (2023).
308. Carter, D. J. *et al.* The impact of social protection and poverty elimination on global tuberculosis incidence: a statistical modelling analysis of Sustainable Development Goal 1. *Lancet Glob. Health* **6**, e514–e522 (2018).

List of Figures

List of Tables

Supplements

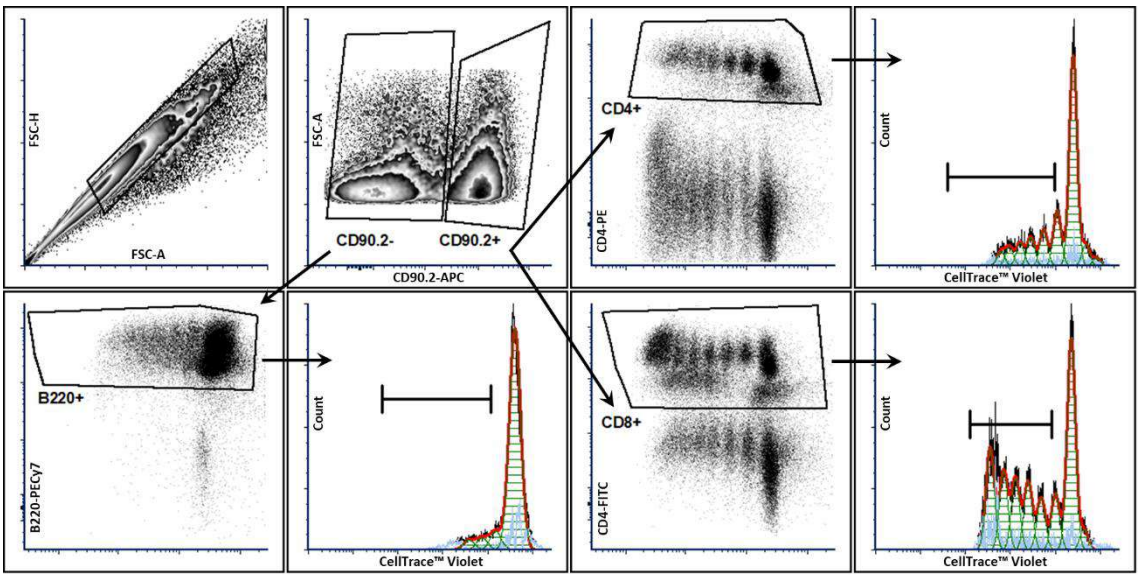

Suppl. Figure S1: Gating strategy to analyse CD8 T cell, CD4 T cell and B cell proliferation in lymph nodes in response to *ex-vivo* restimulation. Representative flow cytometry plots for detection of proliferated CellTrace™ Violet-labeled CD4+, CD8+ or B220+ cells from lymph nodes 28 or 90 days after vaccination in response to restimulation with ConA for 96 hours. Proportion of proliferated cells was determined as the population within marker gate. Gating strategy depicted by an example of cells isolated from the lymph node of a female C57BL/6 mouse shown for day 28 after BCGΔBCG1419c vaccination (data from Harikumar Parvathy et.al., 2024[238]).

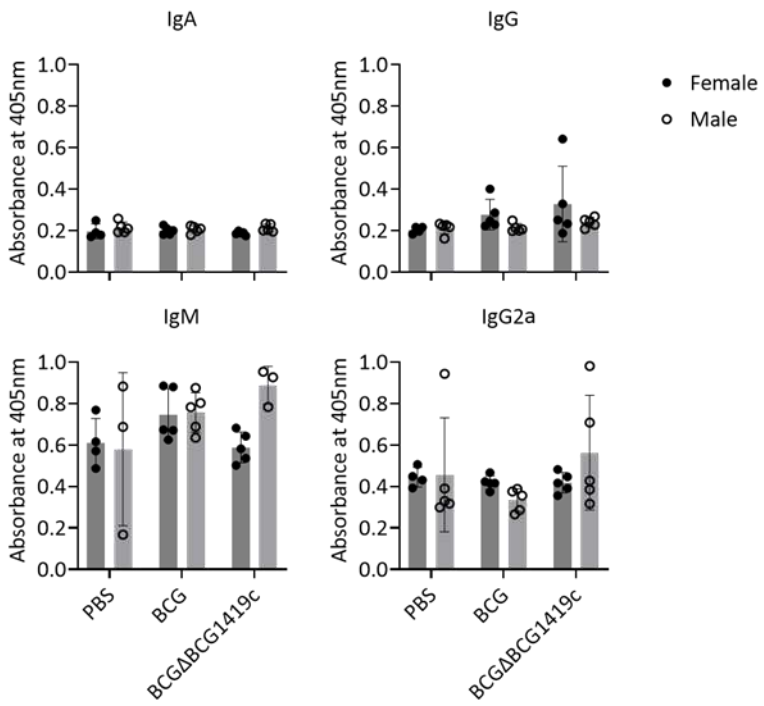

Suppl. Figure S2: *Mtb* whole-cell lysate specific Ig type A, M and G, in lung homogenates. Female and male C57BL/6 mice were vaccinated s.c. with 10^6 BCG or BCGΔBCG1419c, respectively, or PBS (mock control), and immunoglobulin concentrations were determined in lung homogenates at day 28 following aerosol *Mtb* challenge (n = 3-5 mice per group of 1 experiment). Error bars represent SD from mean (data from Harikumar Parvathy et.al., 2024[238]).

```
#These are the utility functions to get subtracted images and Superimposed images. use them accordingly.

import cv2


#Function to calculate and save a subtracted image.

#Input: two image paths used for subtracting images(example: Desktop/gish/images/weighted_final-4.png) and also path to save(example: Desktop/gish/images/weighted_final-4.png).

def subtract_images(path_img_1,path_img_2,path_to_save):
    img0 = cv2.imread(path_img_1)
    img1 = cv2.imread(path_img_2)
    diff = cv2.subtract(img1,img0)
    cv2.imwrite(path_to_save, diff)


#Function to superimpose three subtracted images.

#Input: path to the subtracted images from subtracted_images function above and also path to save superimposed image(example: "Desktop/gish/images/weighted_final-4.png")

def superimpose_difference_images(path_diff_1,path_diff_2,path_diff_3,path_to_save):
    diff_1 = cv2.imread(path_diff_1)
    diff_2 = cv2.imread(path_diff_2)
    diff_3= cv2.imread(path_diff_3)
    x,y,z = np.where(img4 > 0)
    diff_2[x,y] = [255,100,50]
    x,y,z = np.where(img5 > 0)
    diff_3[x,y] = [255,255,0]
    dst = cv2.addWeighted(diff_1,1,diff_2,1,0)
    dst_max = cv2.addWeighted(dst,1,diff_3,1,0)
    cv2.imwrite(path_to_save, dst_max)
```

Suppl. Code S3: Code for subtraction of homeostatic proliferation from restimulation and the superimposition of UMAP images of all restimulated proliferations sex-wise (data from Harikumar Parvathy et.al., 2024[238]).

```
def subtract_images(path_img_1,path_img_2,path_to_save):
    img0 = cv2.imread(path_img_1)
    img1 = cv2.imread(path_img_2)
    diff = cv2.subtract(img1,img0)
    cv2.imwrite(path_to_save, diff)
```

Suppl. Code S4: Code for subtraction of superimposed female and male UMAP images, in order identify proliferating populations unique to females and males.

Acknowledgement

This thesis is dedicated to the memory of my mom – a void that I constantly strive to unsuccessfully fill with my (imperfect) pursuit of immunology – and my partner Parru (Parrvathee Rejitha), who has inspired me and supported me through my toughest days and through my toughest memories over many years. My dad – who has influenced me in his own ways.

My dear gratitude is to Dr. Bianca Schneider – my PI who has given me an opportunity to explore a very fascinating topic – with whom, over time, I have developed a warm and outstanding relationship with freedom to both agree and disagree in scientific topics often with 1-hour meetings stretching out to 2.5-3 hours – the hallmark of an open mentor-mentee relationship. I am forever grateful for my time in her group, our discussions, her support and the project we did together – and how it has enriched my person and my science.

Dr. Jochen Behrends, who has helped me immensely with fluorescence cytometry – teaching me its basics and helping me troubleshoot in preparation for long hours of measurements (16-17 hours per session) - has also been someone with whom I have shared scientific perspectives on and off the scope of the immediate work. He is one of the smartest people I have ever met, with a creative solution for almost every problem that I have discussed with him - and he has been equally generous in sharing his scientific wisdom with me. My time in Borstel has been enriched because of that.

All members of our group – my peers Jaqueline Marschner, Lara Buer, Liisa Knipp, lab Postdoc Dr. David Hertz, TAs Lars Eggers and Linda von Borstel, our former master students Laura and Pauline as well as Martina Hein from Jochen's fluorescence cytometry core facility – are all people who have taught me one thing or another, often many things, that has become a part of my experience which I will take with me. Lars, Linda, Martina, Jaqueline and David also collaborated with me on the experimental part of the project. Further, Prof. Dr. Torsten Goldmann and Dr. Sebastian Marwitz from our histo-pathology division have kindly offered their department's services in tissue/organ processing and automated H&E staining of lung sections.

As with any place of study or work, our relationships make or break us. That way, I have been very fortunate to have developed really great friendships in Borstel. Among others, Alejo,

Claire, Emilie and Vidhisha need a special mention. We have shared laughter, had fun, provided advice to one another, helped one another and have supported each other through our toughest days. On the private side, I have been enormously fortunate to have the greatest group of friends anyone could ever hope to have – in Bonn, my flatmate Dhananjay Bhandiwad (Jay) - and Apsi, his girlfriend (who have now gone on to marry each other) - who was in Passau at the time, have become best friends, to cherish at heart – having survived the covid lockdown together. Jay, with several years of industry experience, went on to do his PhD in Artificial Intelligence in TU Dresden – came around and collaborated with us on our work. We have spent time talking science and concepts in data analysis, developed a concept that was selected for Falling Walls Young Entrepreneurs in Science – Bohringer Ingelheim Venture Fund start-up pitch event, co-developed the code of analysis of UMAP images – in these beautiful years of friendship. Similarly, from my undergraduate days - Faisbin Shah, Brian Issac Pothen, Mariya Ann Tom, Hari Mangalath and John Francis Herbin – people who have come into my life over my years in medical school and despite having taken very different paths, have remained very much present in each other's life – and have supported each other through our toughest moments, deserve a particular mention.

Many students in university will have a phase that would serve as a turning point in their perspectives on what to pursue (for better or worse). For me, I was extraordinarily fortunate to have two extraordinary mentors, Prof. Dr. Sanjay Zachariah and Dr. Dominic Winter, from my medical school in India and my Master studies in Bonn, respectively – mentors who have supported and discussed with me about my interests, sometimes when I was doubting my own evolving tastes and encouraged me to have the courage to welcome change – and to discover myself a bit better at each stage.

A special mention should go to Prof. Dr. Stefan H.E. Kaufmann, Prof. Dr. Hanna Lotter, Dr. Mario Alberto Flores-Valdez, Dr. Zane Orinska – people who have collaborated with us on the project and who have extensively reviewed our work particularly over the course of preparing our manuscript (that is currently available as a preprint) and/or over course of regular reviews, often asking very thorough and critical questions - and never shying away from discussions – which has enormously benefitted all of us together. Zane has also trained me in lymph node harvests from mice and generously shared her advice and reagents with me. Another special note of thanks is to Prof. Dr. Ulrich Schaible, our CEO, for his insightful questions in seminars

(with a particular emphasis on his friendliness) and for his advice on certain experimental matters (such as our observational study post *Mtb* challenge).

In the end, my dearest gratitude is for PD Dr. Norbert Reiling – very pleasant, friendly, supportive head of microbial interface biology, who have generously agreed to review my thesis, offering his insight and wisdom. Norbert, who is in campus, occasionally used to pass by and say hello in the evenings – offering some "tips" on-the-go that have generally turned out to be very insightful; such conversations lasting a couple of minutes have deeply informed me about various aspects that was the topic of those few minutes of conversations.

Further gratitude is to all staff at our institute, especially Ms. Silvia Maaß and Ms. Doreen Beyer, for all the help and support they have given to our work including advice shared by Silvia on culture of BCG vaccine strains, as well as the staff of the animal facility and the Spülküche. My acknowledgement is also due for DFG, for the funding that made this undertaking possible, as well as Lübeck University, for the opportunity to enroll as a doctoral student there. Translation of English language summary to German language was kindly advised and helped by Dr. Bianca Schneider.

Finally, I wish to acknowledge that a significant part of this work was performed during the peak of Covid-19 pandemic, including the years 2020-2022 – a time where we faced innumerable delays in having meetings, getting reagents, plastic-ware and antibodies (sometimes having a delay of several months), delays in setting long experimental schedules, among others. I wish to acknowledge the effort of all my fellow graduates and colleagues, who as a group have pulled together during this time in Borstel.

Erklärung

Hiermit versichere ich, dass ich die vorliegende Arbeit selbstständig verfasst und keine anderen als die angegebenen Hilfsmittel benutzt habe. Weder vorher noch gleichzeitig habe ich andernorts einen Zulassungsantrag gestellt oder diese Dissertation vorgelegt. Ich habe mich bisher noch keinem Promotionsverfahren unterzogen.

Bad Oldesloe, _____ _____

Gishnu Harikumar Parvathy

Publication List

- **Gishnu Harikumar Parvathy**, Dhananjay Bhandiwad, Lars Eggers, Linda von Borstel, Jochen Behrends, Martina Hein, David Hertz, Jaqueline Marschner, Zane Orinska, Stefan H E Kaufmann, Mario Alberto Flores-Valdez, Hanna Lotter, Bianca E Schneider. Sex differences in vaccine induced immunity and protection against Mycobacterium tuberculosis. bioRxiv 2024.04.20.590403; doi:10.1101/2024.04.20.590403.
  (in preparation for journal submission)
- David Hertz, Sebastian Marwitz, Lars Eggers, Linda von Borstel, **Gishnu Harikumar Parvathy**, Jochen Behrends, Danny D. Jonigk, Rudolf A. Manz, Torsten Goldmann, Bianca E. Schneider. Ablation of B cell-derived IL-10 increases tuberculosis resistance. bioRxiv 2024.07.17.603865; doi: 10.1101/2024.07.17.603865.
  (submitted to journal)

Conference Presentations

- NDI3 Symposium, Research center Borstel, Germany. 11.11.2021 to 12.11.2021
  Oral presentation

- DGfI Rothenfels Symposium, Burg Rothenfels, Germany. 27.04.2022 to 29.04.2022
  Oral presentation

- DGfI Rothenfels Symposium, Burg Rothenfels, Germany. 22.03.2023 to 24.03.2023
  Oral presentation

- DGfI Autumn School, Merseburg-Halle. 09.10.2022 to 14.10.2022
  Poster presentation

- DGfI-SFI Joint Meeting 2023, Strasbourg, France. 26.09.2023 to 29.09.2023
  Poster presentation